

**FINAL  
CONTRACT REPORT  
VTRC 10-CR4**

**A CELLULAR AUTOMATA APPROACH TO  
ESTIMATE INCIDENT-RELATED TRAVEL TIME  
ON INTERSTATE 66 IN NEAR REAL TIME**

**ZHUOJIN WANG**  
Graduate Research Assistant

**PAMELA M. MURRAY-TUITE**  
Assistant Professor

Department of Civil and Environmental Engineering  
Virginia Polytechnic Institute & State University



**Standard Title Page—Report on State Project**

Report No.: VTRC 10-CR4	Report Date: March 2010	No. Pages: 81	Type Report: Final Contract Period Covered: July 2007 - May 2009	Project No.: 86493 Contract No.:
Title: A Cellular Automata Approach to Estimate Incident-Related Travel Time on Interstate 66 in Near Real Time			Key Words: Incident, travel time, congestion, real-time data, cellular Automata	
Author(s): Zhuojin Wang and Pamela M. Murray-Tuite				
Performing Organization Name and Address: Virginia Transportation Research Council 530 Edgemont Road Charlottesville, VA 22903				
Sponsoring Agencies' Name and Address: Virginia Department of Transportation 1401 E. Broad Street Richmond, VA 23219				
Supplementary Notes:				
<p>Abstract:</p> <p>Incidents account for a large portion of all congestion and a need clearly exists for tools to predict and estimate incident effects. This study examined (1) congestion back propagation to estimate the length of the queue and travel time from upstream locations to the incident location and (2) queue dissipation. Shockwave analysis, queuing theory, and cellular automata were initially considered. Literature indicated that shockwave analysis and queuing theory underestimate freeway travel time under some conditions. A cellular automata simulation model for I-66 eastbound between US 29 and I-495 was developed. This model requires inputs of incident location, day, time, and estimates of duration, lane closures and timing, and driver re-routing by ramp. The model provides estimates of travel times every 0.2 mile upstream of the incident at every minute after the start of the incident and allows for the determination of queue length over time. It was designed to be used from the beginning of the incident and performed well for normal conditions and incidents, but additional calibration was required for rerouting behavior. We recommend that the Virginia Department of Transportation (1) further pursue cellular automata approaches for near-real time applications along freeways; and (2) consider adopting an approach to address detector failures and errors. Adopting these recommendations should improve VDOT's freeway real-time travel time estimation and other applications based on detector data.</p>				

**FINAL CONTRACT REPORT**

**A CELLULAR AUTOMATA APPROACH TO ESTIMATE INCIDENT-RELATED  
TRAVEL TIME ON INTERSTATE 66 IN NEAR REAL TIME**

**Zhuojin Wang**  
**Graduate Research Assistant**

**Pamela M. Murray-Tuite**  
**Assistant Professor**

**Department of Civil and Environmental Engineering**  
**Virginia Polytechnic Institute & State University**

*Project Manager*

Catherine C. McGhee, P.E., Virginia Transportation Research Council

Contract Research Sponsored by  
the Virginia Transportation Research Council  
(A partnership of the Virginia Department of Transportation  
and the University of Virginia since 1948)

Charlottesville, Virginia

March 2010  
VTRC 10-CR4

## **DISCLAIMER**

The project that was the subject of this report was done under contract for the Virginia Department of Transportation, Virginia Transportation Research Council. The contents of this report reflect the views of the author(s), who was responsible for the facts and the accuracy of the data presented herein. The contents do not necessarily reflect the official views or policies of the Virginia Department of Transportation, the Commonwealth Transportation Board, or the Federal Highway Administration. This report does not constitute a standard, specification, or regulation. Any inclusion of manufacturer names, trade names, or trademarks was for identification purposes only and was not to be considered an endorsement.

Each contract report was peer reviewed and accepted for publication by Research Council staff with expertise in related technical areas. Final editing and proofreading of the report were performed by the contractor.

Copyright 2010 by the Commonwealth of Virginia.  
All rights reserved.

## ABSTRACT

Incidents account for a large portion of all congestion and a need clearly exists for tools to predict and estimate incident effects. This study examined (1) congestion back propagation to estimate the length of the queue and travel time from upstream locations to the incident location and (2) queue dissipation. Shockwave analysis, queuing theory, and cellular automata were initially considered. Literature indicated that shockwave analysis and queuing theory underestimate freeway travel time under some conditions. A cellular automata simulation model for I-66 eastbound between US 29 and I-495 was developed. This model requires inputs of incident location, day, time, and estimates of duration, lane closures and timing, and driver rerouting by ramp. The model provides estimates of travel times every 0.2 mile upstream of the incident at every minute after the start of the incident and allows for the determination of queue length over time. It was designed to be used from the beginning of the incident and performed well for normal conditions and incidents, but additional calibration was required for rerouting behavior. We recommend that the Virginia Department of Transportation (1) further pursue cellular automata approaches for near-real time applications along freeways; and (2) consider adopting an approach to address detector failures and errors. Adopting these recommendations should improve VDOT's freeway real-time travel time estimation and other applications based on detector data.

## **FINAL CONTRACT REPORT**

### **A CELLULAR AUTOMATA APPROACH TO ESTIMATE INCIDENT-RELATED TRAVEL TIME ON INTERSTATE 66 IN NEAR REAL TIME**

**Zhuojin Wang**  
**Graduate Research Assistant**

**Pamela M. Murray-Tuite**  
**Assistant Professor**

**Department of Civil and Environmental Engineering**  
**Virginia Polytechnic Institute & State University**

## **INTRODUCTION**

Traffic congestion continues to increase in the United States and worldwide, causing 4.2 billion hours in delays and costing \$78 billion in 2007 in 437 urban areas in the United States (Schrank and Lomax, 2007). Incidents account for between 25% (Corbin et al., 2007) and 50% of congestion (Booz Allen Hamilton, 1998). With such a large portion of congestion being attributed to semi-random events, a need clearly exists to be able to predict and estimate the effects of incidents, particularly in terms of congestion propagation and delays. Such estimates aid state departments of transportation (DOTs) with congestion mitigation plans and information provision to motorists so they may select alternate routes and plan for delays. Drivers are frequently alerted to the incident occurrence and its location via mass media and advanced technologies, such as Intelligent Transportation Systems (ITS). Other information that aids drivers' decision making includes (1) how long the total trip will take, (2) how to avoid incident-related traffic, and (3) how long it will take to get through the congestion. Drivers might also seek information on incident clearance time; however this aspect is outside the scope of this project. Predicting travel time based on real-time traffic conditions is generally difficult, but important to items (1) and (3).

To monitor real-time traffic conditions, the Virginia Department of Transportation (VDOT) installed numerous inductive loop detectors on Interstate 66 (I-66) for both directions, eastbound and westbound, from Exit 47 to 75. The loop detectors provide real-time traffic information such as traffic volumes, speed, and occupancy. Although these data are valuable in their current presentation to engineers, they are not very informative for the general public, who better understand travel time. Travel times could be predicted based on historical time-of-day data, but the historical travel times might be vastly different from incident-related travel time.

This study involved the development of a cellular automata microsimulation model to estimate incident related travel time, relating to (1) and (3) above. The simulation tool was designed to be used at the beginning of the incident or for hypothetical incidents. This model requires inputs of incident location, day, time, and estimates of duration, lane closures and

timing, and driver re-routing by ramp. The model provides estimates of travel times every 0.2 mile upstream of the incident at every minute after the start of the incident and allows for the determination of queue length over time. Providing upstream drivers with information on the incident location, travel time and distance to the back of the queue, and location of incident-related queues allows them to address item (2) on their own. In particular, drivers would be able to leave the facility at an exit prior to the congestion, provided they were familiar with the network and know or can find alternate routes to their destinations.

Figure 1 indicates where this study and its models fit into the overall timeline of an incident. Depending on vehicle arrival rates, the congestion back propagation and queue building extend from the time the incident occurred until the service rate exceeds the queue arrival rate. Queue dissipation covers the time the incident is cleared to the time that normal flow returns.

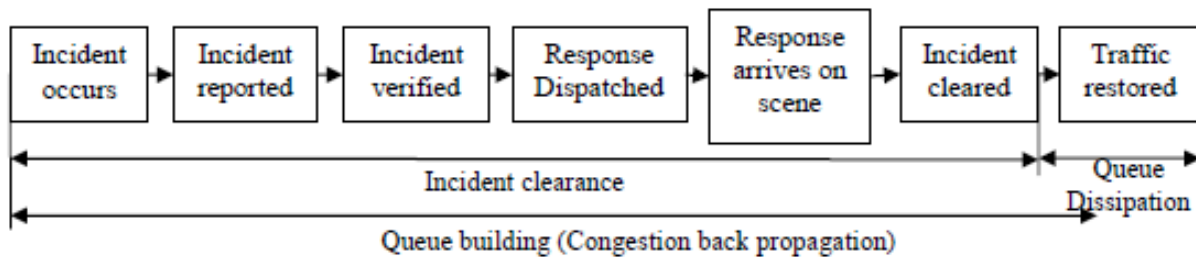


Figure 1. Incident Timeline (Adapted from Hobeika and Dhulopala, 2004).

### Description of Study Area

The focus of the study was a 16-mile eastbound section of I-66. Figure 2 indicates the on- and off-ramps and the number of lanes in each portion of the study area. As can be seen from Figure 2, the number of lanes decreased in the eastern portion of the study area. Some of the lanes had special designations. From US 29 to US 50, three lanes were general purpose and the leftmost was an HOV lane, which was open to general traffic during the off-peak period. Between US 50 and I-495, the road had two general purpose lanes, a right hand shoulder lane, and a left high occupancy vehicle (HOV) lane. The right-side shoulder lane was open as a general purpose (GP) lane during the morning peak period to relieve congestion. East of I-495, the road consisted of three lanes, which narrowed to two lanes at Westmoreland Road. During the peak period, these lanes were all HOV lanes. Normally one auxiliary lane existed in the ramp sections: an acceleration lane for on-ramps and an exit lane for off-ramps.

Peak period eastbound congestion on I-66 routinely started at about 5:30 a.m. and continued until 10:00 a.m. on weekdays. For the purpose of reducing congestion and making full use of the road, VDOT implemented various lane control regulations on eastbound I-66, listed as follows (VDOT, 2008):

1. East of I-495, all eastbound lanes were restricted to vehicles with two or more people (HOV-2) on weekdays from 6:30 a.m. to 9:00 a.m.
2. West of I-495, in the eastbound direction, the far left lane of the GP lanes spanning the entire test area was reserved for HOV-2 from 5:30 a.m. to 9:30 a.m.

3. The right shoulder between US 50 and I-495 was open to all traffic from 5:30 a.m. to 10:00 a.m. (This regulation is for 2007. From 2008, the period changes to 5:30 a.m. to 11:00 a.m.)
4. On weekends, holidays and off-peak hours, shoulder lanes were closed for use and HOV-2 lanes were open to all traffic except trucks.

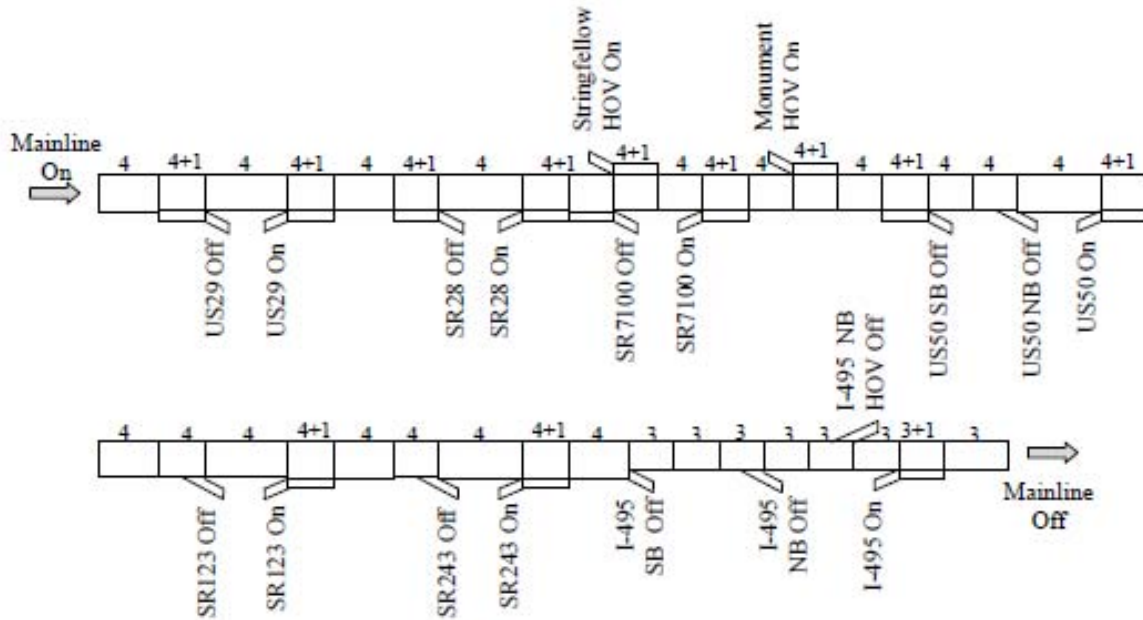


Figure 2. Diagram of the I-66 Study Section.

## PURPOSE AND SCOPE

I-66 in Northern Virginia is particularly fraught with incidents. In 2007, approximately 2,000 incidents were recorded in the Incident Management System (IMS), 22% of which were collisions, 48% were disabled vehicles, 15% were congestion, 6% were road work, and the remainder included debris, vehicle fires, and police activity. (The IMS provided these classifications.) The goal of this study was to identify a feasible approach for estimating incident-related travel time in near-real time for I-66 in Northern Virginia. Given the inputs of incident location, day, time, and estimates of duration, lane closures and timing, and driver re-routing by ramp, the adopted approach provided estimates of travel times every 0.2 mile upstream of the incident at every minute after the start of the incident and allowed for the determination of queue length over time. The study area focused on a 16-mile eastbound portion between US 29 and I-495 using 2007 data. This section of roadway contained 9 on-ramps and 10 off-ramps. In this initial feasibility study, only one type of vehicle was simulated (i.e., trucks and HOVs were not treated separately from general personal vehicles).

## METHODS

This study determined incident-related queue lengths, travel times from upstream locations through the incident location, and queue dissipation. Incident duration was not part of this study. To attain the overall goal, this study addressed the following objectives:

1. Review existing incident-related travel time estimation techniques.
2. Develop origin-destination matrices.
3. Develop methods to model congestion back propagation and queue dissipation based on detector data.
4. Develop methods to calculate travel time.
5. Examine the feasibility of the developed methods performing in near-real time.

Input for the modeling system included start time of the incident, clearance time or an estimated clearance time (which could be refined later), duration, location, and status of lane closure. Outputs of the system were total travel time passing through the incident zone for drivers at different locations, traffic flow, average travel speed and some auxiliary information such as the travel time for drivers to reach the nearest off-ramp especially when a severe incident occurred and people were more likely to exit the freeway prior to reaching the incident.

The methods employed to accomplish the objectives of this study included six tasks:

1. Literature Review
2. Collection of Data
3. Processing of Detector Data
4. Development of Origin-Destination (OD) Trip Tables
5. Development of Model(s)
6. Calibration of Parameters and Application of Model(s).

### **Task 1: Literature Review**

The literature review examined existing models of congestion back propagation and queue clearance, incident travel time prediction methods, studies that incorporated detector data, and previous work specific to the adopted approach.

### **Task 2: Collection of Data**

Two types of data were needed for this study. The first was loop detector data for the study area for the year 2007. In particular, station based speed and flow data for every 5-minute increment were gathered from a database of detector data. The second was incident records for the corresponding area and time period.

## Loop Detector Data

The test site was equipped with 130 detectors on the mainline along with 21 on the ramps. The loop detectors on the mainline were spaced approximately 0.5 mile apart. Parallel detectors with the same milepost, namely, at the same location of the freeway but on different lanes in the same direction, were grouped into logical units called stations. Detectors on the ramps were normally located near the merge or diverge points and detectors on each ramp belonged to individual stations.

The detectors gathered data every minute on speed, volume, and occupancy. Speed at a station was a volume weighted speed in miles per hour. Volume was the number of vehicles detected by the detector within the defined time frame. Occupancy was the percentage of time that vehicles were detected by the detector. Figure 3 shows the station layout on the test site. The integers in the figure represented the station identification (ID) and the numbers in the parentheses indicated the milepost of the station. The station ID numbers were the ones used in 2007 when the data were collected, although station ID numbers have been changed since then.

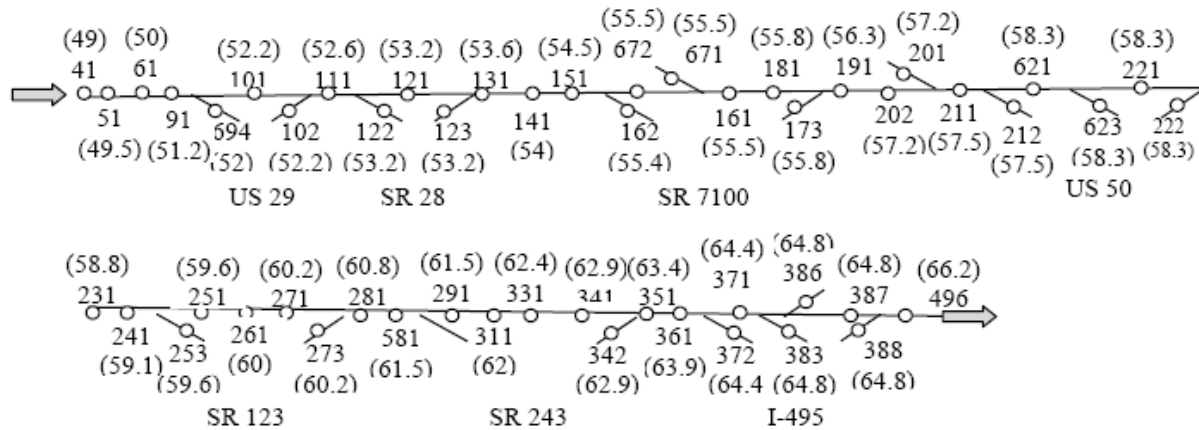


**Figure 3. Station Locations on the Test Section.**

The 1-minute raw data were collected directly from the loop detectors by VDOT in non-delimited flat formats and then translated into a readable format before being stored in the Real-time Freeway Performance Monitoring System (RFPMS), a Microsoft SQL Server database developed by the Virginia Tech Spatial Data Management Lab. This database assembled a history of traffic measurements from all the detectors on I-66 for the last five years. The 1-minute raw data were preliminarily processed by eliminating abnormal and erroneous data based on rules predefined by the database before being aggregated into 5-minute station-level data. The aggregated data were used in this study to minimize random fluctuations. Despite preliminary cleaning, the 5-minute data required further processing, as described in Task 3.

## Incident Data

Incident data were collected from the IMS developed by the University of Maryland CATT Lab and supervised by VDOT. IMS has collected incident records on all freeways in Northern Virginia including I-66, I-496, I-395 and I-95 since 2005. Each incident record

contained the incident ID, incident type and subtype, start time, clear time, close time, location, lane status (closure or open) over time, and a brief description of the incident.

### **Task 3: Processing of Detector Data**

Since preliminary data processing had been conducted on original 1-minute detector data before being transformed into 5-minute station-level data, data processing here refers to system level analysis and eliminating inconsistent and abnormal source data, possibly caused by detector malfunction. System level analysis, differentiated from the individual level where erroneous data were identified on the basis of the relationship between speed, volume and occupancy data from a single detector, considered the relations of data among neighboring stations and trends of daily volume distribution. For example, if data from two stations on the same link (a road section between two junctions, within which the configuration was uniform), were significantly different, the data were further scrutinized and justified based on their consistency.

The objective of data processing was to compile a complete and representative set of flow data for each day of the week representing the normal non-incident daily travel pattern. The data set covering all inflow and outflow in the network was generated as a base case for incident simulation.

In previous studies, one specific day was selected as the typical day after considering the completeness of the data and justifying if its flow data faithfully followed the day-to-day trend (Gomes et al., 2004). However, this method was not suggested for this study due to: (1) no single day had absolute complete data; (2) no single day was incident free throughout the test site; and (3) flow fluctuation from day to day could not guarantee the representativeness of the data.

The procedures to compile a representative data set in this study were (1) integrating data from the same station, same day of a week (except holidays) and same time of a day into one group; (2) eliminating outliers for each group; and (3) averaging flow for each group. Then the average flow data of the same day were ordered chronologically and the combination was the representative entity used for origin-destination trip estimation for each day of the week. The main advantage of this method was that it dramatically reduced the risks of obtaining biased representative data but it required more data processing effort. The most challenging part of data processing was identifying abnormal data.

The procedure for data processing was applied to most stations that had good data quality and small data variance. For some stations with less reliable data quality or mass loss of data, different approaches were utilized, which are indicated in the following procedure. The detailed data processing procedure used in this study is described as follows:

- *Step 1: Choosing representative station data for each link.* This applied to the condition that more than one station was located on a link, which was a road section with uniform configuration. For example, in Figure 3, stations 251, 261, and 271 were located on the same link and only data from one station were selected as representative data for that link. Selection was based on the comparison among these station data assuming the flows should be

close to each other since there was no in- or out-flow within the link. If one station's flow was much smaller than the other two, this station was not selected even if the lower flow was caused by downstream congestion and the data were valid. The higher value should be closer to theoretical flow rate and incident-free conditions, and if lower flow was used in the OD estimation model, the demand would be underestimated. If all the stations had similar data, the station in the middle was chosen since the flow was less likely to be influenced by ramps near the ends of the link. If a link had only one station on it, this station was selected.

- *Step 2: Processing data from station to station.* Data from the same station, same day of a week (except holidays), and same time of day were integrated into one group. Thus, there were at most 52 datum points for each group corresponding to 52 weeks of a year. The detailed steps were:

1. eliminating data in the group where flow equaled zero
2. calculating the average flow and finding the maximum gap between datum points and the average
3. deleting the data with the maximum gap if the gap exceeded a threshold
4. repeating (2) and (3) until the maximum gap was less than the threshold
5. calculating average flow of the reduced data group.

The flow might be zero on some ramps at night. However, eliminating these valid zero data did not significantly affect the results of flow estimation since the average flow on these ramps was low and so was the standard deviation of their flow rates. The results from (5) were considered as the representative link volume for a specific time of day and the "normal" conditions. The maximum gap and threshold were used here to obtain a data set with higher convergence in order to increase the reliability of the results. The thresholds were defined as (1) 100, if the average volume was greater than 250 veh/5min; (2) 80, if the average was between 150 and 250 veh/5min; and (3) 50, if the average was less than 150 veh/5min. The thresholds were based on preliminary manual tests on multiple data sets. Some abnormal data were easily observed from the data set; for example, observations that were 200 veh/5 min higher or lower than the other values could easily be identified. Several thresholds were tested and the one that excluded all of the abnormal data and did not eliminate too much of the good data was selected. These thresholds were then verified by analyzing the least square error, standard deviation, and percentage of values excluded from the data set. The least square error and standard deviation were compared to the before conditions.

However, this method was not applicable to some stations with erroneous data caused by detector malfunction. These stations were identified and specific methods applied. For example, at Station 387, the 5-minute volumes from the first half year double the value from the second half year. Additional scrutiny revealed that the volume in the first half of the year did not vary by time of day, which was suspicious, especially considering the values at neighboring ramps. In this case, the first half year of data was eliminated before the method was applied since the data were too high to be consistent with downstream and upstream links.

- *Step 3: Processing data on a system level.* The average flow data of the same day were organized chronologically to cover 24 hours and the combination was considered as the

volume on each link. The basic idea of system-level data calibration was that the inflow should be close to outflow for each merge or diverge point. For example, in Figure 3, the flow at Station 91 should be similar to the sum of Station 694 and 101 at the US 29 off-ramp. Similarly, Station 111 data should be similar to the sum of Station 101 and 102 at the US 29 on-ramp. On the basis of this approach, it was easy to identify erroneous station data, which were replaced with an average value calculated from neighboring stations. For example, erroneous data in Station 101 could be replaced by  $[(\text{flow at Station 91} - \text{flow at Station 694}) + (\text{flow at Station 111} - \text{flow at Station 102})] / 2$ . Apart from using the spatial relations among stations, the daily trend was another method to identify abnormal data. If the flow at one time increased or decreased unaccountably (i.e., no incident was recorded) and was much higher or lower than the value in its neighboring time steps, the volume was substituted by interpolation from the data in neighboring time steps. Reasonable flow fluctuation within the boundary of 100 veh/5min on the mainline was not eliminated since it was possibly caused by platoon or queue discharge.

- *Step 4: Justifying the data, especially data that has been modified through video.* The real time images from video cameras were available online from TrafficLand.com (TrafficLand). The images did not offer exact flow data but provided a rough idea whether the modified flow data were reasonable or not; this was a qualitative assessment to ensure that the data processing yielded reasonable results.

#### **Task 4: Development of Origin-Destination Trip Tables**

The final flow data from Task 3 were transformed into origin-destination formats required for incident modeling using the software package QueensOD. This software was a macroscopic statistical OD estimation model developed by Van Aerde and his colleagues at Queens University (Van Aerde & Assoc., 2005) that translated the observed link flows to a set of OD matrices. OD matrices were developed for the full 24 hours of each day of the week, with a resolution of 5 minutes.

These OD matrices should be used for regular traffic days. Specifically, they should not be used for holiday weeks, which might have atypical patterns. Different OD matrices would be required for these days, but the model could be used with these revised inputs.

#### **Task 5: Development of Model(s)**

The study required the development of a new simulation model for a few reasons. First, the expense of obtaining real time versions of some existing simulation tools was excessive. Second, other simulation tools had proprietary code that would be difficult to tailor to this study's needs. Finally, the literature indicated that the commonly considered shockwave and queuing approaches underestimate freeway travel times.

Cellular automaton (CA) was the approach selected for further investigation, based on the outcomes of Task 1. This approach showed great promise in studies from Germany. The model was developed based on previous models found in the literature with some modification. New

rules that incorporated some freeway driving behavior that was previously overlooked were included in this model. The model was developed in the C# programming language.

### Task 6: Calibration of Parameters and Application of Model(s)

The CA models must reproduce regular (“incident-free”) traffic flow for each day of the week; parameters of the model were calibrated to achieve the desired results. The CA models must also reproduce incident conditions where driving behavior may be different from those under normal conditions.

The calibration involved both quantitative and qualitative measures. For both incident-free and incident situations, volumes were calibrated using two statistics: mean absolute percentage error (MAPE) and GEH (named after its creator). Equations (1) and (2) provide the formulae for these statistics.

$$MAPE = \frac{1}{n} \sum_{i=1}^n \left| \frac{Vol_{obs,i} - Vol_{sim,i}}{Vol_{obs,i}} \right| \quad (\text{Eq. 1})$$

where

- $n$  = number of time intervals,
- $I$  = index representing the time,
- $Vol_{obs,i}$  = observed volume at time  $i$ , and
- $Vol_{sim,i}$  = simulated volume at time  $i$

For a good fit between the observed (detector) values and the simulated values, MAPE should be small. A perfect fit would yield a MAPE value of 0. Determining what constituted a poor value of MAPE was subjective as there is no upper bound. The threshold established for this study is discussed in the results section.

Similar to the MAPE statistic, the GEH statistic incorporated both the observed volumes and the simulated volumes. GEH was specifically created for traffic analyses and allows scaling of the volumes so that freeway sections and ramps could be evaluated with the same “statistic,” which was an empirical formula rather than a true statistic.

$$GEH = \sqrt{\frac{2(Vol_{obs} - Vol_{sim})^2}{(Vol_{obs} + Vol_{sim})}} \quad (\text{Eq. 2})$$

where the terms were analogous to those described for Equation 1.

The Highways Agency in the United Kingdom considered GEH statistics of less than 5 for individual flows for at least 85% of the cases as acceptable for validation (Highways Agency, 1996). These criteria for acceptability have been followed by other researchers (e.g., Chu et al., 2004) and were used in this study as well.

Speed contour plots were used as a visual tool to examine the daily morning congestion of the network in terms of initial time and end time of the congestion along with queue length. The columns, or x-axis, presented the list of stations on the mainline from upstream to downstream and the rows, or y-axis, provided the time of day in 5-minute intervals. The numbers in the table represented the average speed for each specific location on the freeway and time of day. The speed contour plots could easily identify the location and time of congestion and incidents by marking the segments with speed less than normal speed. The threshold used in this study to distinguish between congestion and normal conditions was 45 mph, corresponding to the value VDOT's NRO freeway operations group considered mild congestion.

Due to the possible oscillation of this information from day to day, reflected by the severity of the congestion, a range was set. If the simulation results were located within the range, the model was considered to be capable of reproducing the morning bottlenecks.

The evaluation of incident simulation was mainly based on flow data. MAPE values and GEH analysis were used for justifying the models. The flow data with 5-minute resolution covered the whole incident duration along with a half hour before the incident and one-half to 1 hour after the incident clearance, covering the queue dissipation period. The threshold of MAPE values was defined as 20% (see the "Results" section for the justification) and the threshold GEH percentage was 85%.

## **RESULTS**

### **Literature Review**

The results of the literature review were divided into two sections. The first discussed models frequently used in the past and a key paper that tested several previous approaches against field observations. According to this paper, queuing theory and shockwave analysis underestimated travel time (Yeon and Elefteriadou, 2006). With this in mind, a relatively new microscopic simulation approach, based on cellular automata models was explored. The second part of the literature review focused on the development of CA approaches.

#### **Previous Approaches to Travel Time Estimation**

Several earlier works estimated general travel time from detectors. For example, Petty (1998) developed a methodology to estimate link travel time directly from a single loop detector and occupancy data based on the assumption that all vehicles arriving at an upstream point during a certain period of time had a common probability distribution of travel time to a downstream point. The distribution of travel time was calculated by minimizing the difference between actual output volume and output volume estimated from upstream input flow and its travel time distribution. Coifman (2002) also used individual loop detectors to calculate travel time as a function of the headway, vehicle velocity, and speed at capacity, which was derived on the basis of linear approximation of the flow-density relationship. The method was reported accurate except at changes of traffic streams, which were frequently found on freeways. Oh et al. (2003) based their calculations on section density and flow estimates from point detectors.

These previous works were not necessarily capable of capturing the complex dynamics that occur during incident scenarios, especially if detectors were widely spaced or conditions between detectors were desired.

Numerous approaches to forecasting travel time under incident conditions have also been developed, including statistics-based approaches, such as probabilistic distributions (Giuliano, 1989; Garib et al., 1997; Sullivan, 1997; Nam and Mannering, 2000), linear regression models (Garib et al., 1997; Ozbay and Kachroo, 1999), and time sequential models (Khattak et al., 1995), decision trees (Ozbay and Kachroo, 1999; Smith and Smith, 2001), Artificial Neural Network (ANN) models (Wei and Lee, 2007), and macroscopic and microscopic models. Queuing analysis and shockwave models were two commonly used macroscopic models to estimate the travel time through a bottleneck (Nam and Drew, 1999; Zhang, 2006; Xia and Chen, 2007), and microscopic packages such as VISSIM and PARAMICS were often used to address the issue (Park and Qi, 2006; Khan, 2007).

Statistical analysis, macroscopic calculation and microscopic simulation were the three main methods to estimate incident-related travel time. Statistical approaches typically covered the entire incident period and provided average travel time by incident type; these were not directly applicable to the current study, due to their general nature. The macroscopic and microscopic models each had advantages along with drawbacks due to their features. Macroscopic models considered the whole traffic flow as a “flow of continuous medium based on a continuum approach” (Li et al., 2001). The models focused on the relations between three macroscopic parameters, namely, flow, density and average speed. Microscopic traffic simulation analyzed traffic flow through detailed representation of individual drivers’ behavior (Choudhury, 2005). The disadvantage of macroscopic methods was that they could be too generalized for specific situations despite their computational efficiency. Microscopic simulation, on the other hand, could reproduce the traffic flow more realistically and precisely, however, computational efficiency was sacrificed. Due to the flexibility and uncertainty of incidents, real time travel time forecasting, requiring both accuracy and efficiency, was necessary, and the models mentioned above left room for improvements in the incident area.

### *Macroscopic Approaches*

Macroscopic models were developed on the basis of traffic flow theories to estimate travel time in terms of flow, speed and occupancy. Most of these models were based on comparison between the inflow and outflow of a specific section in sequential time periods. The advantage of these models was their ability to capture the dynamic characteristics of traffic (Vanajakshi, 2004). The macroscopic approaches considered in this review generally focused on shock wave theory and queuing theory.

Historically, shock waves have been used to identify and model the interface between two distinct states (i.e., congested and non-congested). They modeled both the backward propagation of queues as well as the dissipation of congestion once a bottleneck was passed. Shock waves could be identified using time space diagrams or from density-flow graphs.

In time-space diagrams, vehicle trajectories were plotted (see, for example, Lawson et al., 1997). The slope of the trajectory line represented the speed of the vehicle. As vehicles approached the back of a queue, they reduced their speeds (possibly from free-flow speed). From the diagram, the upstream free flow state could be distinguished from the queued state from the change in slope of the trajectory line. A line drawn connecting these change points among adjacent vehicle trajectories represented the location of the end of the queue as a function of time. The diagram also indicated the speed at which the back of the queue was moving. Individual vehicle delay and total time spent in queue could also be determined from the diagram (Lawson et al., 1997). A drawback to using the basic shock wave approach (as just described) for incident-related travel time prediction was that individual vehicle trajectories had to be plotted. These disaggregate data were not readily available from detectors, which collected aggregate data; thus density-flow graphs were more useful for detector data approaches.

Muñoz and Daganzo (2003) used detector data and kinematic wave theory to identify shocks in traffic flow and examined non-equilibrium flow and the transition zone between congested and non-congested conditions during rush hours. Their detector data indicated that a transition zone with decelerating vehicles existed just behind a queue. From the data, they estimated trip times, the speed of the transition propagation, and the amount of time that drivers spent in transition. The insights gained from Muñoz and Daganzo's work suggested that it was feasible to use detector data to model the transition into the congested regime and the transition into the free-flow regime, at least for recurrent congestion at pre-specified locations as in the peak period.

Another way to avoid constructing vehicle trajectories was to use input-output diagrams for queuing theory applications. Input-output diagrams, also known as cumulative plots (Rakha and Zhang, 2005), depicted the relationships between the cumulative number of vehicles and time at one upstream point (input/arrival) and one downstream point (output/departure). The arrival  $A(t)$  and departure  $D(t)$  curves recorded the associated times for each vehicle. The horizontal distance between these two curves for an individual vehicle was the total travel time between the two observation points (see Figure 4). One could also plot the virtual departure curve  $V(t)$  based on travel at free-flow speeds. Delay was then the horizontal distance between the departure and virtual curves (Lawson et al., 2007). The authors also introduced a fourth curve  $B(t)$  to represent the cumulative number of vehicles reaching the back of the queue. Queue length was the vertical distance between  $B(t)$  and  $D(t)$  and the time spent in the queue was the horizontal distance between  $B(t)$  and  $D(t)$  (Lawson et al., 2007).

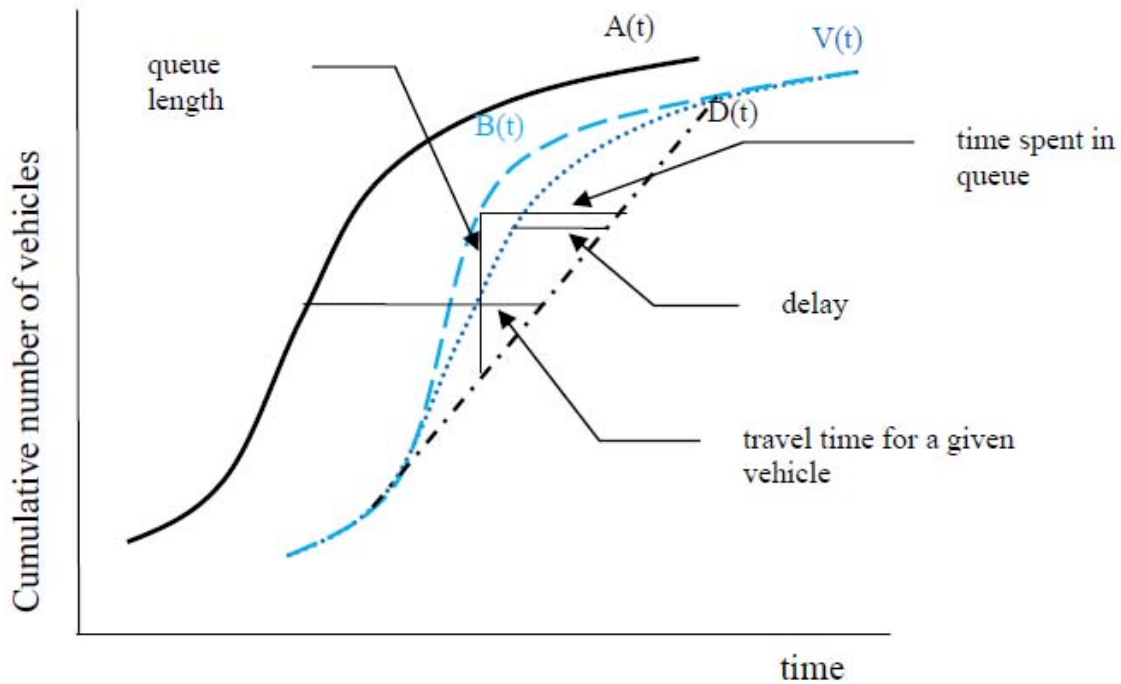


Figure 4. Queuing Curves (Adapted from Lawson et al., 2007).

Using queuing models, Nam and Drew (1999) estimated vehicles' travel time under normal flow conditions and congested flow conditions separately. In normal flow conditions, vehicles entered and left the section within the time interval concerned, while this was not true for the congestion situation. Based on cumulative flow plots, the authors developed two different equations for travel time calculations, one for uncongested and one for congestion conditions.

Rakha and Zhang (2005) identified three errors in Nam and Drew's (1998) earlier work that compared delay calculated by shockwave and queuing theory approaches. Rakha and Zhang corrected Nam and Drew's equations and showed that delay computations for shockwave analysis and queuing theory were consistent.

Using Rakha and Zhang's corrections for queuing analysis, shockwaves, and a third technique called rescaled cumulative curves, Yeon and Elefteriadou (2006) examined the accuracy of these three methods compared with field-measured travel time. Yeon and Elefteriadou noted that all three approaches had typically been applied to freeway sections without entering/exiting ramps. With the presence of ramps between detectors, the rescaled cumulative curves could not be applied. Although the other two methods could be applied in the presence of ramps, the authors concluded that they were inadequate. Comparison of shockwave analysis and queuing theory with field-measured travel time revealed underestimates in certain section configurations for congested conditions (Yeon and Elefteriadou, 2006).

Based on Yeon and Elefteriadou's (2006) work and their recommendation that alternate methods capable of handling ramp considerations be developed for estimating travel time along freeways, we considered microscopic approaches, which were described next.

### *Microscopic Approaches*

Car-following (CF) models are classical microscopic models to simulate traffic networks and the models were incorporated into several simulation packages such as VISSIM and PARAMICS. Simulation models were frequently used for “what-if” scenarios and to examine travel times and queue lengths, but a potential drawback was the computational time.

Cellular automata models are relatively new methods when compared to CF models, with the advantage of high computational speed. Cellular automaton is a dynamic system with discrete and finite features in time and space. “Cellular” pointed out the discrete feature of the system while “automaton” implied the feature of self-organization, free of requiring extra controls from the outside. Cellular automata were “sufficiently simple to allow detailed mathematical analysis, yet sufficiently complex to exhibit a wide variety of complicated phenomena” (Wolfram, 1983). The discrete feature enabled CA models to simulate the network more efficiently along with all advantages of microscopic models. Moreover, CA models could capture the features of observed driving behaviors and translate them into rules. All these advantage made CA models promising for real time forecasting.

### **Cellular Automata Models**

CA models were initially proposed by Von Neumann in 1952 (Ulam, 1952) and introduced into the field of transportation by Cremer and Ludwig in 1986 (Cremer and Ludwig, 1986). CA models have been widely used to simulate a variety of traffic networks including one-way (Nagel and Schreckenberg, 1992; Larraga et al., 2005) and two-way arterials (Simon and Gutowitz, 2008; Fouladvand and Lee, 1999), freeways (Hafstein et al., 2004), intersections (Brockfeld et al., 2001), roundabouts (Fouladvand et al., 2004), and toll stations (Zhu et al., 2007), and were capable of reproducing various traffic conditions such as congestion and free flow at a microscopic level. CA models specifically applied to freeway traffic are discussed further below.

### *CA Basics*

The CA models separated the roads into a sequence of cells, each of which was either occupied by a vehicle or empty. At each time step, a given vehicle remained in its current cell or moved forward at a speed determined by the relationships between the given vehicle and surrounding vehicles in terms of their relative speed and distance. The relationships were defined by rules. One of the great advantages of CA models was that “the dynamical variables of the model were dimensionless, i.e., lengths and positions were expressed in terms of number of cells per second and times were in terms of number of seconds” (Hafstein et al., 2004). The dimensionless feature simplified the application of the models and improves computational efficiency.

Vehicle updating in CA models was either synchronous or sequential. Synchronous updating meant that in each time step all vehicles were updated in parallel; while in sequential updating, an update procedure was performed from downstream to upstream. Each driver was assumed to have full information about the behavior of his predecessor in the next time step (Knospe et al., 1999) under sequential updating rules, which yielded a higher value of average

flow due to a succession of driver overreaction (Jia et al., 2007; Knospe et al., 1999). Therefore, most CA models followed synchronous updating rules.

The boundary conditions in CA models fell into two categories: periodical and open (Jia et al., 2007). According to periodical boundary conditions, the lead vehicles passing through the end of the road reentered the system at the beginning of the road. The total number of vehicles and density in the system were constant. Under open boundary conditions, new vehicles were injected into the beginning of the road with a probability  $\alpha$  and the vehicles were deleted from the system with a probability  $\beta$  once they reached the end of the road (Jia et al., 2007). Periodical boundary rules were normally used when testing the CA model and calibrating its parameters with a general purpose, where the roads could be hypothetical. Open boundary rules were more adaptable for realistic road networks.

### *CA Models of Single Lane Freeways*

Nagel and Schreckenberg (1992) initially presented a single lane CA model (NaSch model) for highways and most of the later CA models were developed based on this model with additional rules. The original rules included four steps (Nagel and Schreckenberg, 1992):

1. *Acceleration*: if a vehicle ( $n$ )'s velocity ( $v$ ) was lower than the maximum speed and the distance ( $d_n$ ) to the next downstream car was larger than its desired speed, the speed was advanced by one cell/ sec.
2. *Deceleration*: if distance  $d_n$  was less than the vehicle's speed, the vehicle reduced its speed to  $d_n$ . (It was implied that  $d_n$  was divided by 1 second to match the units of speed.)
3. *Randomization*: the velocity of each vehicle was decreased by one with probability  $p$  if it was greater than zero.
4. *Car motion*: each vehicle was advanced according to its speed.

Simple as it was, the CA model for traffic flow was able to reproduce some characteristics of real traffic, like jam formation (Hafstein et al., 2004). However, NaSch models missed some observed traffic features, such as metastability, synchronized traffic flow, and the hysteresis phenomenon. These deficiencies motivated additional model developments.

Two models, the TT model and the BJH model were developed to capture metastability by introducing slow-to-start behavior. The first did so by modifying the NaSch model's acceleration step (Takayasu and Takayasu, 1993), and the second added a separate step after the NaSch acceleration step (Benjamin et al., 1996). The idea behind the modified rules of the BJH and TT models was to mimic the delay of a car in restarting, i.e., due to "a slow pick-up of engine or loss of the driver's attention" (Schadschneider and Schreckenberg, 1999). The delay caused by slow starting behavior was considered the main reason for metastable status.

Barlovic et al. (1998) proposed a velocity-dependent-randomization model (VDR model) that modified the randomization step of the NaSch model so the probability for random slowing was one value if the speed of the vehicle was zero in the previous time step and another value if velocity was greater than zero. The other rules remained the same as the NaSch model, and similar to the TT and BJH models, the VDR model was capable of reproducing metastable states.

Li et al. (2001) suggested that the speed of a following vehicle depended not only on the distance between itself and the preceding car but also on the anticipated speed of the preceding car in the next time step. The authors confirmed that neglecting this effect underestimated traffic speed and flow if simulating real road networks. Li et al. (2001) proposed a Velocity Effect (VE) model and modified step 2 in the NaSch model. The deceleration rule in the VE model stated that the speed of a vehicle was the minimum of (a) the maximum speed, (b) current speed plus one, and (c) the gap (with implied division by 1 second) plus the estimated velocity of the preceding car at the next time step. Compared with the NaSch model, the output from the VE model was claimed to be consistent with real data (Li et al., 2001).

Larraga et al. (2005) also considered the speed of the preceding vehicle, but used the preceding vehicle's speed at the same time step rather than the estimated speed at next time step. Their deceleration rule involved a parameter representing driver aggressiveness. The difficulty of determining these parameter values for different drivers created problems in applying this particular model to real traffic flow analysis (Liu, 2006).

Also concerned with the effects of preceding vehicles, Knospe et al. (2000) introduced a comfortable driving (CD) model that accounted for the effects of brake lights. The main ideas of the model were: (1) if the preceding gap was sufficiently large, the driver proceeded at maximum speed; (2) with an intermediate gap, the following driver was affected by changes in the downstream vehicle's velocity as indicated by brake lights; (3) with a small gap, drivers adjusted their speed for the sake of safety; and (4) the acceleration for a stopped vehicle or a vehicle braking in the last time step would be retarded (Knospe et al., 2000). Moreover, Knospe et al. (2000) allowed multiple choices of the safety gap (unlike the VE model, where the safety gap was one cell), which facilitated model calibration and led to more realistic results. The model proved to be capable of reproducing three phases and hysteresis status (Knospe et al., 2000).

Jiang and Wu (2003) modified the first step of Knospe's CD model claiming that the drivers were still very sensitive to restart their cars when they had just stopped until they reached a certain time. The modified model successfully simulated synchronized flow and the results were consistent with real traffic data.

### *CA Models of Lane Changing*

One significant deficiency of single-lane models was that overtaking was not allowed in the system. CA approaches to multi-lane facilities naturally needed to consider this behavior. Lane changing behavior was classified into two categories (Ahmed, 1999): Discretionary Lane Changing (DLC) and Mandatory Lane Changing (MLC). DLC was performed when the driver perceived that the target lane was better than the current lane, for example, higher speed could be achieved by switching. MLC was performed for lane reductions, such as incidents and ramps.

Lane changing rules could be symmetric or asymmetric (Rickert et al., 1996). Symmetric rules were used in systems where lane changing on both sides was permitted while asymmetric rules applied to systems where the motivations of lane changing from left to right or from right to left were different. For example, in Germany, vehicles may only pass on the left, and slow moving vehicles always drove on the right. However, this was not guaranteed to be the case in

the United States. Nagel et al. (1998) pointed out that American drivers usually did not use the rightmost lane in order to avoid disturbances from ramps. Furthermore, simple observation revealed that some American drivers passed on the right. Thus, symmetric rules could be more useful to describe actual American driving behavior than the asymmetric rules.

All lane changing rules consisted of two parts: a reason, or trigger criterion, and a safety criterion (Chowdhury et al., 1997). The trigger explained why people want to change lanes and a safety criterion determined if it was safe for the driver to do so. If both conditions were satisfied, lane changing behavior would be taken.

Rickert et al. (1996) introduced a set of lane changing rules to the NaSch model. If one vehicle was retarded in its current lane, the travel condition in the target lane was better, and lane changing would lead to neither collision nor blockage of another vehicles' way, the vehicle would change to the target lane with probability  $p_{change}$ . The first two conditions were the trigger criteria and the second were the safety criteria. These conditions were adaptable to both changing to the left and to the right lane.

Lane changing for inhomogeneous traffic (e.g., cars and trucks) with different speeds was investigated by Chowdhury et al. (1997). They developed rules that were "symmetric with respect to the vehicles as well as with respect to the lanes" (Chowdhury et al., 1997). The safety criteria were the same as above while the trigger criteria were defined as the forward gap in the current lane being less than the minimum of the maximum speed and the expected speed for the next time step and the forward gap in the target lane being larger than that of the current lane.

The model generated good results in homogenous traffic systems but had some problems in simulating inhomogeneous traffic (Chowdhury et al., 1997; Knospe et al., 1999). Jia et al. (2007) pointed out that the effects of slow vehicles in the system were exaggerated in the model. Even a small number of slow vehicles initiated the formation of platoons at low densities and the queue would not dissipate after a very long time, which was not the case in reality. Jia et al. (2005) addressed this problem by proposing a two-lane CA model with honk effects. Jia's model added two rules to the trigger criteria in Chowdhury's model: (1) the following vehicle honked at the leading vehicle due to blockage and (2) the leading vehicle could drive at its desired speed on either of the lanes free of collision. If all of the trigger and safety criteria were met, the slower vehicle would change lanes. The results showed that fast vehicles could pass slow vehicles quickly at low densities and side effects aroused by slow vehicle were suppressed.

Li et al. (2006) pointed out that fast vehicles usually exhibited more aggressive lane changing behavior when the preceding vehicle was a slow vehicle compared with other cases (i.e., the fast vehicle hindered by a fast one, or a slow vehicle hindered by a slow one). Their model incorporated rules to allow more aggressive behavior for the faster vehicles and improved the simulation of mixed traffic systems.

### *CA Models of Freeway Ramps*

During roughly the same time period as the development of lane changing rules, CA models were extended to include freeway ramps. Diedrich et al. (2000) implemented the on- and

off-ramps as connected parts of the lattice where the vehicles might enter or leave the system. Their procedure for randomly placing vehicles in a vacant cell on the on ramp was recommended for injecting vehicles into the system by Jia et al. (2007).

Campari et al. (2000) extended CA models to two-lane networks with on and off ramps. The study was able to reproduce synchronized flow based on Diedrich's approach. Ez-Zahraouy et al. (2004) also used methods similar to Diedrich's but with open boundary conditions.

Jiang et al. (2003) argued that the above models only considered the influence of the ramps to the main road but the main road actually influenced the ramps. For example, when the density of the main road reached a certain level, it would become a bottleneck for the ramps (Jia et al., 2007). Jiang et al. (2003) adjusted the vehicle updating sequence based on the estimated time vehicles on the mainline and the ramp would reach the junction point; the shorter travel time indicated the road segment that was updated first. Ties were broken according to distance to the junction. Further ties went to the mainline. Jiang et al. (2003) further modified their model to consider randomization effects in an on-ramp system, but the essential idea was that the ramp traffic yielded to the mainline traffic.

The authors also investigated the on-ramp system where the main road had two lanes. The update rules were based on two steps: (1) the vehicles on the main lanes shifted to the left according to Chowdhury's lane changing rules regardless of the on-ramp traffic and (2) vehicles in the left lane were updated according to NaSch rules while those in the right follow Jiang's rules (Jiang et al., 2002, 2003).

Jia et al. (2005) considered the effects of an acceleration lane in an on-ramp system with one lane on the main road. Along the mainline (not including the acceleration lane) and on-ramp, vehicles were updated according to NaSch models. In the section containing both the mainline and the acceleration lane, which was a two-lane network, the authors proposed forbidding the vehicles on the main lane from changing to the accelerating lane (Jia et al., 2005).

Based on similar rules, Jia et al. (2004) simulated off-ramp systems with a CA model with and without an exit lane. Regardless of the configuration, exiting vehicles changed to the right lane and slowed immediately upstream of the off-ramp. In the case where no exit lane existed, exiting vehicles were not permitted to change to the left lane. In the case where an exit lane existed, exiting vehicles already on the exit lane were not allowed to change to the left and the through vehicles could not enter the exit lane. For both cases, the exiting vehicles changed to the right when the trigger and safety criteria were met. If an exiting vehicle was not able to access the right lane before some given point, it stopped there and waited for an opportunity to change lanes.

### *CA Models of Incidents*

On and off ramps, work zones, accidents, and toll booths could be considered typical reasons for the formation of bottlenecks. Bottlenecks reduced the capacity of roads and changed driver behavior and thereby the flow pattern. CA models of ramp simulation were discussed in the previous section. Here, we mainly discuss CA models proposed for incident simulation.

Incidents could be premeditated, like work zones, and accidental such as crashes. The existing literature focused more attention on intentional incidents.

Jia et al. (2003) proposed a model for a two-lane road with a work zone. They focused on the upstream section where drivers perceived the work zone and began to change lanes. According to the rules, the driver on the blocked lane changed to the free lane if the driving situation was at least marginally better than on the blocked lane. Moreover, the lane changing behavior should obey safety criteria. The authors also allowed the vehicle on the free lane to change to the blocked lane if the vehicle was blocked on its current lane while the neighbor lane provided better conditions.

Nassab et al. (2006) proposed similar lane changing models referring to work zone networks. Similar with Jia’s model, the vehicles were not only allowed to change from the blocked lane to the free lane but also from the free lane to the blocked lane. For the first situation, the authors adopted Rickert’s lane changing models and for the second situation, the authors simply reversed the criterion of the first situation.

All of these previous studies played a role in the rule determination for the CA model developed in this study.

### Data Collected

The detector data were obtained as indicated above. The incident data for the same time period (all of 2007) were also obtained. In 2007, a total of 1714 incidents occurred on I-66; these were categorized in Table 1. Nearly half of the incidents were disabled vehicles and nearly a quarter involved collisions.

**Table 1. Incident Categorization.**

Category	Collision	Disabled vehicle	Road Work	Congestion	Debris	Vehicle Fire	Other	Police Activity
<b>Number</b>	407	842	120	264	362	6	29	10
<b>Percentage</b>	24%	49%	7%	15%	2%	0.4%	2%	0.6%

### Processing of Detector Data

The data processing results are presented in terms of standard deviations and relative least square errors, representative daily flow, and scale factors.

#### Standard Deviation and Relative Least Squares Error

The convergence of link flow data used to calculate the average flow was important to justify the reliability of results since the flows of one location were normally similar from day to day (at least for weekdays). In order to quantify the variability in flow data, standard deviation (STDEV) and relative least-squares error (LSE) were used. Relative LSE was computed by dividing the average squared error by the average flow volume (Rakha et al., 1998).

Standard deviation represented the absolute variation of the data set while relative LSE indicated the relative variation related to its average value. Relative LSE was more applicable to justify a data set with higher average value while STDEV provided more intuitional judgments on data sets with lower values. Therefore, in this study, comparison between original data and modified data of mainline stations was mainly based on relative LSE since the flows on the mainline were very high especially in the morning peak. Comparison of stations on ramps was mainly based on the STDEV value. Table 2 lists the average STDEV and relative LSE value for each station before and after data processing (before step 3) for the Friday dataset as an example (tables for the other days are provided in Appendix B). The stations listed were the selected representatives for each link (from step 1). Table 2 also lists the percentage of data that was removed from the set (i.e., the percentage considered outside the normal range). The stations selected but not listed lacked complete data.

Comparison of the “before” and “after” statistics in Table 2 indicated dramatic decreases in most cases. STDEV for mainline stations were over 30 veh/5 min before data processing and the value for Station 387 even reached 153. After data processing, all values dropped below 50 veh/5 min and most were less than 30. Relative LSE for most stations decreased below 20%, which meant the average variance of the data was less than 20% of the mean flow. The decrease of STDEV and LSE for ramp stations was not as dramatic as mainline stations due to the lower flow on the ramps. Standard deviations for all stations were less than 20 veh/5 min. The percentage of data eliminated was no more than 20% of the total original data set. The results showed that the link flow came to a satisfactory convergence level after data processing and yielded a reliable data set over which the representative flow was averaged.

**Table 2. Station Standard Deviation and Relative Least Square Errors Before and After Data Modification.**

<b>Mainline</b>	<b>61</b>	<b>111</b>	<b>121</b>	<b>141</b>	<b>672</b>	<b>161</b>	<b>191</b>
STDEV Before (veh/5 min)	44.07	44.35	41.27	48.56	37.04	37.83	46.33
STDEV After (veh/5 min)	26.69	26.51	21.96	28.76	23.53	23.67	28.34
LSE Before	23.62%	23.47%	26.06%	22.36%	25.95%	24.52%	25.85%
LSE After	15.10%	14.88%	16.32%	13.71%	16.56%	15.32%	16.36%
Delete%	4.89%	5.05%	4.78%	5.23%	3.88%	3.79%	5.72%
<b>Mainline</b>	<b>211</b>	<b>221</b>	<b>231</b>	<b>261</b>	<b>291</b>	<b>351</b>	
STDEV Before (veh/5 min)	53.01	38.79	58.58	65.46	48.85	52.96	
STDEV After (veh/5 min)	37.25	24.23	30.65	30.31	28.21	30.29	
LSE Before	31.16%	23.55%	21.47%	25.54%	22.86%	21.58%	
LSE After	21.69%	14.55%	11.67%	12.97%	13.67%	12.70%	
Delete%	11.41%	4.04%	6.50%	8.03%	5.34%	6.13%	
<b>Ramp</b>	<b>694</b>	<b>102</b>	<b>122</b>	<b>123</b>	<b>162</b>	<b>173</b>	<b>212</b>
STDEV Before (veh/5 min)	74.10	8.01	13.60	19.78	9.22	5.83	9.59
STDEV After (veh/5 min)	14.70	7.10	9.70	16.10	8.39	5.08	6.73
LSE Before	92.68%	35.92%	31.55%	23.72%	31.50%	44.51%	46.43%
LSE After	54.36%	32.79%	24.79%	19.55%	29.53%	44.22%	42.97%
Delete%	34.92%	0.78%	3.08%	2.24%	0.92%	0.05%	0.96%
<b>Ramp</b>	<b>623</b>	<b>222</b>	<b>273</b>	<b>342</b>	<b>386</b>	<b>388</b>	
STDEV Before (veh/5 min)	7.01	28.20	7.83	14.00	43.19	18.89	
STDEV After (veh/5 min)	5.11	19.17	6.90	10.71	11.26	7.55	
LSE Before	50.95%	23.28%	37.90%	30.20%	55.81%	73.15%	
LSE After	50.58%	17.74%	36.95%	28.13%	25.62%	36.61%	
Delete%	0.09%	2.80%	0.29%	1.06%	3.41%	4.34%	

## **Representative Daily Flow**

The flow patterns between weekends and weekdays were different. On weekdays, the flow increased dramatically in the morning peak period and dropped to about half in the afternoon. On weekends, however, plots from all stations showed that the flow gradually increased in the morning and reached the apex in the afternoon. Flow at stations near I-495 showed differences from other stations located to the west. In particular, an abrupt drop in flow occurred after 6 a.m. on weekdays, due to HOV restrictions east of I-495.

## **Scale Factors**

Scale factors, defined as the ratio of the total inflow of the system to the total outflow for each given interval, could be used to identify possible problems with real data (Gomes et al., 2004). The scale factor was expected to fall within 10% of 1.00 for an incident-free condition and the average over a day should be close to 1.00 (Gomes et al., 2004).

For this study, the scale factors around midnight for all days of the week were relatively low because the absolute flow value was small and the quotient of two small values exaggerated the difference between the numerator and denominator. On the other hand, the scale factors were relatively high (approximately 1.1) from 4:00 to 6:00 a.m. for weekdays and 8:00 to 10:00 a.m. (0.95-1.08) for all days due to the morning congestion. By and large, the scale factors were within the reasonable range, justifying the calibrated link flow and qualifying the data as inputs for OD estimation.

## **Origin-Destination Trip Tables**

QueensOD was used to convert the on- and off-ramp flow data into a sequence of 2016 OD matrices for an entire week – 288 for each day: one for each 5-minute time interval in the 24-hour period. The dimension of each matrix was 21\*21 (10 origins and 11 destinations).

Volumes calculated from OD tables were compared with loop detector data to justify the assignment results and evaluate the performance of QueensOD. Figure 5 shows a sample of the results for four locations and presents their volumes from OD tables and from detectors.

As can be seen in Figure 5, the volumes calculated from OD tables matched the detector flow data very well. Table 3 presents the average and variance of volume difference for all of the ramps on Friday as an example. As indicated in the table, the variance of volume difference between OD tables and loop detectors was within the range of 20 veh\*veh/5 min and the average difference was no more than 5 veh/5 min. The difference between volumes of these two sources was within a small scope, indicating QueensOD was consistent with the detector data. Data from other days also showed a good match between the two sources.

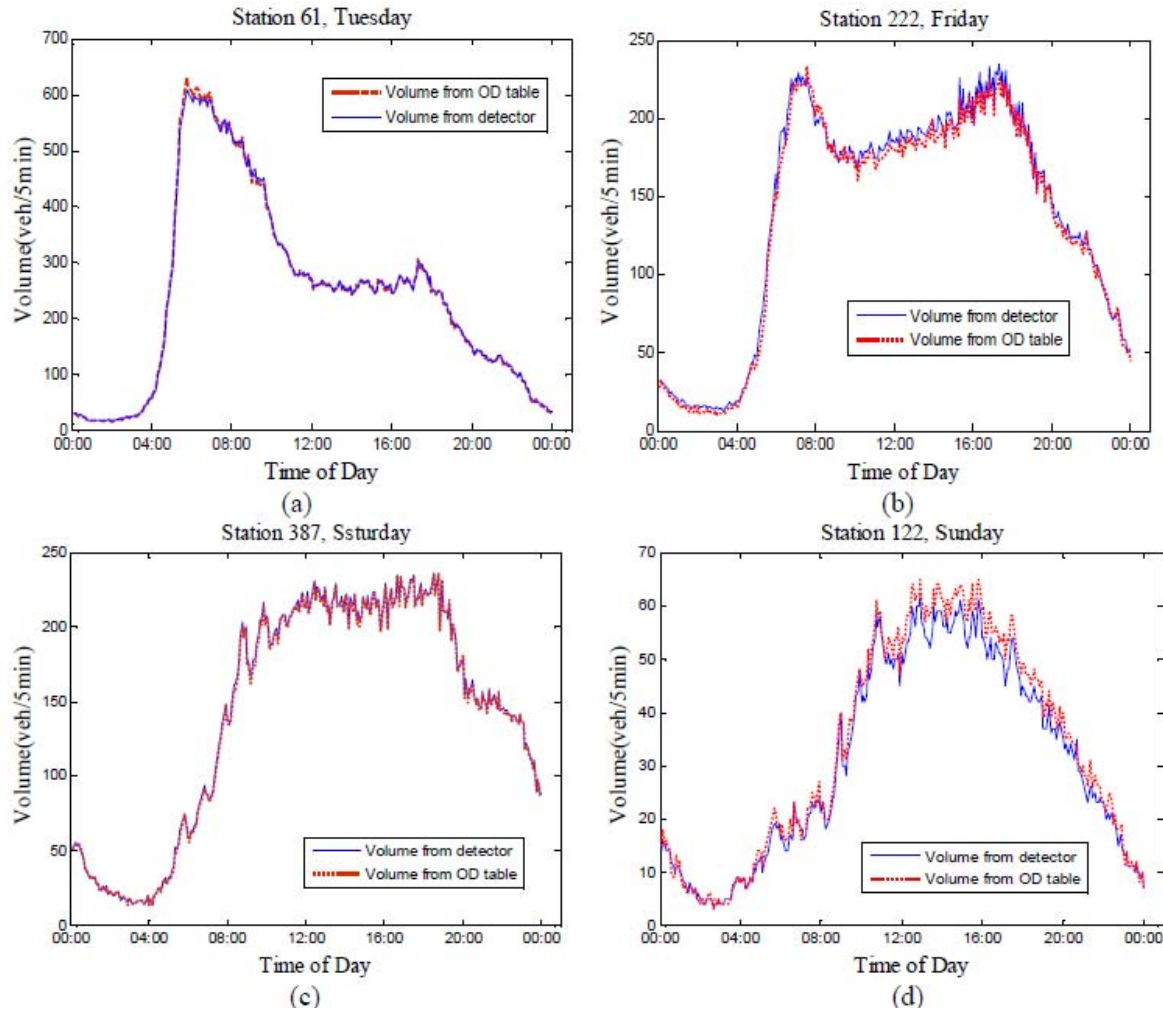


Figure 5. Comparison of Volumes from the Estimated OD Tables and Loop Detectors.

Table 3. Mean and Variance of Gap Volume between OD Tables and Link Flow (Friday).

	I-66 On	US29 Off	US29 On	SR28 Off	SR28 On	SR7100 Off	Stringfellow HOV On	SR7100 On	Monument HOV On	US50 SB Off	US50 NB Off
Average (veh/ 5 min)	1	0	1	3	1	1	1	1	1	2	2
Variance (veh*veh / 5 min)	17	2	3	11	13	10	2	5	1	11	4
	US50 On	SR123 Off	SR123 On	SR243 Off	SR243 On	I-495 SB Off	I-495 NB Off	I-495 NB HOV Off	I-495 On	I-66 Off	
Average (veh/ 5 min)	4	4	5	3	0	1	2	3	2	4	
Variance (veh*veh / 5 min)	19	8	17	13	8	4	4	17	2	14	

## Model Development

Although existing microscopic and mesoscopic simulation packages were capable of precisely simulating traffic networks, the run times, along with the difficulty in setting some features or making some changes in the software, excluded them as ideal tools for this study.

The CA model developed for this study derived many of its rules from the previous works mentioned in the Task 1 results. In particular, symmetric lane changing rules were employed with both triggers and safety criteria. Other rules based on the previous studies related to slow-to-start parameters and the basic speed oscillation parameter (P). Innovative features developed for this study include the incorporation of lane changing aggressiveness parameters and speed oscillation parameters near on and off ramps. Models simulating unplanned incidents were not found in the literature; as such, this was a further point of departure for this study.

In this initial study, only one type of vehicle (the personal vehicle) was considered. Vehicles were not designated HOV or low occupancy at this time. For incident scenarios with blocked lanes, VDOT might remove the HOV restriction and drivers might violate the restriction when congestion is significant.

### Overview

The model kept track of every vehicle in the network, specifically their individual speeds and locations. The inputs to the model were the OD tables from Task 4 and the network. The study area network was converted into cells of 7.5 m in length and a lane wide.

For near-real time applications, the network status can be saved every 5 minutes, including vehicles' locations, speeds, and destinations. Once the initial data were entered into the system, we could directly navigate to the traffic network status with the nearest timeframe and load the corresponding network. For example, if the accident occurred at 5:32 p.m., the system would automatically load the network recorded at 5:30 p.m. from which the simulation would begin. Based on the loaded network when vehicles have distributed according to average conditions, incident CA models could directly be applied here without taking time to run the model from the beginning of the 24-hour period representing that day. This approach saved computational time and thus aided near-real time simulation.

The travel time information was extracted from the model by considering all vehicles, the locations of which were recorded at each time step. Vehicles' travel times under incident conditions were affected by two factors: distance from the downstream edge of the incident zone, denoted by  $x$ , and elapsed time since the beginning of the incident, denoted by  $t$ . The corresponding travel time at location  $x$  at time  $t$  was averaged over data from vehicles that were located between  $x - \Delta x$  and  $x$  during the time span from  $t - \Delta t$  to  $t$ . Small values of  $\Delta t$  and  $\Delta x$  provided precise information of travel time. In this study,  $\Delta t$  was set as 1 minute and  $\Delta x$  was 0.2 mile.

Queue dissipation was reflected in speed changes. When the speeds returned to normal after an incident, the queue had dissipated. The queue length could be tracked based on the vehicles or interpreted from speed contour plots.

### Simulation Setup

The length for each cell was 7.5 m (24.6 ft), which was the average length occupied by one vehicle in a complete jam condition (Nagel and Schreckenberg, 1992). Each cell was occupied by one vehicle or empty. The maximum speed defined here was 4 cells/sec (67 mph), rather than 5 cells/sec (84 mph) normally adopted in previous studies. Since the speed limit of the test site was 55 mph and the average free flow speed observed was 65 mph, 4 cells/sec was consistent with realistic conditions. The time step was one second.

The notation is visually represented in Figure 6. The large “X” indicated the given vehicle to which the measurements pertained and a smaller “x” indicated another vehicle.

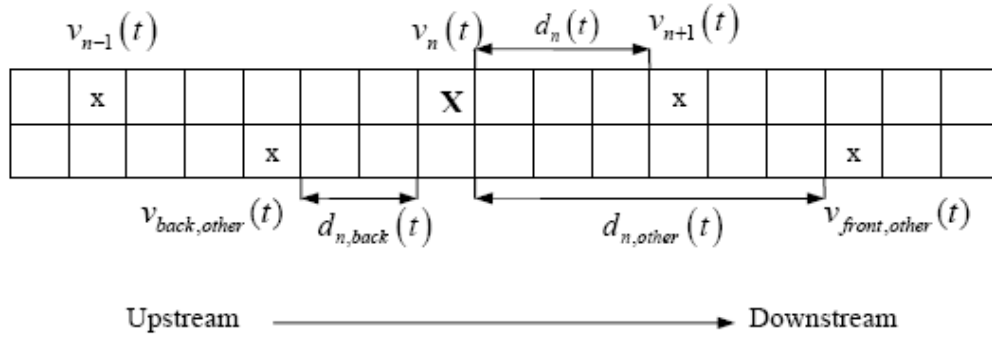


**Figure 6. Illustration of CA Notation.**

$v_n(t)$ : speed of given vehicle  $n$  at time  $t$ , in units of cells/second;  $v_{n+1}(t)$ : speed of leading vehicle  $n + 1$  at time  $t$ , in units of cells/second;  $v_{n-1}(t)$ : speed of following vehicle  $n - 1$  at time  $t$ , in units of cells/second;  $v_{front,other}(t)$ : speed of leading vehicle in the neighboring lane at time  $t$ , in units of cells/second;  $v_{back,other}$ : speed of following vehicle in the neighboring lane at time  $t$ , in units of cells/second;  $d_n(t)$ : distance between given vehicle and its leading vehicle at time  $t$ , in units of cells;  $d_{n,other}(t)$ : distance between given vehicle and its leading vehicle in the neighboring lane at time  $t$ , in units of cells;  $d_{n,back}(t)$ : distance between given vehicle and its following vehicle in the neighboring lane at time  $t$ , in units of cells.

The distance between the given vehicle and its following vehicle  $n - 1$  was not given specific notation since it could be expressed as  $d_{n-1}(t)$ .

The model also included look-back distance, look-ahead distance, and ramp influence zones. The look-back distance applied to areas near off-ramps where the appropriate exiting vehicles changed lanes in order to reach their intended off-ramps. This distance was 60 cells (450 m or 0.28 mi) and essentially represented the part of the network where the exiting vehicles started moving to the right lane in preparation for exiting. The look-ahead distance applied to bottleneck sections with lane reductions where the vehicles on a blocked or disappearing lane began switching to other lanes. This distance was 30 cells (225 m or 0.14 mi) for this model.

Finally, the ramp influence zones, as defined in the *Highway Capacity Manual* (Transportation Research Board, 2000) were the areas where merging and diverging vehicles affected the mainline flow and were 1500 ft (457.2 m) long. In this model, the on-ramp influence zone was 60 cells (1476 ft) from the merge point. The off-ramp influence zone covered the 60 cells upstream from the diverge point, equivalent to the look-back distance, and the freeway section with a deceleration lane since speed oscillation in this region could result in lane changes. Figure 7 illustrates the influence zone and look-back distance.

Since the network contained several types of sections and behavior was expected to vary among the sections, a set of indicators was developed to discriminate among the vehicles under the different influences. Table 4 summarizes the different types of sections and their indicators.

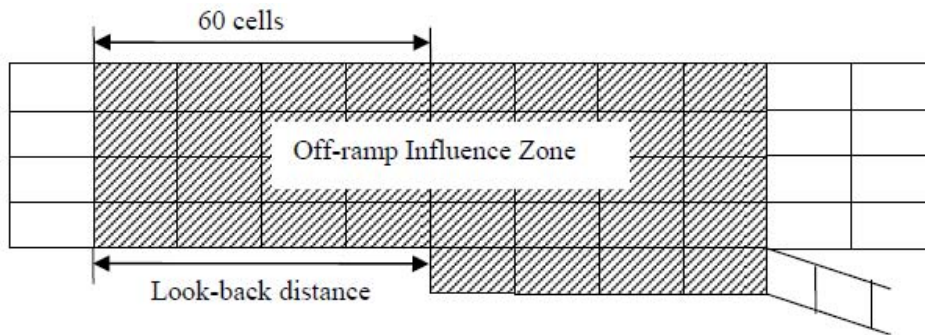


**Figure 7. Off-Ramp Influence Zone and Look-Back Distance Illustration.**

**Table 4. Freeway Section Indicators.**

Freeway Section	Indicator
Shoulder lane	-5
Look-ahead distance	-4
On-ramp influence zone	-3
No vehicle permission zone	-2
Acceleration lane	on-ramp ID
Off-ramp influence zone	off-ramp ID
All other sections	-1

To simplify the division of the 16 mile long network into cells, the entire mainline of the network was initially considered to contain six lanes, a left entrance/exit lane, four main lanes (which includes the HOV and shoulder lanes in the appropriate sections), and a right entrance/exit lane. Then, cells that did not exist in reality were coded with a “-2.” This indicator was also applied to other sections where vehicles were not permitted, such as incident zones and the shoulder lane during its closed time. The indicators also played a role in lane changing, which was described as part of the model in the next section.

## CA Base Model

### *Initializing the System*

The network was empty at the beginning of a simulation. The open boundary condition was applied here to initialize the system and inject vehicles into the network. The probability for a vehicle to enter the system in one time step was  $\alpha$ , defined as total volume divided by the

corresponding time interval. For example, if the volume observed to enter the system of one lane was 150 veh/5 min, the value of  $\alpha$  equaled  $150/(5*60) = 50\%$ . The vehicle would be injected randomly into one of the western most first four cells, corresponding to the farthest location that it could reach in one time step, only if these cells were all empty. However, if the first four cells already contained some vehicles, the system navigated to the location of the last vehicle and as long as the first cell behind it was empty, a vehicle was injected into any cell upstream of the last vehicle. New vehicles were assigned a lane according to the percentages estimated from detector data: approximately 20% to both the leftmost and rightmost lanes and approximately 30% to each of the middle lanes. For vehicles that entered the network from on-ramps, the same injection procedure of searching for empty cells was followed. The initial speeds set for all the vehicles entering the mainline were the maximum speed (4 cells/sec) while 3 cells/sec was applied to those from on-ramps considering that vehicles from on-ramps should have lower initial speeds.

The destination of the new injected vehicle was determined based on volume-weighted percentage, which was calculated from OD matrices. For example, a demand of 100 vehicles from one origin had two destinations: 30 vehicles would go to destination 1 and the remaining 70 would go to destination 2. A vehicle would choose destination 1 and 2 with probability 30% and 70%, respectively. The vehicle was given an indicator representing its origin and destination.

### *Updating Vehicles*

The updating rules were based on NaSch models (Nagel and Schreckenberg, 1992) and Chowdhury's lane changing models (Chowdhury et al., 1997) while some modifications (as outlined at the beginning of this task's results) were made to be more consistent with the study area. The lane changing models were incorporated into the NaSch four-step model and made the total updating steps into five, which are described in detail below. In the following steps, all the values at time  $t-1$  were known and the speed and new location of the given vehicle were found at the current time step  $t$ . The initial value of  $v_n(t)$  was the same as  $v_n(t-1)$  and was updated from step to step. Thus,  $v_n(t)$  at the beginning of each step was the result from the previous step and the value obtained in the last step was the final speed of vehicle  $n$  at time  $t$ .

- *Step 1: Acceleration.* If the vehicle's speed in the last time step was less than the maximum speed  $v_{max}$ , the vehicle increased its speed by 1 cell/sec in the current time step. The rule was expressed as:

$$\text{If } v_n(t-1) < v_{max}, \text{ then } v_n(t) \rightarrow \min(v_n(t-1) + 1, v_{max}).$$

The minimum could be considered the desired speed for the vehicle in the current time step.

- *Step 2: Lane Changing.* Lane changing behavior was classified into discretionary and mandatory. Vehicles changing from on-ramps to the mainline, from the mainline to intended off-ramps, or one main lane to another near lane reduction sections fell into the mandatory lane changing category. Other cases where lane changing was not necessarily required were considered discretionary.

The given vehicle changed lanes with probability  $P_{change,dis}$  (probability for discretionary lane changing) if the following conditions were met:

*Trigger criteria:*

1. the gap in front was less than the desired speed of given vehicle

$$d_n(t) < v_n(t)$$

2. the front gap in the neighboring lane was greater than current lane

$$d_{n,other}(t) > d_n(t)$$

*Safety criteria:*

3. the neighboring site of the given vehicle  $n$  was empty
4. the back gap in the neighboring lane was greater than or equal to the following vehicle's speed at time  $t-1$

$$d_{n,back}(t) \geq v_{back,other}(t-1)$$

Note that the comparison of distance and speed was allowed by the implied multiplication of speed by the time increment of 1 second.

The parameter  $P_{change,dis}$  discriminated between the aggressive and less aggressive drivers.

The last criterion was less restricted compared to Chowdhury's model. Here, if the leading vehicle thought that changing lanes would not reduce the speed of the following vehicle in the target lane, it could switch. This was an indirect way to incorporate the effect of turning signals into the model. Therefore, discretionary lane changing behavior was more freely used here and the frequency should be higher compared to Chowdhury's models given the same lane changing probability.

Mandatory lane changing behavior was more aggressive than the discretionary type, thereby following less restrictive rules. For vehicles to enter the mainline from an on-ramp acceleration lane, to reach the intended off-ramps from the freeway lanes, and to pass through lane reduction sections, they changed to their target lane with probability  $P_{change,man}$  if (1) the speed of given vehicle would drop by less than  $k$  cells/sec in the current time step; and (2) the speed of the following vehicle in the target lane would drop by less than  $b$  cells/sec in the current step. The criteria were expressed as:

$$d_{n,other}(t) \geq v_n(t-1) - k \text{ and } d_{n,back}(t) \geq v_{back,other}(t-1) - b$$

(Note: the comparison of distance and speed was permitted by the implied multiplication of speed by 1 second.)

$P_{change,man}$  represented the probability of mandatory lane changing, which should be greater than  $P_{change,dis}$ . The parameters  $k$  and  $b$  were the maximum speed reduction that the given vehicle and the following vehicle could tolerate because of lane changing behavior. Higher values led to higher frequency of lane changing maneuvers. These two parameters were calibrated in the next task. This rule reflected the fact that vehicles were more likely to yield to those vehicles that had to change lanes. For example, when vehicles got close to a bottleneck with lane reduction, vehicles on the unblocked lane would often show courtesy to those on the blocked lane in the United States.

A specific mandatory lane changing rule was applied to vehicles on the shoulder lane when the lane was closed (i.e., vehicles that were on the lane when it was open just prior to its closure). This rule kept the model from losing vehicles when the lane status switched or causing excessive congestion. The closed shoulder lane in the off-peak was treated as a special area where vehicles were permitted but forced to leave as soon as possible. Aggressive lane changing rules were used here: a vehicle on the closed shoulder lane changed to the main lane if there was at least one empty cell in the forward and backward directions in the target lane. The rule was expressed as:

$$d_{n,other}(t) \geq 1 \text{ and } d_{n,back}(t) \geq 1$$

This rule forced vehicles to leave the closed shoulder lane aggressively but without causing severe congestion. Once the vehicle left the shoulder lane, it was not permitted to return. However, if the vehicle could not change lanes according to the rule, it continued on the lane until it met the criteria.

The lane change direction (left or right) was based on the vehicle's location. The rules that determined the direction were:

1. If the vehicle was on a right acceleration lane, the lane change direction was left.
2. If the vehicle was on a left acceleration lane, the lane change direction was right.
3. If a vehicle was within the look-back distance of its intended off-ramp, which was on the right side, the vehicle changed lanes to the right; if the off-ramp was on the left, the vehicle changed lanes to the left until it reached the exit lane.
4. If a vehicle was within the look-ahead distance of a blocked lane, the vehicle moved toward an unblocked lane (either right or left) until it reached a free lane.
5. If a vehicle was on the shoulder lane, the lane change direction was left since the shoulder lane was on the right.
6. A vehicle was not permitted to change to acceleration lanes, exit lanes not pertaining to its destination, shoulder lanes during the closed period, or any road segment indicated as "-2."
7. On uniform freeway sections (indicated by "-1"), with no ramps or incidents, the vehicle could change to either left or right lanes (provided such a lane exists).

It was possible for the above rules to conflict when an exiting vehicle within the look-back distance encountered a blocked lane section, as in Figure 8. While the exiting vehicle should move to the right, the blocked lane effect was more critical than moving to the right. Therefore, the vehicle went around the blocked section by changing lanes to the left and then moved to the right to reach the exit ramp.

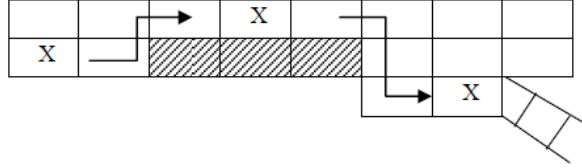


**Figure 8. Lane Changing Illustration.**

Once the lane changing criteria were met, the vehicle's location was changed from its current lane to the target one. Lane changing behavior was updated sequentially, from downstream to upstream, consistent with the fact that the following vehicle would make a lane change decision considering its leading vehicle's behavior. The updating sequence indirectly incorporated the interaction between leading and following vehicles.

- *Step 3: Deceleration.* If the desired speed of vehicle  $n$  exceeded the forward gap, the vehicle would reduce its speed to the gap / 1 second. The rule was expressed as:

$$\text{If } d_n(t) < v_n(t), \text{ then } v_n(t) \rightarrow d_n(t) / 1 \text{ sec.}$$

- *Step 4: Randomization.* This step decreased a vehicle's speed by 1 cell/sec with a certain probability considering possible oscillations on the freeway. The rule was expressed as:

$$v_n(t) \rightarrow \max(v_n(t) - 1, 0)$$

Six probabilities were defined in this study considering the different probabilities in several conditions, which were:

1.  $P_0$ : if the speed of vehicle  $n$  at time  $t-1$  was zero and its forward gap at time  $t$  was 1.
2.  $P_{00}$ : if the speed of vehicle  $n$  at time  $t-1$  was zero and its forward gap at time  $t$  was greater than 1.
3.  $P_{onramp}$ : if the vehicle was in an on-ramp influence zone.
4.  $P_{offramp}$ : if the exiting vehicle was in an off-ramp influence zone.
5.  $P_{following}$ : if the brake lights of the leading vehicle were on.
6.  $P$ : in all other circumstances.

$P_0$  and  $P_{00}$  were used to mimic the "slow-to-start" behavior caused by the reaction time taken to restart stopped vehicles. The adoption of  $P_{00}$  avoided excessive reaction time since if the vehicles had taken "slow-to-start" rules in the last time step, the vehicle should move forward in the current time despite the possibility that some drivers took more time to start their vehicles. Thus, the value of  $P_0$  should be high and  $P_{00}$  was small.

$P_{onramp}$  and  $P_{offramp}$  reflected the possible oscillation in ramp influence areas that were defined according to the *Highway Capacity Manual* (Transportation Research Board, 2000). In the study, specific values were assigned to four bottlenecks in the morning congestion, which were presented as  $P_{offramp} - B1$ ,  $P_{offramp} - B2$ ,  $P_{onramp} - B3$  and  $P_{onramp} - B4$ . The rest of the on-ramps and off-ramps used uniform  $P_{onramp}$  and  $P_{offramp}$  values.

$P_{following}$  accounted for the effect of brake lights of leading vehicles. If the front vehicle within the distance of  $d_{following}$  had brake lights on, the following vehicle was more likely to reduce its speed to avoid stopping abruptly. The parameter  $d_{following}$  was the threshold distance in which the brake lights of the leading vehicle affected the following vehicles. If the vehicles were under both effects of  $P_{onramp}$  and  $P_{following}$  or  $P_{offramp}$  and  $P_{following}$ , the higher one was selected. The brake lights would turn on if (1) the vehicle was stopped or (2) the speed in the current time step was less than that in the previous time step.

$P$  was applied to all other normal conditions where vehicles were driven on a uniform section with no ramps and lane reductions.

- *Step 5: Car motion.* The vehicles advanced with their speed obtained from the previous steps. If a vehicle left the system, it was deleted from the network.

After one loop of updating existing vehicles in the system at one time step, new vehicles were injected with probability determined by the volume as described in the “initializing the system” section.

## CA Incident Models

When an incident happens, some or all lanes are blocked, leading to frequent lane changing and vehicle rerouting. Vehicles on the blocked lane change to an unblocked lane to pass through the bottleneck or they could leave the freeway from the nearest off-ramps instead of their intended ones to avoid the bottleneck. Moreover, input flows from the upstream on-ramps nearest the bottleneck would decrease.

In the incident influence zone, defined as sections upstream of the incident location, only vehicles in the blocked lane were allowed to change to an unblocked lane and the reverse situation was not permitted. The lane change behavior was conducted with probability  $P_{change,lan}$  given that it would bring about  $b$  cells/sec speed reduction of the following vehicle in the target lane. The criterion was expressed as:

$$d_{n,back}(t) \geq v_{back,other}(t-1) - b$$

This lane changing behavior without considering the speed reduction of the given vehicle itself was less restricted when compared to those near ramps since changing lanes instead of speeding was a higher priority for drivers blocked near bottlenecks. The probability used here was the mandatory lane changing probability.

Vehicle rerouting rates were the other concern. The rerouting decisions made by drivers were assumed to be mainly determined by their judgments on capacity reduction at the bottleneck, which affected their speeds approaching and passing through the bottleneck. In this model, the rerouting choice was represented by a probability that was determined by the number of lanes blocked.  $P_{rerouting\_all}$  and  $P_{rerouting\_part}$  denoted the rerouting probabilities when all lanes and only some lanes were blocked, respectively. The parameter  $P_{rerouting\_all}$  was close to 1.0 or equal to 1.0. Meanwhile, probabilities  $P_{re\_onramp\_all}$  and  $P_{re\_onramp\_part}$  were set to represent the possible flow reduction from the nearest onramps when all or some of the lanes were closed, respectively.

### Parameter Calibration and Model Application

For the purposes of this study, a MAPE value of 20% or less was considered acceptable based on the average MAPE value calculated for nine stations on 30 days between 5:00 a.m. and 11:00 a.m. with a resolution of 5 minutes shown in Table 5. In the calculation, the detector data represented the observed volumes and the representative flow corresponding to the OD matrix was the simulated volume. The chosen threshold accounted for normal flow fluctuations.

**Table 5. Average MAPE Value Comparing 30 Days of Detector Data and the Representative Flow.**

Station	61	111	141	161	191	231	261	291	351	Average
MAPE	17.30%	16.73%	16.16%	16.36%	19.50%	14.19%	16.76%	16.41%	15.50%	16.55%

Simulation models need to reproduce recurring congestion as well as capture incident effects. Parameter calibration was based on MAPE and GEH statistics and comparison of speed contour plots between field data and simulation results. Congestion and incidents were identified by marking cells with average speed less than 45 mph in speed contour plots. Parameters of incident-free conditions were calibrated first followed by calibration of incident related parameters. Before calibration, the effects of changing individual parameters were examined.

### Identifying Recurring Congestion Bottlenecks

Recurring congestion emerged on the study area every weekday during the morning peak period. Figure 9 shows a sample congestion pattern where average vehicle speed dropped below 45 mph from 5:40 a.m. to 10:35 a.m. throughout the whole test site. From this and other similar contour plots, four distinct bottlenecks were identified, which were (listed from downstream to upstream):

- Bottleneck 1: upstream of Station 361 (near I-495 southbound off-ramp)
- Bottleneck 2: upstream of Station 581 (near SR243 off-ramp)
- Bottleneck 3: upstream of Station 231 (near US50 on-ramp)
- Bottleneck 4: upstream of Station 131 (near SR28 on-ramp)

Bottleneck 3 experienced the earliest congestion on weekdays at about 6:00 a.m. and ended at about 9:00 a.m. Congestion in bottleneck 4 started at about 6:30 a.m. and ended at 9:00 a.m. Congestion in bottleneck 1 began at 7:00 a.m. and ended at about 10:30 a.m. Congestion in bottleneck 2 started at 7:30 and ended at about 9:35. The start and end time of congestion at each

bottleneck was not exactly the same from day to day but the time oscillation was normally within one-half hour, depending on the severity of the congestion. Queues spilling back on the mainline can clearly be seen in the figure, where the long stretch of the queue indicated the heavy congestion on I-66 eastbound in the morning peak.

Station	49(41)	49(5(5))	50(61)	52(2(10))	52(2(11))	53(2(12))	53(4(11))	54(5(15))	55(5(72))	55(4(16))	56(3(9))	57(5(21))	58(3(6))	58(2(21))	58(2(23))	59(2(24))	60(2(6))	60(2(27))	60(2(28))	61(5(58))	61(5(23))	62(1(3))	62(4(33))	62(3(24))	62(4(25))	63(3(36))	64(3(27))			
5.45	61	62	63	63	60	59	59	46	43	51	61	62	55	64	60	52	45	66	56	57	63	57	62	58	62	61	53	46		
5.50	62	62	64	58	57	51	50	32	41	50	61	61	52	61	56	55	54	61	59	60	63	60	58	61	58	56	53	50		
5.55	61	61	62	60	44	33	35	35	54	55	62	61	44	61	57	44	42	48	54	50	61	58	57	61	60	63	63	55	48	
6.00	60	61	62	28	20	21	54	54	61	60	63	63	52	61	54	31	37	48	56	57	59	51	52	56	61	53	53	54	50	
6.05	51	42	31	22	26	41	54	53	59	58	62	62	55	63	51	28	41	55	55	57	60	56	56	59	62	42	46	40	47	
6.10	25	19	18	51	46	39	52	45	56	56	59	58	53	59	35	24	35	52	56	58	60	55	54	60	54	46	48	36	48	
6.15	22	25	30	61	57	44	53	49	54	53	59	48	54	46	24	21	41	56	58	59	60	58	58	63	59	47	50	45	50	
6.20	37	38	53	56	54	56	55	47	56	56	44	20	53	43	22	20	40	55	57	58	60	54	57	63	59	62	57	47	52	
6.25	53	55	59	60	46	37	54	50	59	55	24	19	53	37	26	23	49	54	58	59	62	56	58	64	59	60	57	55	49	
6.30	60	63	64	60	24	35	53	48	54	43	32	26	50	39	24	19	40	53	58	58	60	57	57	64	59	62	60	54	53	
6.35	59	62	64	63	33	38	55	48	51	45	45	48	27	49	26	17	19	39	51	57	58	59	56	58	64	59	62	61	39	49
6.40	57	60	61	63	43	41	51	37	48	45	54	32	25	27	18	18	37	54	55	56	54	55	53	61	58	59	43	26	54	
6.45	55	59	60	60	43	34	40	49	42	58	47	19	26	18	19	38	53	57	57	53	58	64	59	49	49	26	22	57	47	
6.50	59	59	61	51	31	33	48	35	37	45	57	32	16	28	22	18	36	52	56	58	58	51	57	64	58	48	19	20	53	
6.55	58	61	62	38	34	28	27	35	35	42	54	25	13	29	18	17	36	49	56	57	57	45	55	64	58	15	19	23	54	
7.00	58	61	61	44	14	16	45	27	35	40	52	16	23	28	19	17	36	53	58	58	57	39	54	64	56	10	24	17	62	
7.05	55	58	60	28	7	10	53	50	53	46	50	20	15	32	15	17	39	52	56	56	50	34	55	64	50	11	19	20	49	
7.10	52	52	34	17	7	12	52	51	56	56	56	17	9	36	28	16	37	51	55	54	54	31	53	63	59	13	22	19	55	
7.15	36	19	20	18	9	12	52	53	59	58	46	7	20	34	19	17	38	52	53	33	26	30	50	61	39	14	18	22	49	
7.20	23	21	21	17	13	21	49	46	56	54	27	15	22	33	18	16	36	51	35	21	22	31	50	63	41	10	16	15	53	
7.25	20	21	25	27	32	26	46	45	44	42	33	19	19	29	20	17	36	47	27	20	35	29	51	61	33	11	15	15	46	
7.30	23	21	22	45	33	34	44	30	35	41	28	14	17	30	24	16	31	38	25	16	31	26	50	60	20	9	18	15	56	
7.35	26	29	31	55	44	35	23	26	35	40	26	13	19	28	13	15	33	48	29	15	22	26	47	52	14	7	16	15	52	
7.40	36	37	39	59	50	33	19	23	38	39	33	15	16	30	14	17	35	41	18	16	24	25	48	40	9	11	17	14	54	
7.45	46	36	30	58	33	28	25	28	34	42	36	15	19	30	15	14	31	36	17	10	27	27	50	34	9	7	19	17	48	
7.50	43	39	39	58	18	30	24	29	36	41	40	15	16	24	13	15	24	37	20	13	25	25	54	31	10	9	21	19	55	
7.55	44	36	52	52	22	34	28	28	31	39	49	14	12	27	9	16	38	39	17	13	23	29	48	27	11	10	31	18	54	
8.00	55	59	57	41	27	30	23	24	33	42	58	18	15	27	12	16	32	33	19	14	26	23	48	37	15	12	20	13	54	
8.05	55	61	63	38	15	32	25	32	39	43	56	19	18	29	12	15	31	36	13	11	23	28	49	50	13	7	16	13	53	
8.10	54	59	52	38	28	39	32	29	45	48	50	16	19	28	13	15	37	33	13	14	25	26	51	51	11	6	14	12	50	
8.15	53	45	31	50	45	45	28	31	43	46	58	26	14	27	17	15	27	26	12	13	26	50	52	12	6	14	14	13	52	
8.20	32	35	55	46	41	41	33	33	37	43	59	21	18	21	15	16	26	24	14	10	26	21	52	52	10	7	14	12	48	
8.25	53	56	60	46	48	41	33	27	35	41	59	35	15	27	12	16	28	25	11	11	21	23	49	56	11	6	16	11	47	
8.30	54	60	62	45	39	37	32	28	36	44	58	36	17	31	16	14	17	23	15	13	25	24	50	49	10	6	16	15	47	
8.35	57	61	62	44	38	24	29	37	41	59	29	23	23	22	13	13	29	26	15	16	25	23	45	43	9	7	14	14	47	
8.40	58	59	48	44	38	35	32	30	35	42	60	37	17	26	10	13	20	31	19	17	24	26	50	39	11	7	16	14	53	
8.45	45	37	37	53	44	33	30	29	36	41	60	51	22	23	10	18	34	39	16	18	27	49	44	11	6	15	13	53	53	
8.50	33	31	41	53	50	38	26	27	37	40	59	45	25	31	16	18	34	39	16	17	31	25	47	45	8	5	16	14	52	
8.55	51	38	36	61	43	31	22	25	37	45	58	53	25	28	22	19	32	37	14	15	32	25	52	45	11	5	14	12	50	
9.00	40	44	54	56	32	27	25	34	43	44	59	50	29	31	15	20	29	33	18	18	31	25	47	40	8	5	17	13	50	
9.05	56	58	60	38	25	31	31	40	42	57	55	25	27	18	21	39	47	17	19	40	30	48	37	11	4	21	18	51	50	
9.10	58	61	55	46	11	41	45	29	43	44	59	58	24	30	21	23	34	36	20	22	49	35	48	31	12	12	23	16	46	
9.15	51	49	48	34	22	43	31	49	32	39	40	58	29	32	22	22	26	40	25	24	48	33	47	31	12	11	21	16	49	
9.20	62	61	64	60	38	24	29	36	47	59	29	32	24	9	7	17	18	44	58	50	41	42	62	63	14	14	17	14	47	
9.25	64	65	67	62	42	43	33	35	43	48	60	60	25	19	8	14	19	47	62	62	62	56	52	29	19	13	21	17	49	
9.30	64	66	66	68	61	47	46	29	37	45	60	60	20	20	11	10	15	44	62	63	65	63	62	52	13	12	21	22	50	
9.35	64	64	65	67	61	61	54	46	44	42	59	59	13	25	10	16	16	46	63	64	65	63	63	65	35	18	31	22	50	
9.40	65	64	65	68	63	61	53	54	47	50	64	12	25	8	13	14	45	62	62	65	62	63	64	65	33	29	24	47	47	
9.45	65	66	67	68	63	63	63	62	57	63	60	50	25	20	25	7	9	12	44	62	63	64	62	63	66	61	62	43	23	50
9.50	65	65	65	69	65	64	63	59	63	60	62	36	14	22	12	7	12	46	62	64	66	64	63	66	60	63	65	47	44	
9.55	67	67	67	69	65	63	62	60	64	63	66	43	15	23	9	5	7	40	65	66	68	67	64	65	62	64	66	62	46	
10.00	65	66	65	68	65	64	63	59	63	62	67	47	13	21	7	4	6	42	68	67	69	67	65	68	62	63	67	65	61	
10.05	65	66	66	69	65	65	63	60	65	61	66	55	10	17	12	9	8	44	68	70	71	66	66	69	63	65	66	62	54	
10.10	67	66	66	70	64	64	63	60	65	64	68	51	5	18	10	17	14	45	65	69	66	63	66	66	60	65	65	63	51	
10.15	66	67	66	70	65	65	63	58	63	62	60	14	6	20	10	17	21	46	62	65	67	64	62							

mainline and ramp. This exit connected travelers to the western most Metro station for the orange line.

- *Bottleneck 3*: This bottleneck was upstream of the US50 on-ramp, indicating that the congestion was caused by the high volume from on-ramps and merging behavior. The mainline flow was about 500 veh/5 min in morning rush hour and the flow from on-ramps reached over 200 veh/5 min.
- *Bottleneck 4*: This bottleneck was upstream of the SR28 on-ramp and the cause was the same with bottleneck 3. The mainline flow was about 450 veh/5 min in morning rush hour and the flow from onramps reached 150 veh/5 min.

Speed adjusting by the drivers when perceiving high flow on the mainline and ramps was an indirect reason leading to congestion. High volumes on the road or from ramps increased the likelihood of speed reduction and oscillation near the ramp sections since drivers usually slowed down for the sake of cautiousness. The speed oscillation zone was known as the influence area, defined in the *Highway Capacity Manual* (Transportation Research Board, 2000). Identification of the influence zone and recurring congestion area guided later model development.

### Parameter Examination

Fifteen parameters needed to be calibrated for the model. The range of each parameter and its effects on reproducing the recurring bottlenecks are discussed below. The parameter values that were treated as constants while the sensitivity to a particular parameter was tested are presented in Table 6.

**Table 6. Constants for Parameter Sensitivity Analysis.**

Parameter	Value	Parameter	Value
$P_0$	0.8	$P_{offramp}$	0.1
$P_{00}$	0.1	$P_{offramp - B1}$	0.3
$P$	0.1	$P_{offramp - B2}$	0.3
$P_{following}$	0.4	$P_{onramp}$	0
$d_{following}$	8	$P_{onramp - B3}$	0.1
$k$	2	$P_{onramp - B4}$	0.25
$b$	1	$P_{change,man}$	0.9
		$P_{change,dis}$	0.5

#### *Slow-to-Start Parameters*

Two parameters  $P_0$  and  $P_{00}$ , used to mimic the slow to start driving behavior, affected the driver's reaction time to start his vehicle from stopped. The ranges for  $P_0$  and  $P_{00}$  were [0.6, 0.8] and [0.1, 0.2], respectively. Figure 10 presented the speed contour plots for the range of  $P_0$

and Table 7 presented the GEH and MAPE statistics calculated against the representative flows used in the OD matrix. Figure 11 and Table 8 presented the corresponding results for  $P_{00}$ .

Judging from Figure 10,  $P_0$  affected the congestion levels. Higher values of this parameter caused greater amounts of congestion, as reflected in speed reductions. However, the effect on flow was relatively minimal since the MAPE and GEH statistics were all within the established thresholds.

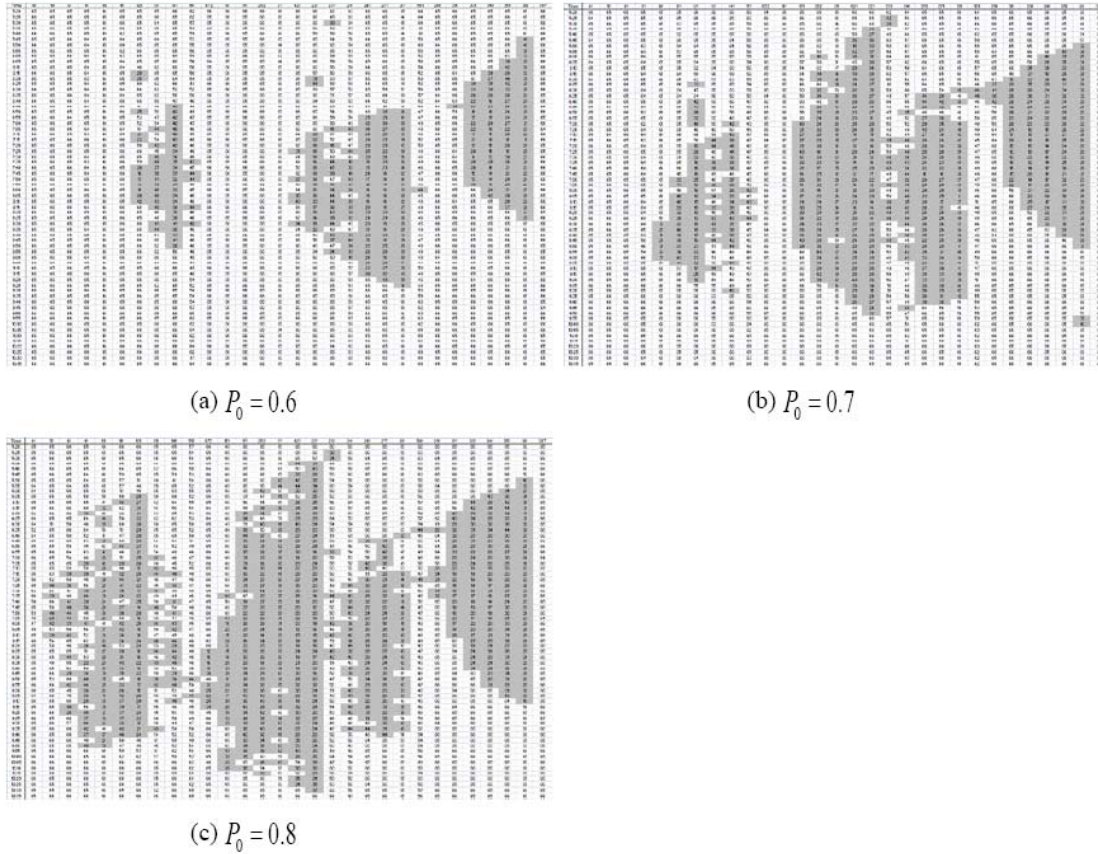
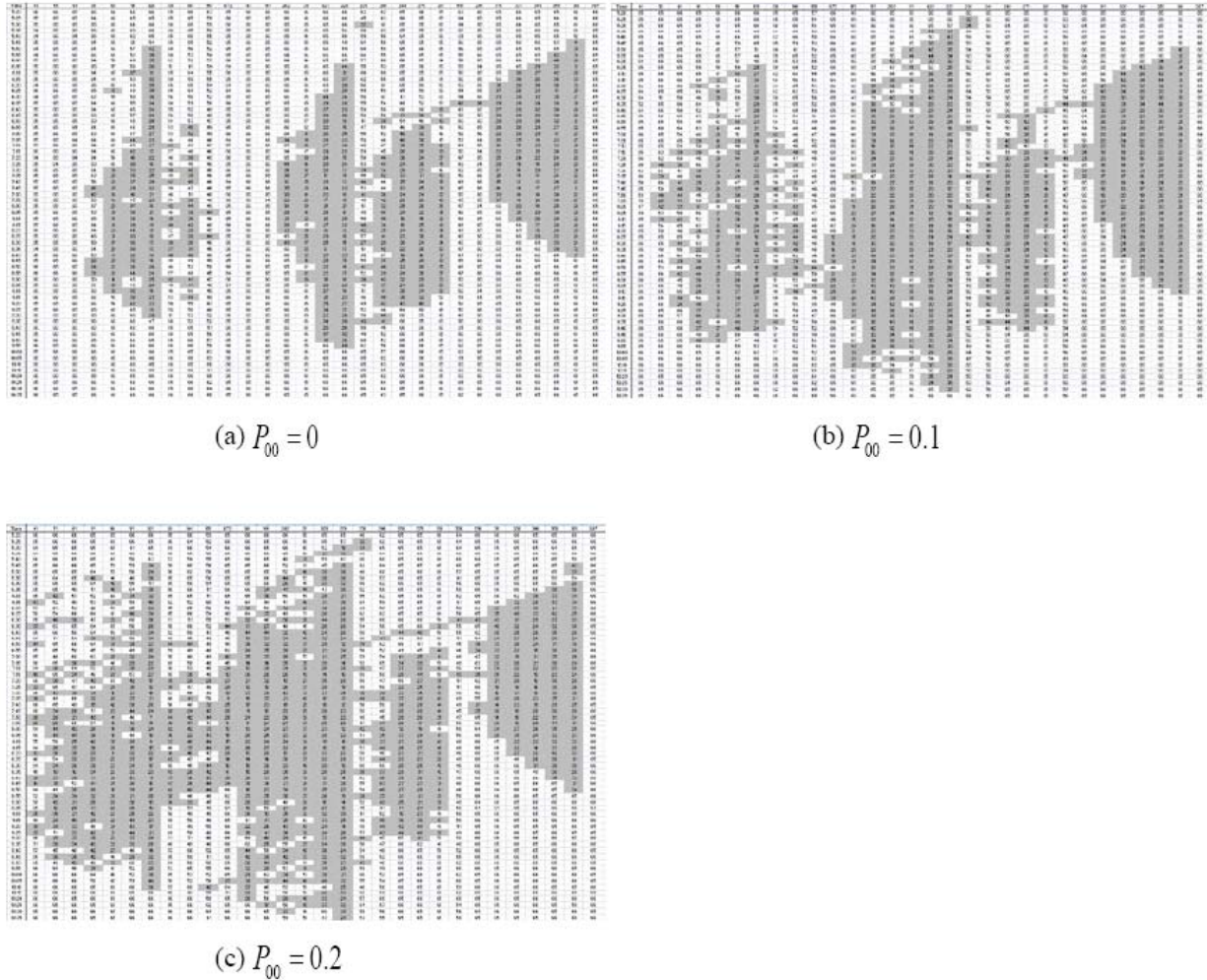


Figure 10. Speed Contour Plots of Morning Congestion for  $P_0$ .

Table 7. MAPE and GEH Analysis on Morning Congestion with Different  $P_0$ .

	Station ID								
	61*	111	141	161	191	231	261	291	351
$P_0 = 0.6$	61*	111	141	161	191	231	261	291	351
MAPE	5.0%	5.1%	5.6%	6.2%	5.6%	6.8%	8.8%	8.2%	8.2%
GEH%	100.0%	100.0%	100.0%	100.0%	100.0%	96.0%	96.0%	98.7%	98.7%
$P_0 = 0.7$	61	111	141	161	191	231	261	291	351
MAPE	5.1%	6.4%	6.7%	7.5%	8.5%	8.7%	9.7%	10.4%	9.4%
GEH%	100.0%	98.7%	100.0%	100.0%	96.0%	93.3%	93.3%	94.7%	97.3%
$P_0 = 0.8$	61	111	141	161	191	231	261	291	351
MAPE	7.5%	8.6%	8.3%	11.1%	11.3%	10.7%	11.8%	10.6%	10.1%
GEH	98.7%	96.0%	96.0%	94.7%	96.0%	86.7%	90.7%	94.7%	100.0%

\*Stations 61, 111 and 141 were located with the influence of bottleneck 4 and Stations 161, 191 and 231 reflect the bottleneck 3. Stations 261 and 291 were affected by bottleneck 2 and Station 351 represents the bottleneck 1.



**Figure 11. Speed Contour Plots of Morning Congestion for  $P_{00}$ .**

As seen from Figure 11, even when  $P_{00}$  took the value 0, four bottlenecks were identifiable. Higher values of this parameter caused greater congestion and average speed reductions, which confirmed intuition given the definition of this parameter. The effects on flow were also important, as shown in Table 8. At the highest value considered, the GEH statistics exceeded the acceptable threshold at five out of nine stations; however, the MAPE threshold was not exceeded.

$P_0$  and  $P_{00}$  affected the congestion duration and queue length. Bottleneck 3 (second from the left) and bottleneck 4 (leftmost) were more sensitive to these two parameters. The queue spillback distance extended to two more stations in Bottleneck 4 when  $P_0$  increased from 0.6 to 0.7. Bottleneck 3 almost disappeared when  $P_0 = 0.6$  was applied. However, the difference between  $P_0 = 0.7$  and  $P_0 = 0.8$  was not as dramatic but the increase in congestion still could be observed such as in bottleneck 3 and bottleneck 4. Bottleneck 3 was also more sensitive to  $P_{00}$  than other bottlenecks.

**Table 8. MAPE and GEH Analysis on Morning Congestion with Different  $P_{00}$ .**

	Station ID								
	61	111	141	161	191	231	261	291	351
$P_{00} = 0$	61	111	141	161	191	231	261	291	351
MAPE	4.8%	6.8%	6.3%	7.3%	6.8%	7.8%	8.6%	8.9%	7.8%
GEH%	100.0%	100.0%	100.0%	100.0%	100.0%	94.7%	94.7%	100.0%	98.7%
$P_{00} = 0.1$	61	111	141	161	191	231	261	291	351
MAPE	7.5%	8.6%	8.3%	11.1%	11.3%	10.7%	11.8%	10.6%	10.1%
GEH	98.7%	96.0%	96.0%	94.7%	96.0%	86.7%	90.7%	94.7%	100.0%
$P_{00} = 0.2$	61	111	141	161	191	231	261	291	351
MAPE	11.8%	13.9%	11.5%	14.3%	14.1%	12.1%	13.3%	11.5%	10.6%
GEH%	84.0%	73.3%	88.0%	86.7%	82.7%	84.0%	88.0%	97.3%	93.3%

### Following Parameters

Parameters  $P_{following}$  and  $d_{following}$  reflected driver cautiousness when approaching leading vehicles; with smaller values, the vehicles were considered more aggressive. The range of  $P_{following}$  was [0-0.7]. Three second rules were used to determine the safety following distance, which was considered the following influence distance, where a vehicle would have a relatively high probability of reducing its speed when the leading vehicle braked. Therefore,  $d_{following}$  was set to range from 6 cells (150 ft) to 12 cells (300 ft), corresponding to the safety distance when the current vehicle's speed was 2 cells/sec to 4 cells/sec. In this study, uniform values were used for all vehicles. Figures 12 and 13 present the speed contours and Tables 9 and 10 present the MAPE and GEH statistics for these parameters.

Examining Figure 12, one can see that higher values of  $P_{following}$  led to greater congestion, as indicated by drops in speed. In particular, Bottleneck 3 was sensitive to  $P_{following}$ ; at lower values of this parameter, the bottleneck showed speed oscillation around the threshold of 45 mph, but at higher values, the congestion was fairly continuous. The duration of congestion at Bottleneck 3 increased severely, indicating this parameter not only affected the queue propagation speed but also queue dissipation duration. Therefore,  $P_{following}$  was recommended to take a moderate value between 0.4 and 0.6, making a trade-off between queue propagation speed and congestion duration. The effects on flow, as shown in Table 9, were less severe. All of the MAPE values remained within the acceptable thresholds while two of the nine stations exceeded the GEH threshold at the highest value of  $P_{following}$ .

The parameter  $d_{following}$  had slight impacts on the four bottlenecks, as shown in Figure 13. It did not have a uniform effect on the four bottlenecks since the congestion in Bottlenecks 3 and 4 were aggravated while those in Bottleneck 1 and 2 were mitigated. The effects on flow were also fairly minimal since all of the MAPE and GEH statistics, shown in Table 10, were within the acceptable thresholds.

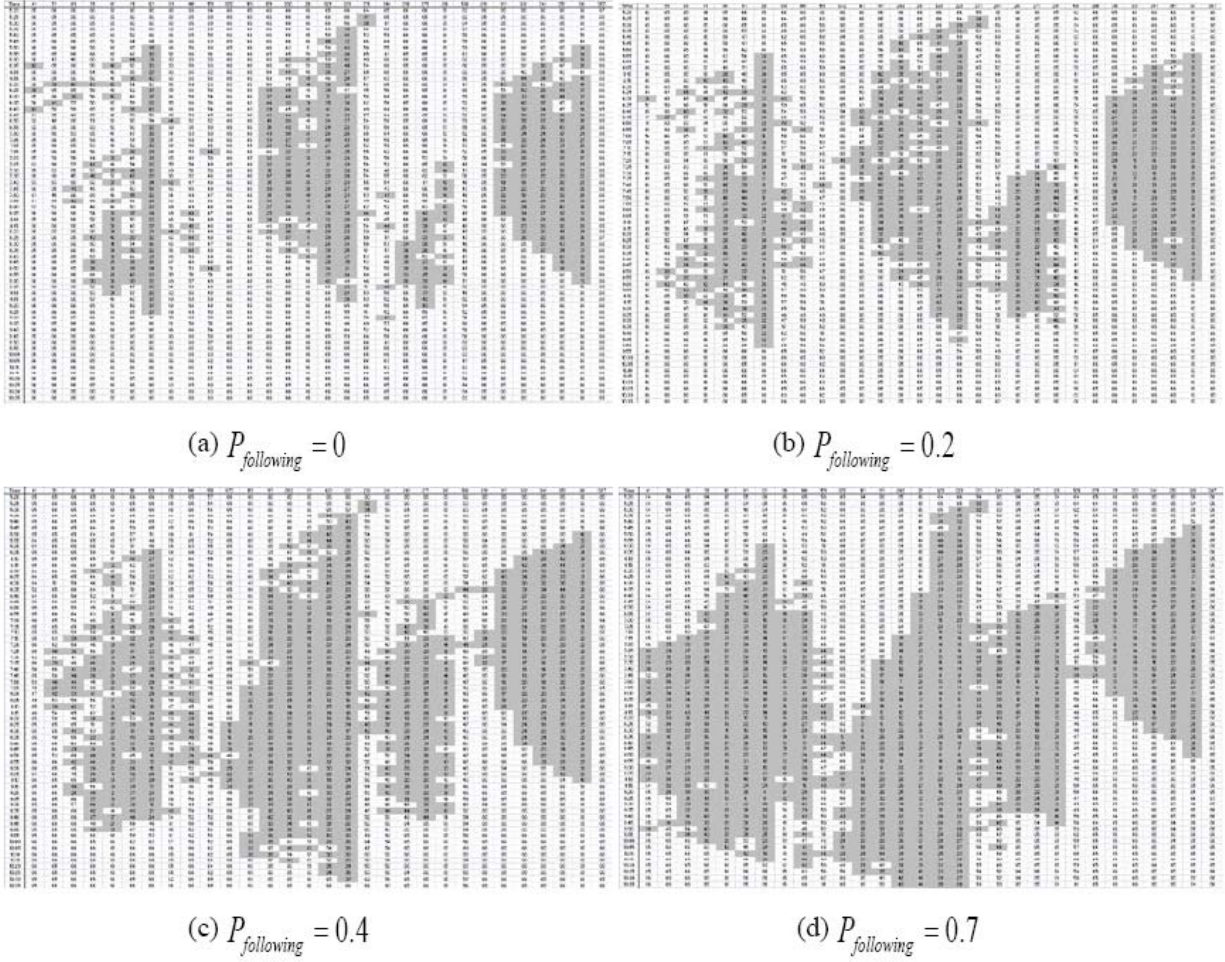


Figure 12. Speed Contour Plots of Morning Congestion for  $P_{following}$  .

Table 9. MAPE and GEH Analysis on Morning Congestion with Different  $P_{following}$  .

	Station ID								
	61	111	141	161	191	231	261	291	351
$P_{following} = 0$									
MAPE	6.2%	7.8%	6.8%	7.8%	8.3%	8.1%	8.9%	8.7%	9.0%
GEH%	97.3%	93.3%	100.0%	100.0%	98.7%	93.3%	97.3%	97.3%	97.3%
$P_{following} = 0.2$									
MAPE	7.3%	8.6%	7.7%	9.2%	10.9%	8.7%	9.8%	9.4%	9.2%
GEH%	93.3%	94.7%	98.7%	97.3%	93.3%	90.7%	97.3%	97.3%	94.7%
$P_{following} = 0.4$									
MAPE	7.5%	8.6%	8.3%	11.1%	11.3%	10.7%	11.8%	10.6%	10.1%
GEH	98.7%	96.0%	96.0%	94.7%	96.0%	86.7%	90.7%	94.7%	100.0%
$P_{following} = 0.7$									
MAPE	10.7%	13.2%	11.3%	13.9%	13.9%	13.0%	13.9%	12.1%	10.1%
GEH%	89.3%	88.0%	92.0%	92.0%	88.0%	82.7%	84.0%	97.3%	97.3%

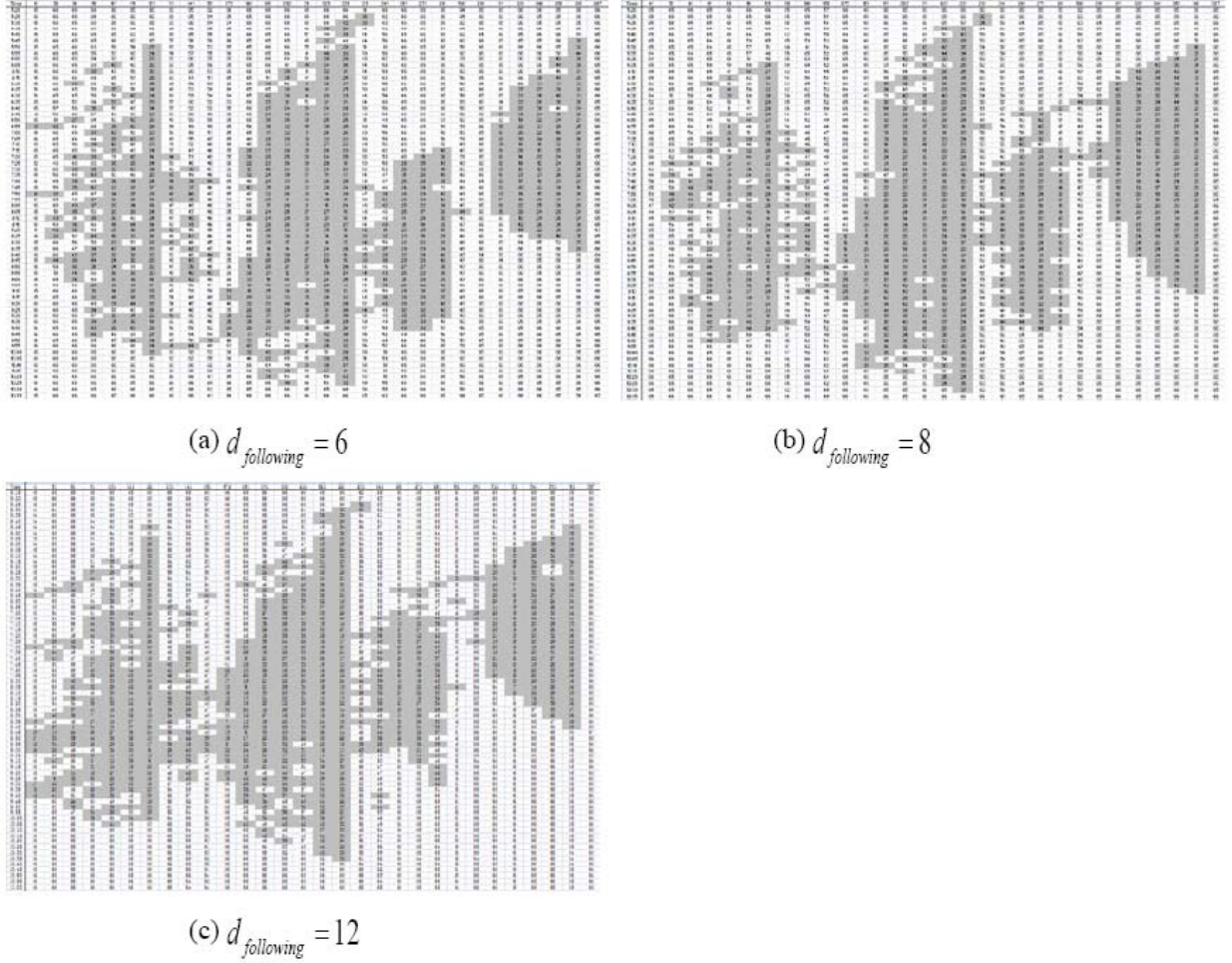


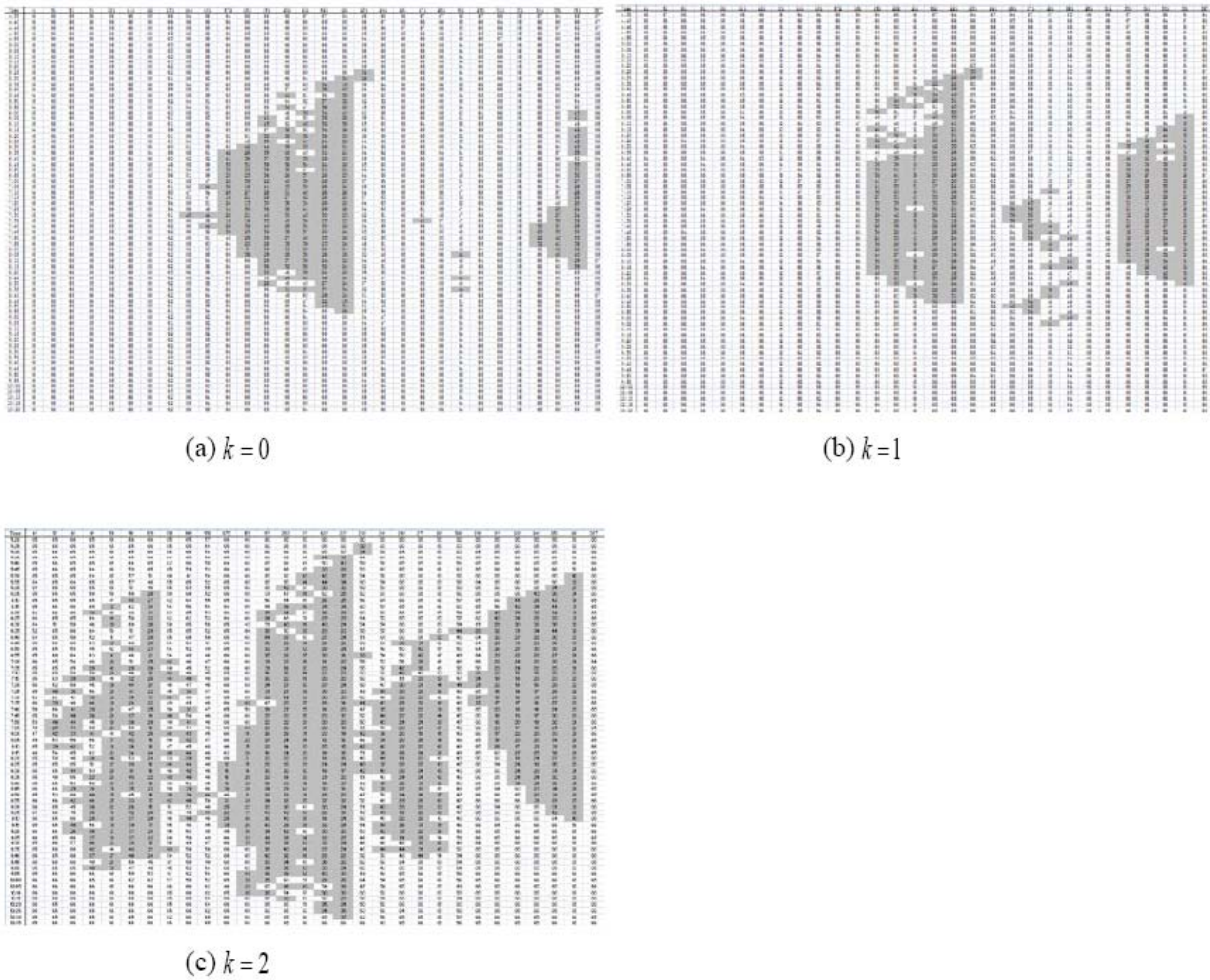
Figure 13. Speed Contour Plots of Morning Congestion for  $d_{following}$  .

Table 10. MAPE and GEH Analysis on Morning Congestion with Different  $d_{following}$  .

	Station ID								
	61	111	141	161	191	231	261	291	351
$d_{following} = 6$									
MAPE	7.8%	8.7%	7.5%	10.4%	11.6%	10.5%	11.5%	10.7%	9.5%
GEH%	93.3%	93.3%	98.7%	96.0%	90.7%	90.7%	94.7%	98.7%	97.3%
$d_{following} = 8$									
MAPE	7.5%	8.6%	8.3%	11.1%	11.3%	10.7%	11.8%	10.6%	10.1%
GEH	98.7%	96.0%	96.0%	94.7%	96.0%	86.7%	90.7%	94.7%	100.0%
$d_{following} = 12$									
MAPE	10.7%	11.0%	10.1%	12.9%	13.1%	11.6%	12.6%	11.4%	9.4%
GEH%	86.7%	85.3%	92.0%	86.7%	88.0%	86.7%	90.7%	97.3%	98.7%

### Lane Changing Aggressiveness Parameters

The parameters  $k$  and  $b$  defined the aggressiveness of mandatory lane changing behavior. The first parameter represented the personal desire for lane changing while the second indicated the tolerance of the following vehicle in the target lane. The parameters also affected the location of lane changes. For example, merging vehicles from an on-ramp changed to the mainline at the beginning of the acceleration lane with higher values of the parameters and closer to the end of the acceleration lane when the values were small. These vehicles might even be blocked until a proper gap emerges. The values of  $k$  and  $b$  considered were 0, 1, and 2. Figure 14, Figure 15, Table 11, and Table 12 present the results for these parameters.

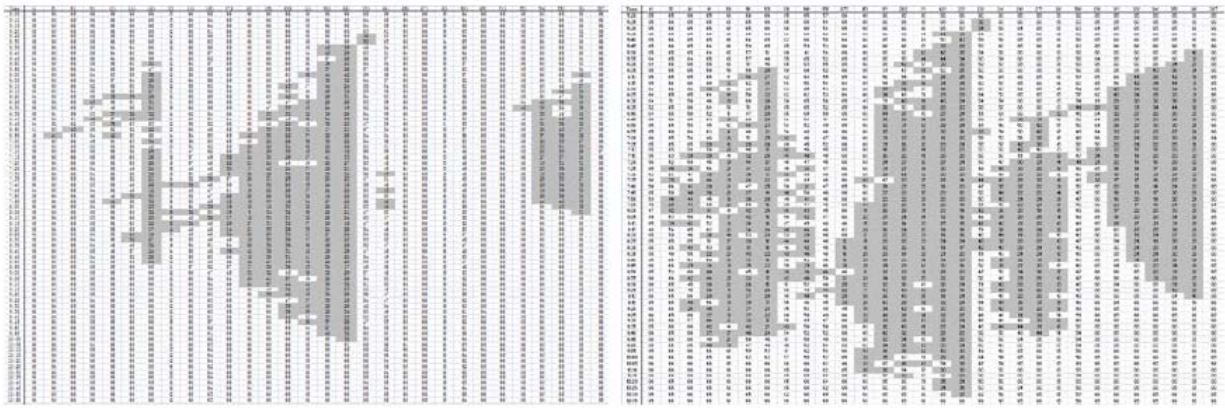


**Figure 14. Speed Contour Plots of Morning Congestion for  $k$ .**

As can be seen from Figure 14, the formation of bottlenecks heavily depended on the value of  $k$ . A higher value led to greater lane changing frequency and affected the mainline speed. The parameters also affected the location of lane changes. The effects on MAPE and GEH were fairly minimal for the range considered since no station exceeded the thresholds.

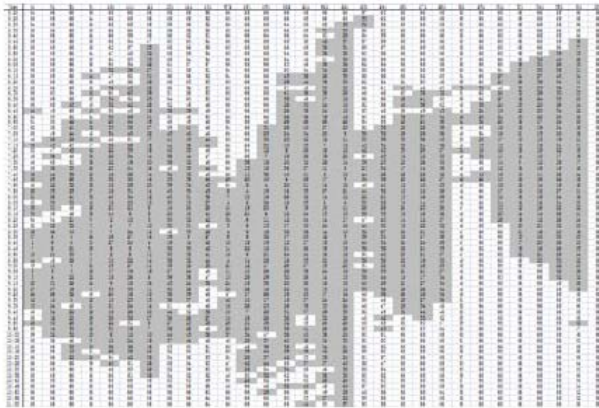
**Table 11. MAPE and GEH Analysis on Morning Congestion with Different  $k$ .**

	Station ID								
$k = 0$	61	111	141	161	191	231	261	291	351
MAPE	5.3%	4.9%	5.4%	7.9%	7.4%	7.9%	8.9%	7.8%	7.5%
GEH%	100.0%	100.0%	100.0%	98.7%	96.0%	94.7%	96.0%	97.3%	98.7%
$k = 1$	61	111	141	161	191	231	261	291	351
MAPE	5.3%	4.7%	4.8%	6.2%	6.5%	7.3%	8.3%	7.6%	9.2%
GEH%	100.0%	100.0%	100.0%	100.0%	97.3%	96.0%	97.3%	97.3%	97.3%
$k = 2$	61	111	141	161	191	231	261	291	351
MAPE	7.5%	8.6%	8.3%	11.1%	11.3%	10.7%	11.8%	10.6%	10.1%
GEH	98.7%	96.0%	96.0%	94.7%	96.0%	86.7%	90.7%	94.7%	100.0%



(a)  $b=0$

(b)  $b=1$



(c)  $b=2$

**Figure 15. Speed Contour Plots of Morning Congestion for  $b$ .**

Figure 15 showed that congestion at the bottlenecks, heavily depended on  $b$ ; higher values led to more congestion. The GEH statistics, shown in Table 12, exceeded the acceptable thresholds for  $b = 2$  and the MAPE values approached their threshold.

Based on these results, the recommended values of  $k$  and  $b$  were 2 and 1, respectively.

**Table 12. MAPE and GEH Analysis on Morning Congestion with Different  $b$ .**

	Station ID								
$b = 0$	<b>61</b>	<b>111</b>	<b>141</b>	<b>161</b>	<b>191</b>	<b>231</b>	<b>261</b>	<b>291</b>	<b>351</b>
MAPE	5.2%	6.6%	5.7%	8.7%	9.4%	9.1%	9.4%	7.9%	7.6%
GEH	98.6%	97.3%	100.0%	97.3%	98.6%	97.3%	95.9%	98.6%	100.0%
$b = 1$	<b>61</b>	<b>111</b>	<b>141</b>	<b>161</b>	<b>191</b>	<b>231</b>	<b>261</b>	<b>291</b>	<b>351</b>
MAPE	7.5%	8.6%	8.3%	11.1%	11.3%	10.7%	11.8%	10.6%	10.1%
GEH	98.7%	96.0%	96.0%	94.7%	96.0%	86.7%	90.7%	94.7%	100.0%
$b = 2$	<b>61</b>	<b>111</b>	<b>141</b>	<b>161</b>	<b>191</b>	<b>231</b>	<b>261</b>	<b>291</b>	<b>351</b>
MAPE	17.1%	18.9%	16.4%	19.1%	17.8%	15.3%	15.8%	14.4%	11.9%
GEH%	77.3%	64.0%	78.7%	73.3%	74.7%	76.0%	80.0%	93.3%	92.0%

*Lane Changing Probability Parameters*

Increasing the lane changing probability would smooth the flow and alleviate the freeway congestion. The  $P_{change\_dis}$  value affected the queue propagation speed and queue length under congested conditions. Lower values of the discretionary lane changing probability led to the reduction of flow and average speed, while a higher value removed the congestion that was supposed to occur. Therefore, the value of  $P_{change\_dis}$  ranged from [0.4, 0.6]. The mandatory lane changing probability was higher than the discretionary one and close to 1. Increasing the  $P_{change\_man}$  enhanced the efficiency of merging, diverging and diverting behavior. This parameter was examined in the range [0.3, 0.9]. Table 13, Table 14, Figure 16, and Figure 17 present the results for these two parameters.

The congestion was mitigated with the increase of  $P_{change\_dis}$  especially at Bottleneck 3. The higher values did not cause enough congestion based on the speed contour plots. For the range of values considered, the MAPE and GEH statistics were all within acceptable thresholds.

**Table 13. MAPE and GEH analysis on Morning Congestion with Different  $P_{change\_dis}$ .**

	Station ID								
$P_{change\_dis} = 0.3$	<b>61</b>	<b>111</b>	<b>141</b>	<b>161</b>	<b>191</b>	<b>231</b>	<b>261</b>	<b>291</b>	<b>351</b>
MAPE	8.5%	10.3%	9.2%	11.9%	12.4%	11.8%	13.5%	11.9%	9.1%
GEH%	98.7%	93.3%	98.7%	96.0%	92.0%	88.0%	90.7%	94.7%	94.7%
$P_{change\_dis} = 0.5$	<b>61</b>	<b>111</b>	<b>141</b>	<b>161</b>	<b>191</b>	<b>231</b>	<b>261</b>	<b>291</b>	<b>351</b>
MAPE	7.5%	8.6%	8.3%	11.1%	11.3%	10.7%	11.8%	10.6%	10.1%
GEH%	98.7%	96.0%	96.0%	94.7%	96.0%	86.7%	90.7%	94.7%	100.0%
$P_{change\_dis} = 0.7$	<b>61</b>	<b>111</b>	<b>141</b>	<b>161</b>	<b>191</b>	<b>231</b>	<b>261</b>	<b>291</b>	<b>351</b>
MAPE	7.4%	8.1%	7.8%	9.1%	9.3%	9.4%	10.7%	9.6%	8.6%
GEH%	97.3%	96.0%	97.3%	97.3%	96.0%	96.0%	96.0%	98.7%	98.7%

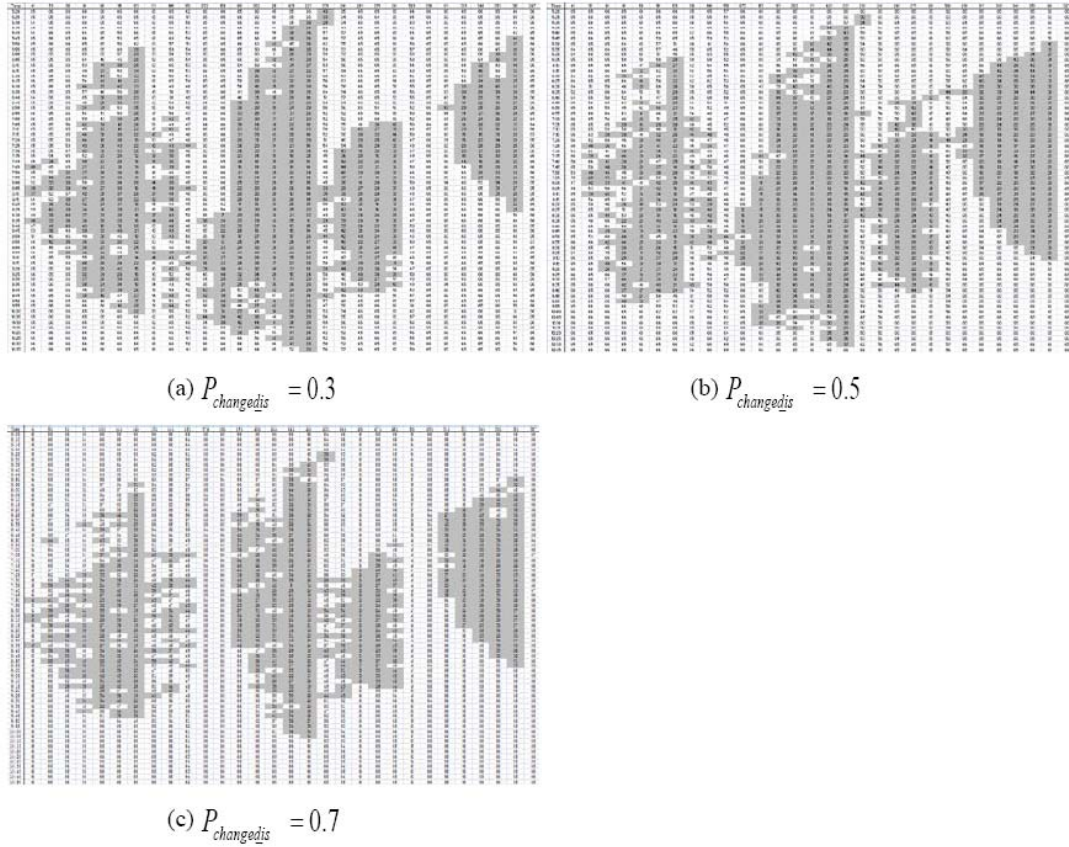
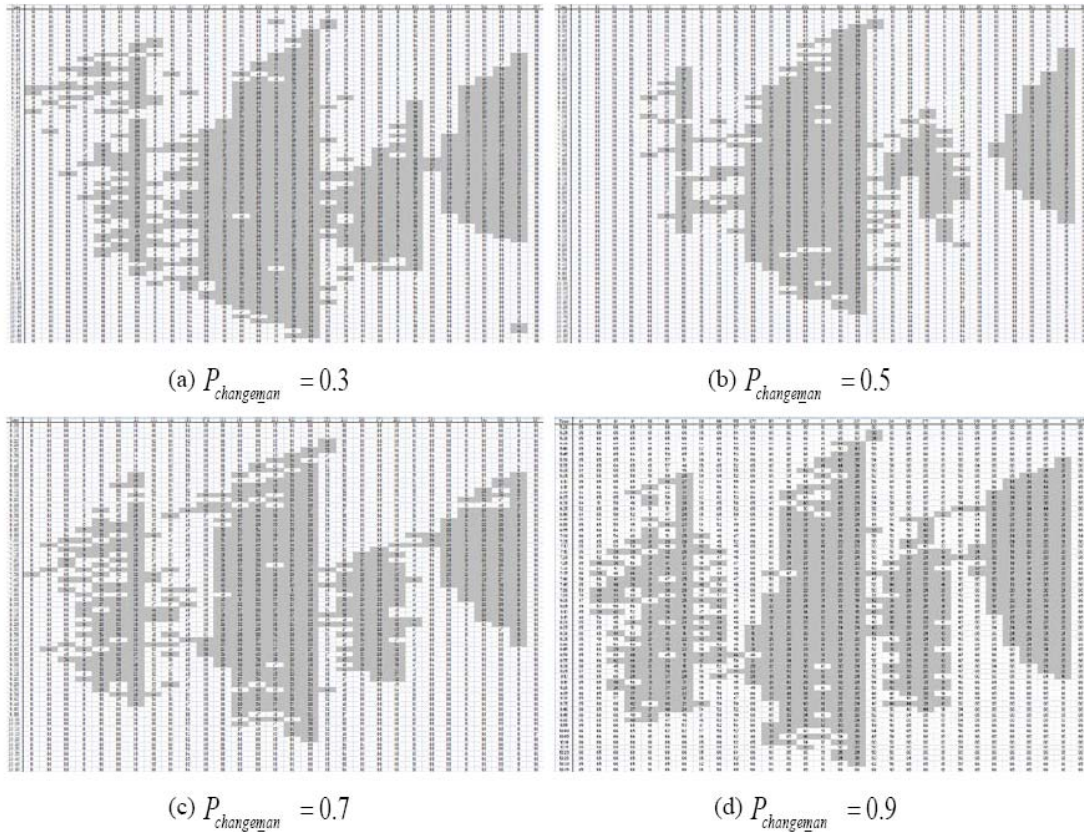


Figure 16. Speed Contour Plots of Morning Congestion for  $P_{change\_dis}$ .

Table 14. MAPE and GEH Analysis on Morning Congestion with Different  $P_{change\_man}$ .

	Station ID								
	61	111	141	161	191	231	261	291	351
$P_{change\_man} = 0.3$	61	111	141	161	191	231	261	291	351
MAPE	7.0%	9.3%	8.6%	12.0%	12.2%	13.0%	13.6%	11.4%	11.7%
GEH%	94.7%	90.7%	92.0%	94.7%	90.7%	85.3%	88.0%	96.0%	94.7%
$P_{change\_man} = 0.5$	61	111	141	161	191	231	261	291	351
MAPE	5.2%	6.1%	6.7%	11.3%	10.2%	10.6%	11.5%	10.2%	10.3%
GEH%	100.0%	100.0%	96.0%	93.3%	93.3%	90.7%	94.7%	97.3%	97.3%
$P_{change\_man} = 0.7$	61	111	141	161	191	231	261	291	351
MAPE	7.4%	7.3%	7.4%	10.7%	11.5%	10.8%	11.2%	10.5%	10.0%
GEH%	96.0%	96.0%	98.7%	96.0%	92.0%	90.7%	93.3%	93.3%	92.0%
$P_{change\_man} = 0.9$	61	111	141	161	191	231	261	291	351
MAPE	7.5%	8.6%	8.3%	11.1%	11.3%	10.7%	11.8%	10.6%	10.1%
GEH%	98.7%	96.0%	96.0%	94.7%	96.0%	86.7%	90.7%	94.7%	100.0%



**Figure 17. Speed Contour Plots of Morning Congestion for  $P_{change\_man}$ .**

### *Speed Oscillation Parameters*

The three parameters  $P$ ,  $P_{onramp}$  and  $P_{offramp}$  represented oscillation of vehicles' speeds when approaching different sections of the freeway. Several ramps used distinct  $P_{onramp}$  and  $P_{offramp}$  values to simulate recurring weekday morning congestion. For all of these parameters, a higher value indicated more oscillation and congestion in the bottlenecks. Figure 18 and Table 15 present the results for  $P$  at 0, 0.1, and 0.2.

With the increase of  $P$ , the congestion at bottlenecks increased. The other oscillation parameters had the same effects. At the higher value of 0.2, the GEH statistic was not considered acceptable at three out of nine stations, with another two being very close (0.4%) to failing. However, the MAPE statistics were all acceptable.



varied from day to day, and was reflected in average speed, queue length, and congestion duration. Table 16 presents the range of start and end times and queue length measured in terms of the furthest station the queue reaches.

**Table 16. Bottleneck Fluctuation Ranges.**

	<b>Bottleneck 1</b>	<b>Bottleneck 2</b>	<b>Bottleneck 3</b>	<b>Bottleneck 4</b>
<b>Start Time</b>	5:35 a.m. – 6:40 a.m.	5:25 a.m. – 6:30 a.m.	6:15 a.m. – 7:15 a.m.	5:30 a.m. – 7:30 a.m.
<b>End Time</b>	8:00 a.m. – 9:45 a.m.	8:45 a.m. – 10:55 a.m.	9:00 a.m. – 10:45 a.m.	8:45 a.m. – 10:10 a.m.
<b>Queue Length</b>	101 - 41	191 - 141	261 - 241	291 - 331

To simulate the incident-free conditions, the OD matrix based on representative flow data was used. The parameters were set so that the bottleneck characteristics fell within the above ranges. Figure 19 presents the speed contour of the simulated Wednesday bottlenecks with the parameter values in Table 17. Table 18 presents the summary of the simulated Wednesday bottlenecks, including start and end times and queue length.

**Table 17. Calibrated Parameter Values.**

$P_0$	$P_{00}$	$P$	$P_{offramp - B1}$	$P_{offramp - B2}$	$P_{offramp}$	$P_{onramp - B3}$
0.8	0.1	0.1	0.3	0.3	0.1	0.1
$P_{onramp - B4}$	$P_{following}$	$d_{following}$	$k$	$b$	$P_{change,man}$	$P_{change,dis}$
0.25	0.4	8	2	1	0.9	0.5

B\_ indicates the bottleneck to which the parameter applies.

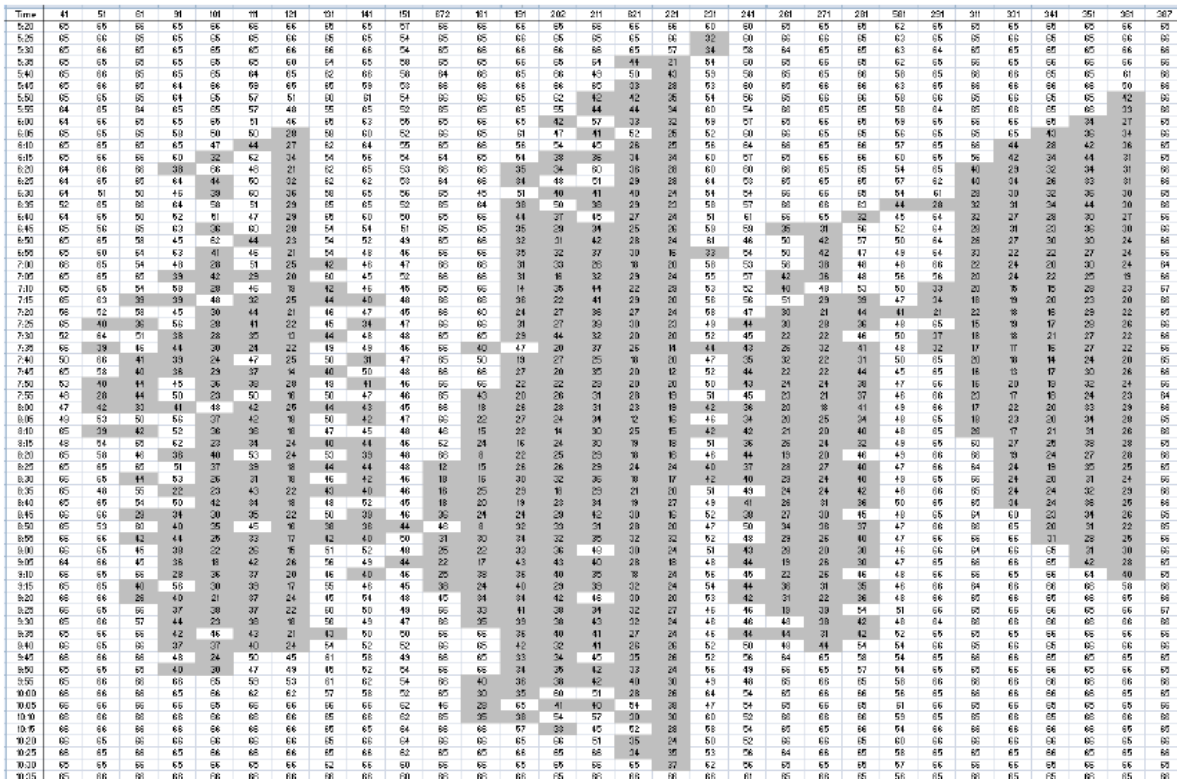


**Figure 19. Speed Contour of Simulated Wednesday Morning Congestion.**

Comparing Tables 18 and 17, one can see that the characteristics were within the ranges, indicating that the model appropriately reproduced the bottlenecks based on speed contours.

**Table 18. Summary of Simulated Wednesday Bottlenecks.**

	<b>Bottleneck 1</b>	<b>Bottleneck 2</b>	<b>Bottleneck 3</b>	<b>Bottleneck 4</b>
<b>Start Time</b>	6:05 a.m.	5:35 a.m.	6:40 a.m.	5:50 a.m.
<b>End Time</b>	9:40 a.m.	10:30 a.m.	9:35 a.m.	9:10 a.m.
<b>Queue Length</b>	51	672	241	291

The success in reproducing the bottlenecks was also checked using MAPE and GEH statistics for major stations on the mainline. The comparison was based on the representative flows from 5:00 a.m. to 11:00 a.m. with a resolution of 5 minutes. Table 19 shows these results, all of which were within the acceptable thresholds.

**Table 19. MAPE and GEH for Bottlenecks.**

<b>Station</b>	<b>61</b>	<b>111</b>	<b>141</b>	<b>161</b>	<b>191</b>	<b>231</b>	<b>261</b>	<b>291</b>	<b>351</b>
MAPE	7.5%	8.6%	8.3%	11.1%	11.3%	10.7%	11.8%	10.6%	10.1%
GEH	98.7%	96.0%	96.0%	94.7%	96.0%	86.7%	90.7%	94.7%	100.0%

Since the MAPE and GEH statistics were within the specified thresholds and the simulated bottlenecks' characteristics fall within the typical range, the parameters in Table 17 were accepted as the calibrated values.

### Incident Simulation

To simulate an incident, one must specify the start time, end time, location, incident zone length, and lane closure status. For complicated incidents, i.e., ones with multiple lane closure states, an input file such as the one in Figure 20 must be created.

```

*Incident 47661 Saturday:
*Start Time;End Time;Location;Length;Lane Closure
20:15;20:25;1900;10;1,2,3,4
20:25;20:40;1900;10;2,3,4
    
```

**Figure 20. Sample Incident Input File.**

Comments were indicated with an asterisk. The system ignored comments, this data should be inputted using the interface described next. The actual inputs were in the third line. Semicolons separated the inputs corresponding to the five characteristics of the incident. The start and end times should be expressed without "a.m." or "p.m." and should not include zeros between the hour and the minute. The hour should be in 24-hour time. For example, five past three in the afternoon should be expressed as "15:5" rather than "15:05" or "3:5 p.m." The location of the incident was expressed by the cell indicator in the system, which could be looked up in a cell look-up diagram (see Appendix A). The incident zone length was also input in the units of cells rather than meters or feet. Lane closure status listed the closed lane number where 1 represented the leftmost lane and these numbers were separated with commas.

Simpler incidents with only one set of lane closure information could use a user-interface, shown in Figure 21. This interface required nine inputs: (1) incident ID; (2) day of week; (3) simulation start time; (4) simulation end time; (5) incident start time; (6) incident end time; (7) incident location; (8) incident zone length; and (9) lane closure status. The incident start and end time, incident location, incident zone length and lane closure status were directly typed into the system through the interface.

The screenshot shows a software window titled "Form1" with a light green border. The interface contains several input fields and checkboxes arranged in a grid-like fashion. At the top, there are fields for "Day of Week" (set to "Friday"), "Incident ID" (set to "32421"), and a checkbox "Read Incident Data From File?". Below these, a text prompt reads: "If you do not read incident data from file, please fill the following blanks:". This is followed by fields for "Simulation Start Hour" (17), "Simulation Start Minute" (0), "Simulation End Hour" (20), and "Simulation End Minute" (0). To the right of these are fields for "Incident Start Hour" (17), "Incident Start Minute" (40), "Incident End Hour" (18), and "Incident End Minute" (40). Further down are fields for "Incident Location" (2350) and "Incident Zone Length" (10). Below these are fields for "Lane Closed (separated in comma)" (3,4). At the bottom, there are two columns of checkboxes and text boxes. The left column has checkboxes for "Load snapshot to initiate the system?" and "Save snapshot for incident-free period?", with corresponding "Load" and "Save" buttons. The right column has checkboxes for "Load snapshot for incident simulation (used when lane closure status is changed)?" and "Save snapshot during incident period?", with corresponding "Load" and "Save" buttons. A large "Start" button is centered at the very bottom of the window.

**Figure 21. Simulation Tool Interface.**

Simulation start and end times determined the horizon of interest, which should cover the entire incident duration and enough time to dissipate resulting congestion. If the incident duration was not known prior to incident clearance (as would be the case for real time applications), a rough simulation end time should be selected (e.g., for a major incident during the peak period, the simulation end time should be during the off-peak). Based on inputs (2) and (3), the corresponding OD tables would be loaded into the system. At the beginning of the simulation, the initial network could be either empty or initialized by loading snapshots saved from previous incident-free simulations. The snapshots included the layouts of the vehicles and their related information such as origins, destinations, trajectories, and so forth. If the network was initially empty, the simulation start time should be at least one-half hour earlier than the incident start time in order to distribute vehicles throughout the network. This advance time was not required if snapshots were loaded. Incident start and end times define the incident duration and corresponding incident location, zone length (the length of the lanes occupied by incident activities) and lane closure status (which lanes were closed) would be applied to the system.

In its current state, the model required incident-related re-routing to be hard coded. The re-routing time and the percentage of the relevant entries of the OD matrix to be used in this study were determined by trial and error by comparing the MAPE and GEH% so that they met

the same thresholds of 20% and 85%. The trial and error process began with running the model with no rerouting. Then the time point where the flow dropped on a ramp, indicating that the queue reached the ramp and the entrance/exit was blocked and/or drivers had started rerouting in significant numbers, was identified. This was the starting point for the re-routing. The end time of re-routing was considered the point when flow recovered on the ramp to levels close to the OD matrix. The percentage was determined by the MAPE and GEH statistics.

With the inputs just discussed and the model described in Task 5, the simulator generated travel times from upstream locations to the incident location every minute after the incident. Travel time indicated the total time from the vehicle's current location through the incident zone. It was affected by two factors: upstream distance from the bottleneck and elapsed time since the incident. Travel times as a function of time and distance were averaged over all relevant vehicles. These travel times were produced for every 0.2 mile upstream of the incident location, although this value could be changed. If these data were not available throughout the simulation period, due to the closure of all lanes and no vehicles being able to reach and pass the incident location, travel times to the nearest off-ramps were provided. Other desired measures, such as the queue length and dissipation could be determined from speed contour plots, which were generated when the simulation was complete. At this point, these measures required user interaction with output files.

Using the calibrated parameters, four incidents of varying characteristics were simulated.

### *Incident 1*

Incident 1 is described as follows and is illustrated in Figure 22:

- Incident ID: 35091
- Duration: 12:50 - 13:55, May 19, 2007, Saturday
- Location: Between SR243 Off-ramp and SR243 On-ramp
- Type: Disabled
- Severity: Major
- Lane closure status: 12:50-13:55 (65 min): One lane was blocked.

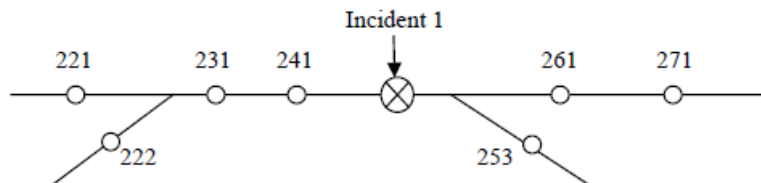


**Figure 22. Location of Incident 1.**

Rerouting inputs were defined based on ramp detector data. Two off-ramps upstream of the incident location were affected by the incident: US50 NB Off-ramp (Station 623) and US50 SB Off-ramp (Station 212). Rerouting inputs for relevant ramps are listed in Table 20.

**Table 20. Rerouting Start Time, End Time and Percentage for Incident 1.**

	US50 NB Off (623)	US50 SB Off (212)
Start Time	13:00	13:05
End Time	13:25	14:20
Percentage	10% more use this ramp	18% more use this ramp

Figures 23 and 24 present comparisons of the detector data and simulation results for incident 1. The stations involved cover all the mainline stations upstream of the incident with reliable detector data and all ramps affected by the incident.

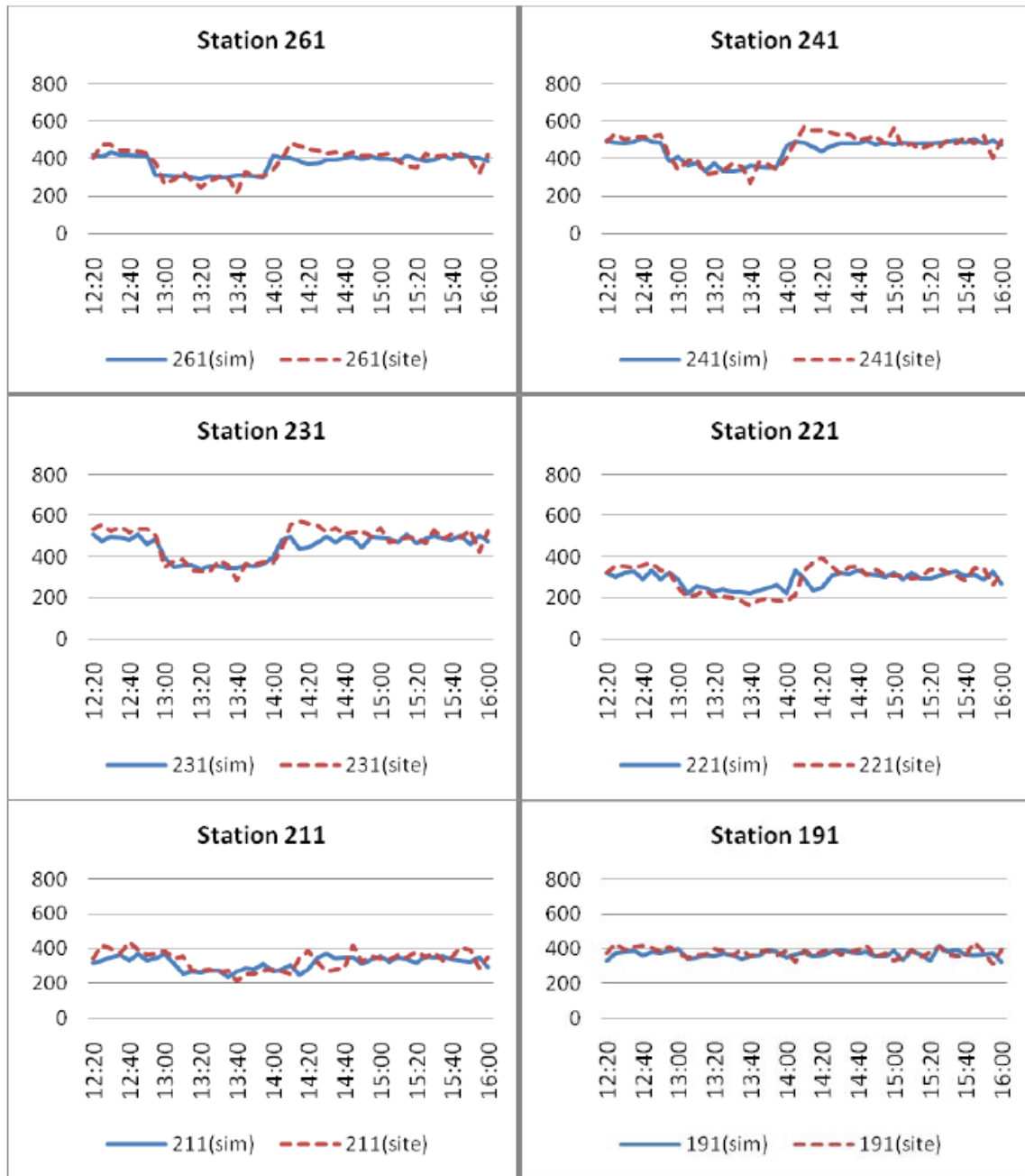


**Figure 23. Traffic Counts (veh / 5 min) at Freeway Measurement Stations Upstream of Incident 1.**

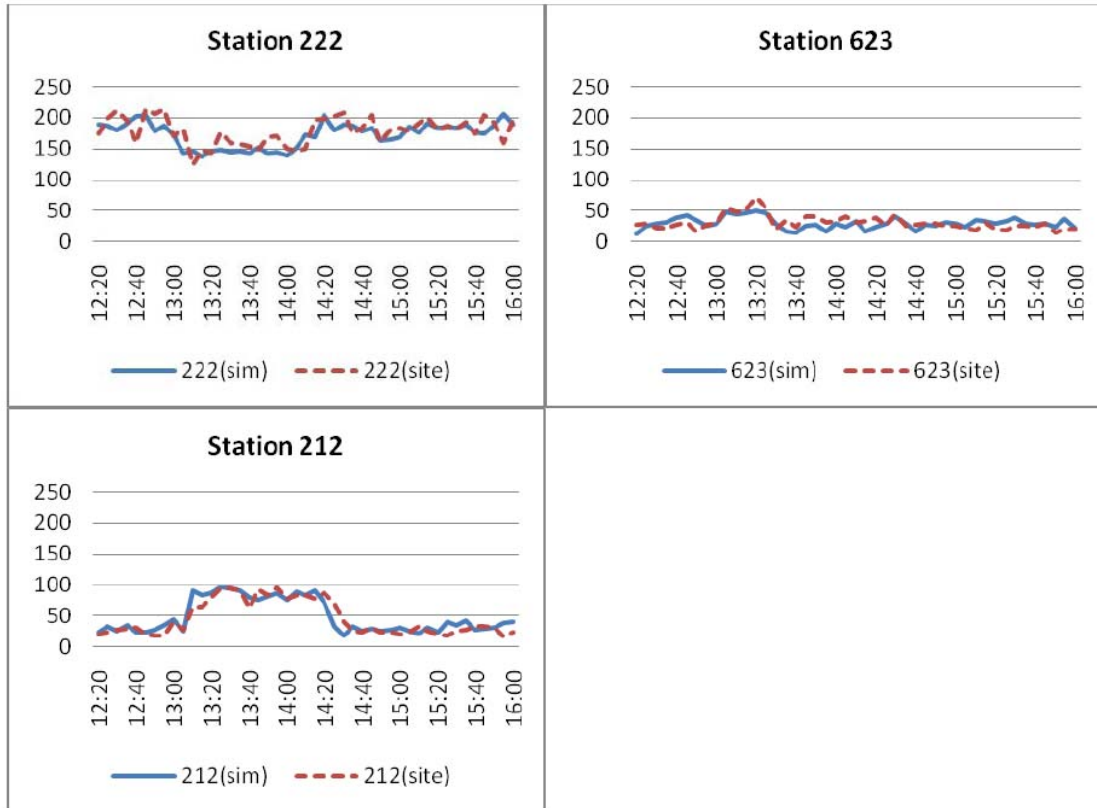


**Figure 24. Traffic Counts (veh / 5 min) at Ramps Upstream of Incident 1.**

Some of the simulated flows were underestimates for some time periods but then they were overestimates so the overall flows matched well. The general shapes of the curves were approximately the same in most cases. According to Figures 23 and 24, queue propagation speed and length followed the field data. The time difference of the queue arrival and dissipation was no more than 5 minutes between the simulation results and detector data. Also recall, that the demands were not exactly equivalent since the simulation results were based on the estimated OD matrix formed from multiple days while the site flows only represented the specific day. The average MAPE and GEH% for each upstream station are listed in Table 21. Data involved in the calculations covered vehicle counts from 12:20 to 14:25 with a resolution of 5 minutes.

**Table 21. MAPE and GEH% for Flow (veh / 5 min) for Incident 1.**

<b>Mainline</b>	<b>261</b>	<b>241</b>	<b>231</b>	<b>221</b>	<b>211</b>	<b>191</b>	<b>161</b>	<b>672</b>
MAPE	10.39%	9.25%	8.90%	18.64%	12.30%	5.86%	6.40%	5.90%
GEH%	96.15%	92.31%	92.31%	84.62%	84.62%	100%	100%	100%
<b>Mainline</b>	<b>151</b>	<b>141</b>	<b>121</b>	<b>111</b>	<b>91</b>	<b>61</b>	<b>51</b>	
MAPE	6.15%	6.80%	7.46%	5.75%	7.10%	6.02%	6.80%	
GEH%	100%	100%	100%	100%	100%	100%	100%	
<b>Ramp</b>	<b>222</b>	<b>623</b>	<b>212</b>					
MAPE	10.06%	29.61%	19.78%					
GEH%	100.00%	100.00%	96.30%					

As indicated in Table 21, the MAPE values of all the mainline stations were less than 20%. Meanwhile, most of the GEH% values were greater than 85% except Stations 221 and 211 whose values were very close to the threshold. For the ramps, the GEH% values were very good, but one of the MAPE values exceeded the threshold while another was very close to the threshold. Some improvement might be made by improving the rerouting inputs. According to these statistical results, incident 1 was properly simulated based on the calibrated parameters and proper rerouting inputs.

The simulation duration for this incident was 5 hours and 30 minutes from 10:30 to 16:00. Starting from an empty network (not using snapshots), the simulation took approximately 9 minutes on an older desktop computer.

An excerpt of the output travel time table is shown in Table 22. The table gives distance upstream of the incident on the x-axis and time of day on the y-axis. The entries in the table are travel times from that upstream point through the incident location. One can see that travel times increased during the incident period. Some fluctuation existed during the period but all were higher than when the incident first occurred. Some of the times seemed counterintuitive with vehicles closer to the incident taking slightly longer to pass through the incident zone than those that were further away. This result was caused by the rules associated with overtaking and the uneven distribution of vehicles on the lanes. Vehicles in the blocked lane had difficulty changing lanes during this incident due to the volumes on the other lanes. This counterintuitive situation did not arise when the entire road upstream of the incident was heavily congested because little to no overtaking occurred, nor did the situation arise under low traffic flow conditions. Thus, the remaining incidents did not demonstrate counterintuitive travel times.

**Table 22. Travel Times Associated with Incident 1.**

	0.2	0.4	0.6	0.8	1.0	1.2	1.4	1.6	1.8	2.0	2.2	2.4	2.6	2.8	3.0	3.2	3.4	3.6	3.8	4.0	4.2	4.4	4.6	4.8
12:50	0.28	0.80	1.40	2.76	4.58	2.79	2.76	2.72	2.60	2.89	3.14	3.49	3.53	4.06	4.38	4.89	5.11	5.84	5.83	5.79	5.68	5.69	5.70	5.98
12:51	0.43	1.17	2.07	4.56	4.64	3.17	2.41	2.62	3.03	3.26	3.72	4.07	4.51	4.60	4.86	5.03	5.25	5.02	5.14	5.46	5.76	6.11	6.74	7.06
12:52	0.51	1.59	3.90	5.45	4.32	3.13	3.26	3.57	3.67	3.97	4.15	4.45	4.53	4.79	5.29	5.53	5.84	5.91	6.21	6.74	6.89	7.11	6.98	7.17
12:53	0.42	1.89	4.95	5.10	5.54	3.46	3.63	3.57	3.92	4.39	4.75	5.03	5.39	5.76	5.91	6.09	6.05	6.01	6.16	6.16	6.73	7.34	8.07	8.49
12:54	0.24	1.67	4.69	5.26	4.95	4.07	4.10	4.65	4.82	5.03	5.21	5.06	5.35	5.66	5.71	6.23	6.90	7.28	7.47	7.50	7.52	7.86	8.06	8.21
12:55	0.44	1.92	4.22	4.96	5.92	4.92	4.14	4.52	4.73	4.89	5.37	6.21	6.36	6.53	6.85	7.04	7.32	7.10	7.37	7.73	8.22	8.78	9.03	9.70
12:56	0.39	1.92	4.52	4.70	5.32	5.22	5.34	5.42	5.64	5.86	6.22	6.48	6.70	7.00	7.38	7.99	8.46	8.23	8.84	9.12	9.16	8.97	8.84	8.97
12:57	0.32	2.25	4.50	4.91	4.72	6.00	5.54	5.97	6.05	6.54	7.26	7.55	8.16	8.69	8.94	8.80	8.83	7.75	8.09	8.87	9.92	10.42	10.75	10.98
12:58	0.48	2.71	4.38	4.43	4.88	6.58	6.81	7.35	7.79	7.88	7.80	7.78	7.94	8.44	8.89	9.57	9.56	10.00	9.78	10.11	9.42	9.30	9.80	10.44
12:59	0.48	2.42	4.11	4.54	5.18	7.43	6.88	7.02	7.31	8.19	8.89	8.78	9.08	8.96	8.92	8.71	9.16	8.96	9.74	9.84	10.37	10.78	10.87	10.34
13:00	0.45	2.31	3.53	4.64	6.23	7.32	7.64	8.08	8.17	7.86	8.03	8.34	8.70	9.15	9.32	9.50	9.93	9.73	9.18	9.58	9.67	9.86	11.06	11.73
13:01	0.46	2.19	3.71	4.60	7.51	6.82	8.38	8.02	8.12	8.41	8.75	9.01	8.61	8.67	9.27	9.36	9.25	10.26	10.60	10.68	10.31	9.94	8.73	9.20
13:02	0.44	2.10	3.70	4.62	8.02	6.56	8.94	7.49	8.17	8.31	8.18	9.21	10.18	10.64	10.37	10.26	9.46	7.85	8.45	9.21	11.23	11.34	12.00	12.78
13:03	0.40	1.98	3.80	4.52	7.88	6.73	9.88	10.22	9.45	9.41	9.17	8.04	7.54	8.12	10.03	10.45	10.95	11.37	11.89	11.49	10.54	10.71	10.63	9.71
13:04	0.48	2.05	3.12	4.66	8.30	7.83	9.17	7.86	7.97	9.48	9.49	9.61	10.50	10.34	9.09	8.83	9.68	8.96	9.23	10.17	10.74	11.13	11.38	11.70
13:05	0.38	2.02	3.00	4.28	8.21	9.65	8.48	9.96	8.74	7.73	8.00	9.01	8.31	9.52	10.06	11.02	11.56	10.81	10.40	9.47	8.57	9.21	9.34	9.60
13:06	0.37	1.76	3.09	4.41	7.99	10.29	7.85	8.40	9.00	9.28	10.50	10.71	10.88	10.22	9.60	8.80	8.07	8.52	8.39	8.48	9.07	8.71	9.15	10.51
13:07	0.41	1.61	3.07	4.77	7.27	10.06	8.38	10.90	8.64	8.95	7.54	7.11	7.30	7.13	7.56	7.71	7.49	8.82	9.59	9.62	9.37	9.61	10.16	9.18
13:08	0.39	1.79	2.66	4.36	7.38	10.50	8.78	6.82	6.19	6.81	6.57	6.50	8.12	8.53	8.37	8.60	9.05	8.77	8.43	9.65	10.08	10.21	9.97	10.26
13:09	0.49	1.97	2.68	4.03	8.41	10.10	8.14	7.38	7.49	7.50	7.80	8.09	7.07	7.82	8.39	8.88	9.42	8.75	9.52	9.32	9.54	9.80	9.90	9.56
13:10	0.48	1.76	3.49	4.36	7.48	12.62	7.70	6.21	7.03	7.64	8.00	8.45	8.65	8.67	8.87	9.12	8.87	9.04	8.45	8.87	9.25	9.22	9.34	9.26
13:11	0.35	1.63	3.41	5.02	7.78	9.92	8.64	7.70	7.77	7.90	8.19	7.93	7.64	7.91	8.04	8.62	8.63	8.31	8.25	8.17	7.69	7.55	8.29	8.67
13:12	0.46	1.73	3.40	4.99	8.52	10.10	8.74	6.55	7.04	7.46	7.55	7.81	7.84	8.00	8.06	7.46	7.62	7.57	7.82	8.31	8.62	8.98	9.22	9.48
13:13	0.46	1.73	3.35	5.20	9.25	10.10	7.88	6.98	7.05	6.67	6.60	6.79	7.19	7.75	8.46	8.84	9.17	8.30	8.53	8.20	8.25	8.08	8.20	8.22
13:14	0.39	1.82	3.36	5.01	9.75	8.86	7.71	6.42	7.12	7.55	7.98	8.46	8.64	8.49	8.09	8.08	7.88	7.23	7.57	8.33	9.33	10.10	10.15	10.42
13:15	0.44	1.82	2.94	5.11	9.40	8.40	8.14	7.73	7.37	7.09	6.98	6.89	6.69	7.05	7.80	8.83	9.43	9.27	9.38	9.15	8.85	8.34	8.50	8.94
13:16	0.32	1.47	3.61	4.26	10.08	8.73	7.46	5.67	6.44	7.18	8.08	8.46	8.54	8.60	8.60	8.25	7.94	7.83	7.96	8.25	9.17	9.39	9.20	9.27
13:17	0.23	1.32	3.33	5.32	9.04	8.52	8.60	7.78	7.54	7.49	7.13	7.27	7.92	8.37	8.86	8.92	8.89	8.16	8.52	8.81	7.80	7.78	7.89	8.62
13:18	0.62	1.72	3.44	5.11	10.02	8.49	7.89	7.07	7.53	8.00	7.90	7.89	7.74	7.75	7.71	7.19	7.02	6.92	8.08	8.46	8.62	9.33	9.48	9.91
13:19	0.73	2.25	3.48	5.20	9.56	8.50	8.34	6.69	6.91	6.29	6.20	5.81	5.92	7.07	7.32	7.58	8.39	8.67	8.77	8.74	8.98	8.63	8.62	8.10
13:20	0.60	1.88	4.70	5.23	9.20	8.78	6.61	5.61	6.23	6.16	6.96	7.34	7.80	7.69	7.70	7.88	7.41	7.46	7.22	7.67	7.89	8.14	8.53	8.47

## Incident 2

The description of Incident 2 is as follows, and the location is shown in Figure 25:

- Incident ID: 31852
- Duration: 13:00 - 14:10, Apr 5, 2007, Thursday
- Location: Between SR28 On-ramp and SR7100 Off-ramp
- Type: Road Work
- Severity: Major
- Lane closure status: 13:00-14:10 (70 min): Two lanes were blocked

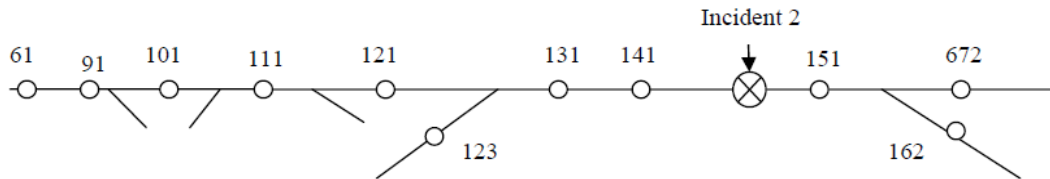


**Figure 25. Location of Incident 2**

The rerouting inputs were initially undefined in this simulation due to lack of ramp data on that day.

The flow plots comparing the detector data and simulation results for upstream stations are presented in Figure 26. Station 51 was upstream of station 61. The associated MAPE and GEH% values are presented in Table 23. Data involved in these calculations covered the vehicle counts ranging from 12:30 p.m. to 14:40 with a resolution of 5 minutes.

**Table 23. MAPE and GEH% for Flow (veh / 5 min) for Incident 2.**

	141	111	91	61	51
MAPE	13.12%	9.55%	9.79%	8.97%	9.74%
GEH%	92.59%	100%	100%	100%	100%

The MAPE and GEH% values were all well within the thresholds. Those values, in addition to the plots in Figure 26 suggested that even without accounting for rerouting during this off-peak incident, the simulated flows well matched those from the detectors.

The simulation of 5 hours duration (from 11:00 to 16:00) starting with an empty network took approximately 7 minutes. Using snapshots would speed this simulation time.

Table 24 provides an excerpt of the travel times associated with Incident 2. As expected, travel times increased during the incident period.

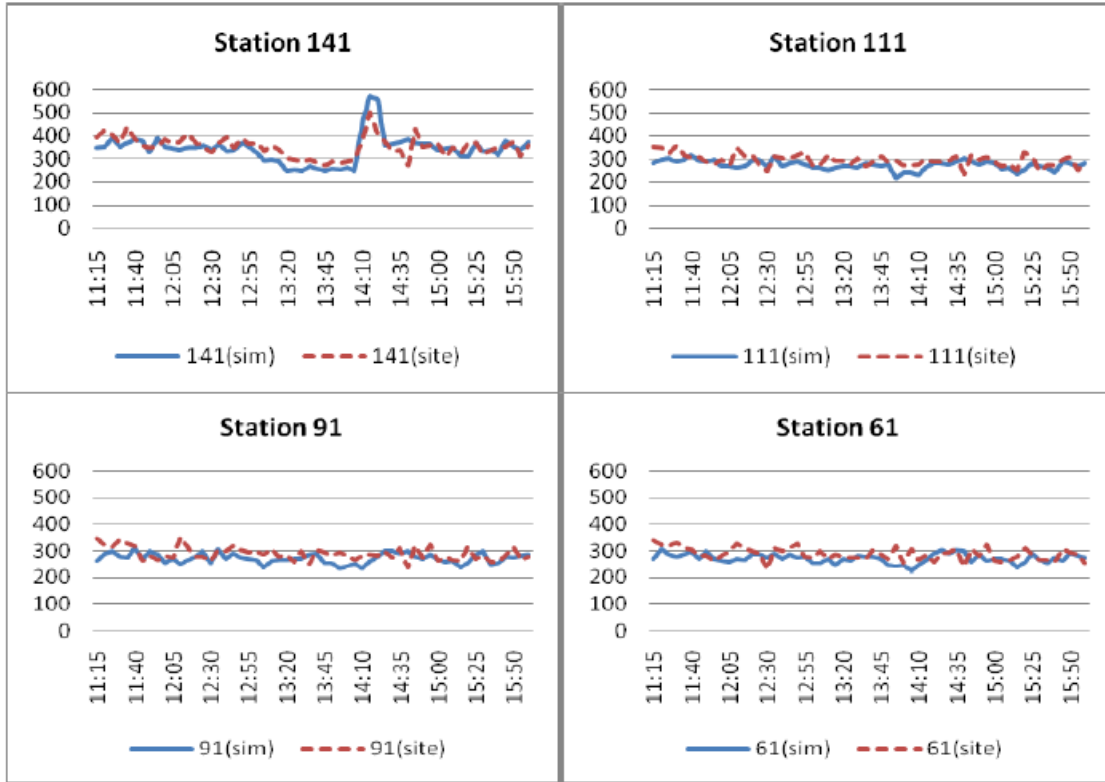


Figure 26. Traffic Counts (veh / 5 min) at Freeway Measurement Stations Upstream of Incident 2.

Table 24. Travel Times for Incident 2.

	0.0	0.2	0.4	0.6	0.8	1.0	1.2	1.4	1.6	1.8	2.0	2.2	2.4	2.6	2.8	3.0	3.2	3.4	3.6	3.8	4.0	4.2	4.4	4.6
13:00	0.01	0.13	0.31	0.50	0.71	0.93	1.13	1.30	1.47	1.64	1.86	2.09	2.30	2.48	2.62	2.78	2.93	3.10	3.31	3.51	3.70	3.88	4.05	4.23
13:01	0.01	0.14	0.34	0.53	0.72	0.92	1.13	1.33	1.52	1.72	1.88	2.04	2.22	2.39	2.58	2.77	2.95	3.14	3.32	3.49	3.66	3.85	4.04	4.22
13:02	0.01	0.16	0.38	0.58	0.78	0.95	1.11	1.29	1.48	1.66	1.85	2.04	2.22	2.39	2.56	2.74	2.93	3.12	3.32	3.54	3.75	3.96	4.16	4.36
13:03	0.01	0.15	0.35	0.53	0.72	0.91	1.12	1.29	1.46	1.64	1.82	2.01	2.20	2.42	2.63	2.84	3.05	3.25	3.43	3.61	3.77	3.93	4.11	4.32
13:04	0.01	0.14	0.33	0.51	0.70	0.89	1.10	1.29	1.51	1.73	1.94	2.14	2.33	2.51	2.68	2.84	3.00	3.20	3.40	3.62	3.83	4.03	4.22	4.41
13:05	0.01	0.14	0.36	0.58	0.80	1.01	1.24	1.42	1.60	1.77	1.92	2.09	2.30	2.50	2.71	2.91	3.12	3.30	3.49	3.67	3.85	4.02	4.23	4.44
13:06	0.01	0.21	0.48	0.67	0.84	0.99	1.17	1.38	1.60	1.81	2.00	2.19	2.38	2.57	2.75	2.92	3.11	3.33	3.53	3.73	3.95	4.19	4.41	4.62
13:07	0.01	0.19	0.46	0.69	0.94	1.13	1.30	1.51	1.69	1.87	2.01	2.21	2.41	2.61	2.82	3.06	3.28	3.51	3.71	3.89	4.06	4.22	4.45	4.64
13:08	0.01	0.34	0.67	0.85	1.05	1.16	1.34	1.54	1.73	1.96	2.17	2.37	2.61	2.78	2.97	3.13	3.32	3.53	3.75	3.95	4.15	4.40	4.51	4.64
13:09	0.01	0.32	0.67	0.88	1.14	1.31	1.50	1.71	1.89	2.07	2.21	2.42	2.61	2.85	3.04	3.26	3.45	3.58	3.71	4.00	4.27	4.57	4.82	5.09
13:10	0.01	0.45	0.84	1.04	1.26	1.38	1.55	1.74	1.95	2.15	2.38	2.50	2.64	2.86	3.13	3.40	3.69	3.94	4.19	4.36	4.54	4.81	5.07	5.16
13:11	0.01	0.51	0.95	1.13	1.33	1.47	1.59	1.82	2.10	2.38	2.58	2.80	3.08	3.28	3.43	3.63	3.96	4.12	4.20	4.47	4.75	4.77	4.83	5.05
13:12	0.01	0.56	0.99	1.28	1.60	1.82	1.98	2.26	2.43	2.59	2.81	3.05	3.15	3.26	3.61	3.81	3.75	3.92	4.22	4.56	4.70	4.91	5.18	5.41
13:13	0.01	0.79	1.73	1.82	2.14	2.17	2.24	2.27	2.51	2.74	2.81	2.81	3.02	3.40	3.64	3.77	4.03	4.30	4.42	4.56	4.77	5.08	5.35	5.56
13:14	0.01	1.35	1.80	1.94	2.16	1.97	1.95	2.29	2.72	2.91	2.93	3.16	3.39	3.46	3.62	3.90	4.25	4.41	4.73	5.18	5.44	5.56	5.96	6.35
13:15	0.01	1.41	1.90	2.07	2.33	2.43	2.58	2.91	3.10	3.29	3.23	3.35	3.51	3.91	4.34	4.56	4.61	5.27	5.32	5.02	5.20	5.52	5.41	5.57
13:16	0.01	1.38	2.22	2.61	2.85	2.78	2.75	2.85	3.17	3.46	3.57	3.88	4.37	4.18	4.06	4.32	4.60	4.42	4.64	4.93	5.16	5.36	5.60	5.83
13:17	0.01	1.55	2.27	2.63	3.00	2.82	3.31	3.51	3.32	3.50	3.64	3.41	3.55	3.76	4.04	4.24	4.49	4.67	4.97	5.39	5.88	6.45	7.10	7.59
13:18	0.01	1.74	2.29	2.52	2.67	3.15	2.70	2.87	3.13	3.44	3.46	3.58	3.81	4.15	4.64	5.05	5.75	6.29	6.70	6.83	7.09	7.07	6.84	6.95
13:19	0.01	1.78	2.15	2.61	2.84	2.82	2.87	3.15	3.43	3.86	4.31	5.02	5.53	5.76	5.97	6.17	5.90	5.90	6.09	6.38	6.59	6.97	7.42	7.71
13:20	0.01	1.67	2.11	2.92	3.31	3.62	4.18	4.61	4.82	5.01	5.11	4.86	4.94	5.29	5.46	5.75	6.18	6.53	6.75	6.87	7.11	7.39	7.44	7.67
13:21	0.01	1.50	2.57	3.86	4.16	4.03	3.83	4.00	4.29	4.58	4.93	5.37	5.68	5.77	5.97	6.22	6.42	6.56	6.79	7.08	7.36	7.47	7.77	8.05
13:22	0.01	1.33	2.83	3.71	4.04	4.25	4.49	4.84	4.98	5.21	5.43	5.45	5.64	5.94	6.21	6.41	6.57	6.91	7.15	7.19	7.49	7.73	7.98	8.23
13:23	0.01	1.55	2.58	4.03	4.51	4.60	4.72	4.85	5.12	5.37	5.47	5.73	6.02	6.18	6.29	6.59	6.87	7.08	7.29	7.52	7.64	7.97	8.18	8.50
13:24	0.01	1.64	2.62	3.91	4.57	4.63	4.95	5.27	5.34	5.64	5.74	5.98	6.21	6.38	6.55	6.79	7.07	7.36	7.55	7.99	8.33	8.69	8.87	8.91
13:25	0.01	1.67	2.60	4.05	4.86	4.93	5.05	5.24	5.46	5.59	5.93	6.14	6.49	6.71	7.17	7.49	7.81	7.86	8.05	8.08	8.11	8.20	8.46	8.87
13:26	0.01	1.67	2.43	4.07	4.94	5.05	5.28	5.54	5.91	6.28	6.65	6.88	6.87	7.10	7.10	7.14	7.30	7.65	7.95	8.27	8.50	8.80	8.94	9.11
13:27	0.01	1.52	2.39	4.21	5.33	5.65	5.89	6.12	6.29	6.32	6.28	6.42	6.84	7.09	7.38	7.62	7.89	8.01	8.25	8.33	8.56	8.70	8.84	9.22
13:28	0.01	1.42	2.34	4.30	5.35	5.52	5.80	6.03	6.32	6.54	6.75	6.95	7.08	7.30	7.43	7.61	7.76	8.02	8.24	8.42	8.70	8.91	9.27	9.49
13:29	0.01	1.21	2.39	4.40	5.58	5.83	6.02	6.16	6.27	6.49	6.68	6.81	7.16	7.28	7.52	7.82	8.04	8.34	8.69	9.12	9.58	9.97	10.36	10.46
13:30	0.01	1.22	2.36	4.45	5.57	5.79	5.89	6.21	6.41	6.77	6.94	7.21	7.50	7.91	8.33	8.73	9.16	9.37	9.47	9.68	9.84	10.04	10.18	10.47

### Incident 3

The description of Incident 3 is as follows, and the location is shown in Figure 27:

- Station ID: 32099
- Duration: 7:45 – 8:10, Apr 9, 2007, Monday
- Location: Between SR28 On-ramp and SR7100 Off-ramp
- Type: Collision
- Severity: High profile
- Lane closure status: 7:45-8:10 (25 min): Two lanes were blocked.

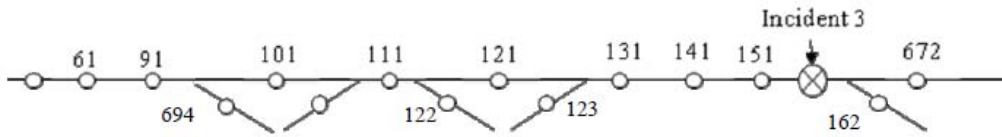


**Figure 27. Location of Incident 3.**

Two off-ramps and one onramp upstream of the incident location were affected by the incident including the SR28 Off-ramp (Station 122), US29 Off-ramp (Station 694) and SR28 On-ramp (Station 123). Rerouting inputs for relevant ramps are listed in Table 25.

**Table 25. Rerouting Start Time, End Time and Percentage for Incident 3.**

	SR28 Off (122)	US29 Off (694)	SR28 On (222)
Start Time	8:00	8:10	8:00
End Time	8:20	8:30	8:30
Percentage	40% more used this ramp	20% more used this ramp	20% fewer used this ramp

The resulting flow plots comparing the simulated flow and the detector data are found in Figure 28.

The curves showed the same general shape but a slight shift in time. However the time difference of queue arrival at different stations and the dissipation time was off by no more than 5 minutes. The MAPE and GEH% associated with the flows are provided in Table 26. The data involved in the calculation covered vehicle counts from 7:15 a.m. to 8:50 a.m. with a resolution of 5 minutes.

**Table 26. MAPE and GEH% for Flow (veh / 5 min) for Incident 3.**

	151	141	111	91	61	51	41
MAPE	11.20%	9.30%	12.79%	10.28%	9.17%	10.65%	10.28%
GEH%	95.00%	95.00%	90.00%	90.00%	90.00%	85.00%	85.00%

For this peak period incident, the simulation period was 4 hours in duration from 5:30 to 9:30, starting with an empty network. This period required about 29 minutes on a desktop computer. Using the snapshot approach would cut the simulation time.



Figure 28. Traffic Counts (veh / 5 min) at Freeway Measurement Stations Upstream of Incident 3.

The travel time excerpt is provided in Table 27. After the incident was cleared, the travel times started to decrease, as would be expected.

**Table 27. Travel Time Excerpt for Incident 3.**

	0.2	0.4	0.6	0.8	1	1.2	1.4	1.6	1.8	2	2.2	2.4	2.6	2.8	3	3.2	3.4	3.6	3.8	4	4.2	4.4	4.6	4.8
7:45	1.45	2.86	2.93	4.18	5.37	5.83	7.86	9.97	11.90	12.76	13.76	14.89	15.41	16.78	17.53	18.19	18.82	19.65	20.20	20.89	21.52	21.58	22.09	21.79
7:46	1.75	2.55	3.72	4.86	6.46	7.03	8.35	10.81	12.80	13.96	14.78	15.67	16.24	17.65	19.52	19.95	20.41	20.88	20.99	21.37	21.56	21.91	22.19	22.54
7:47	1.53	2.74	4.39	5.73	7.06	8.13	9.35	11.76	13.73	14.89	15.73	17.51	18.95	19.55	20.36	20.68	21.08	21.26	21.70	21.92	22.24	22.38	22.39	22.74
7:48	1.79	2.57	4.81	6.52	7.51	9.43	11.23	12.62	14.39	16.36	17.88	18.85	19.86	20.63	21.00	21.29	21.35	21.57	21.73	21.80	22.06	22.28	22.56	22.77
7:49	1.62	2.48	4.65	6.96	9.01	9.98	12.18	14.42	15.49	17.34	18.70	19.90	20.40	20.75	20.89	21.17	21.36	21.65	21.83	22.03	22.12	22.24	22.37	22.52
7:50	1.27	2.54	4.67	7.06	9.37	10.84	12.69	15.47	17.07	17.70	18.90	19.65	20.59	20.83	21.08	21.14	21.27	21.43	21.63	21.79	21.92	22.09	22.24	22.33
7:51	1.07	2.46	4.60	7.13	9.27	11.73	14.03	16.24	17.69	17.93	18.55	19.50	20.25	20.66	20.83	20.98	21.18	21.27	21.39	21.51	21.72	21.87	21.99	22.15
7:52	0.98	2.34	4.44	6.89	9.24	12.05	15.83	17.31	17.83	18.17	18.45	19.12	20.03	20.38	20.60	20.80	20.90	21.05	21.19	21.37	21.52	21.62	21.76	21.92
7:53	0.94	2.29	4.53	6.87	9.20	12.12	15.94	17.65	17.90	18.19	18.41	18.84	19.55	20.19	20.44	20.56	20.68	20.82	20.98	21.00	21.01	21.01	21.04	21.21
7:54	0.97	2.14	4.39	6.64	9.28	12.39	15.91	17.49	17.82	18.23	18.46	18.76	19.21	19.82	19.98	20.02	19.98	20.12	20.27	20.45	20.69	20.89	21.07	21.26
7:55	0.72	2.27	4.33	6.52	9.26	12.53	15.63	17.24	17.85	18.06	18.41	18.83	18.95	19.14	19.56	19.74	20.00	20.13	20.33	20.48	20.58	20.73	20.86	20.87
7:56	0.70	2.37	4.28	6.53	9.07	12.42	15.24	16.95	17.73	17.94	18.11	18.27	18.85	19.08	19.38	19.68	19.73	19.89	19.86	19.96	20.23	20.41	20.58	20.81
7:57	0.81	2.32	4.31	6.70	9.02	12.18	14.77	16.59	17.40	17.70	17.99	18.43	18.59	18.84	19.06	19.29	19.48	19.67	19.90	20.14	20.10	20.22	20.33	20.47
7:58	0.72	2.51	4.11	6.63	8.97	11.88	14.16	16.21	17.28	17.80	18.02	18.27	18.48	18.92	19.13	19.17	19.26	19.40	19.50	19.62	19.75	19.86	20.03	20.14
7:59	1.09	2.26	4.58	6.43	8.89	11.58	13.59	15.73	17.20	17.54	17.81	18.15	18.41	18.53	18.65	18.82	18.93	19.06	19.21	19.39	19.43	19.52	19.49	19.55
8:00	1.25	2.22	4.49	6.46	8.84	11.07	13.09	15.30	16.73	17.20	17.55	17.86	18.12	18.28	18.42	18.46	18.51	18.50	18.59	18.67	18.69	18.75	18.88	18.99
8:01	1.00	2.36	4.29	6.43	8.71	10.58	12.45	14.70	16.13	16.75	17.30	17.46	17.58	17.63	17.70	17.71	17.80	17.93	18.01	18.10	18.22	18.39	18.50	18.68
8:02	1.00	2.41	4.17	6.46	8.32	10.08	11.90	14.18	15.49	16.16	16.59	16.75	16.97	17.05	17.14	17.29	17.43	17.56	17.74	17.86	17.99	18.08	18.23	18.36
8:03	1.06	2.27	4.23	6.38	8.03	9.55	11.32	13.67	14.92	15.46	15.70	16.21	16.64	16.78	16.93	17.01	17.15	17.32	17.40	17.54	17.62	17.74	17.86	17.87
8:04	1.33	2.26	4.26	6.10	7.65	9.08	10.83	13.09	14.29	14.60	14.95	15.64	16.25	16.47	16.57	16.66	16.79	16.87	16.90	16.98	17.14	17.22	17.39	17.55
8:05	1.45	2.21	4.23	5.78	7.17	8.54	10.39	12.48	13.55	13.69	14.28	14.98	15.72	15.91	16.05	16.19	16.27	16.44	16.64	16.84	16.95	17.07	17.10	17.12
8:06	1.15	2.20	4.01	5.45	6.71	7.94	9.89	11.88	12.59	12.97	13.54	14.34	15.06	15.64	15.87	16.00	16.09	16.11	16.13	16.15	16.32	16.47	16.59	16.72
8:07	0.96	2.16	3.64	4.96	6.07	7.44	9.43	11.25	11.99	12.28	12.79	13.69	14.45	15.04	15.24	15.39	15.51	15.62	15.77	15.90	15.91	16.08	16.22	16.36
8:08	0.81	2.00	3.25	4.47	5.53	6.92	8.88	10.55	11.22	11.59	12.18	12.87	13.76	14.46	14.88	14.97	15.15	15.31	15.38	15.55	15.74	15.88	15.95	16.10
8:09	0.77	1.60	2.81	3.85	4.98	6.40	8.29	9.85	10.62	10.93	11.58	12.01	12.92	13.75	14.46	14.82	14.90	14.99	15.20	15.36	15.50	15.67	15.92	16.15
8:10	0.39	1.17	2.33	3.31	4.46	5.96	7.71	9.17	10.14	10.57	10.80	11.45	12.23	13.09	14.03	14.54	14.76	14.99	15.23	15.44	15.69	15.87	16.08	16.28
8:11	0.20	0.81	1.75	2.76	3.93	5.47	7.09	8.55	9.58	9.86	10.11	10.73	11.49	12.41	13.51	14.55	14.97	15.17	15.35	15.65	15.88	16.13	16.30	16.48
8:12	0.27	0.63	1.25	2.23	3.36	4.89	6.50	8.02	8.93	9.15	9.64	10.11	10.73	11.82	13.02	14.39	15.18	15.37	15.54	15.57	15.68	15.83	16.01	16.14
8:13	0.20	0.55	1.03	1.78	2.89	4.33	5.83	7.40	8.10	8.58	9.08	9.56	10.15	11.15	12.61	14.08	14.73	15.04	15.22	15.42	15.69	15.89	16.09	16.40
8:14	0.26	0.62	1.03	1.50	2.39	3.78	5.15	6.77	7.69	7.99	8.38	9.00	9.80	10.67	12.14	13.49	14.47	15.20	15.51	15.70	15.84	16.09	16.30	16.42
8:15	0.24	0.68	1.05	1.49	2.14	3.16	4.51	6.13	6.92	7.33	7.70	8.46	9.42	10.64	11.85	12.90	14.04	15.05	15.48	15.65	15.80	15.90	15.95	16.11

*Incident 4*

The description of Incident 4 is as follows, and the location is shown in Figure 29:

- Incident ID: 33910
- Duration: 8:20 – 8:45, Might 2, 2007, Wednesday
- Location: Between SR28 On-ramp and SR7100 Off-ramp
- Type: Collision
- Severity: High profile
- Lane closure status: 8:20-8:45 (25 min): Three lanes were blocked

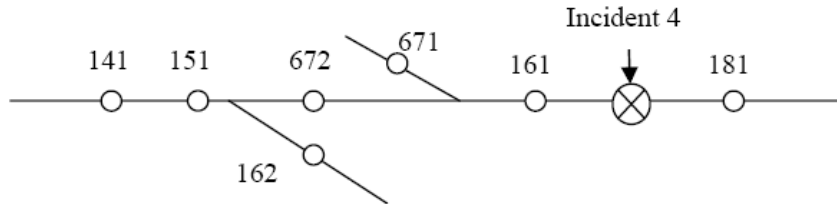


**Figure 29. Location of Incident 4.**

Three off-ramps and two on-ramps upstream of the incident location were affected by the incident including the SR7100 Off-ramp (Station 162), SR28 On-ramp (Station 123), SR28 Off-ramp (Station 122), US29 On-ramp (Station 102) and US29 Off-ramp (Station 694). Rerouting inputs for the relevant ramps are listed in Table 28.

**Table 28. Rerouting Start Time, End Time and Percentage for Incident 4.**

	<b>SR7100 Off (162)</b>	<b>SR28 On (123)</b>	<b>SR28 Off (122)</b>	<b>US29 On (102)</b>	<b>US29 Off (694)</b>
Start Time	8:25	8:45	8:35	8:55	8:45
End Time	8:50	8:55	9:05	9:10	9:05
Percentage	20% more used this ramp	40% fewer used this ramp	10% more used this ramp	40% fewer used this ramp	10% more used this ramp

With this re-routing information, the simulation was conducted. Figures 30 and 31 show the graphical comparison of simulated flow and the detector data. Table 29 presents the MAPE and GEH% for the upstream locations. The data involved in the calculation covered 7:50 a.m. to 9:15 a.m. with a resolution of 5 minutes.

The GEH% results were perfect. However, two of the ramps had MAPE values higher than the threshold, suggesting that additional refinements to the re-routing might be needed. Recall that the re-routing for this study was determined by trial and error. For near-real time use, these values could be estimated by comparing the real time detector data with the OD matrices.

**Table 29. MAPE and GEH% of Incident 4.**

<b>Mainline</b>	<b>161</b>	<b>151</b>	<b>141</b>	<b>121</b>	<b>111</b>	<b>91</b>	<b>61</b>	<b>51</b>
MAPE	10.53%	10.99%	9.35%	11.99%	12.03%	16.61%	13.39%	11.47%
GEH%	100.00%	100.00%	100.00%	100.00%	100.00%	100.00%	100.00%	100.00%
<b>Ramp</b>	<b>162</b>	<b>123</b>	<b>122</b>	<b>102</b>	<b>694</b>			
MAPE	9.61%	13.57%	27.31%	18.77%	20.51%			
GEH%	100.00%	100.00%	100.00%	100.00%	100.00%			

The 4 hour 30 minute simulation period from 5:30 to 10:00, required approximately 30 minutes on the desktop computer starting from an empty network. Comparing among the incidents, one can see that the peak period simulation required more time than the off-peak.

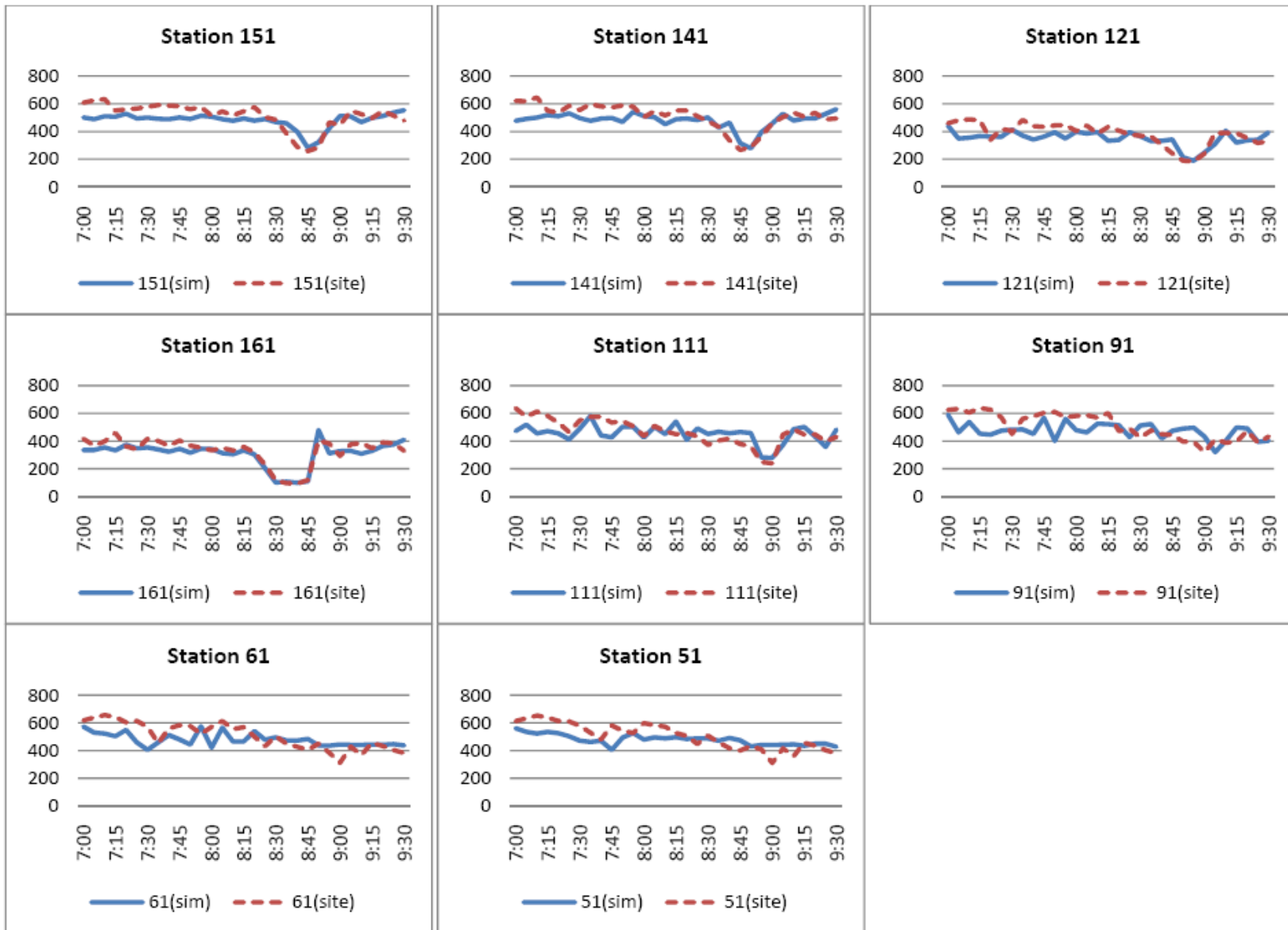


Figure 30. Traffic Counts (veh / 5 min) at Freeway Measurement Stations Upstream of Incident 4.

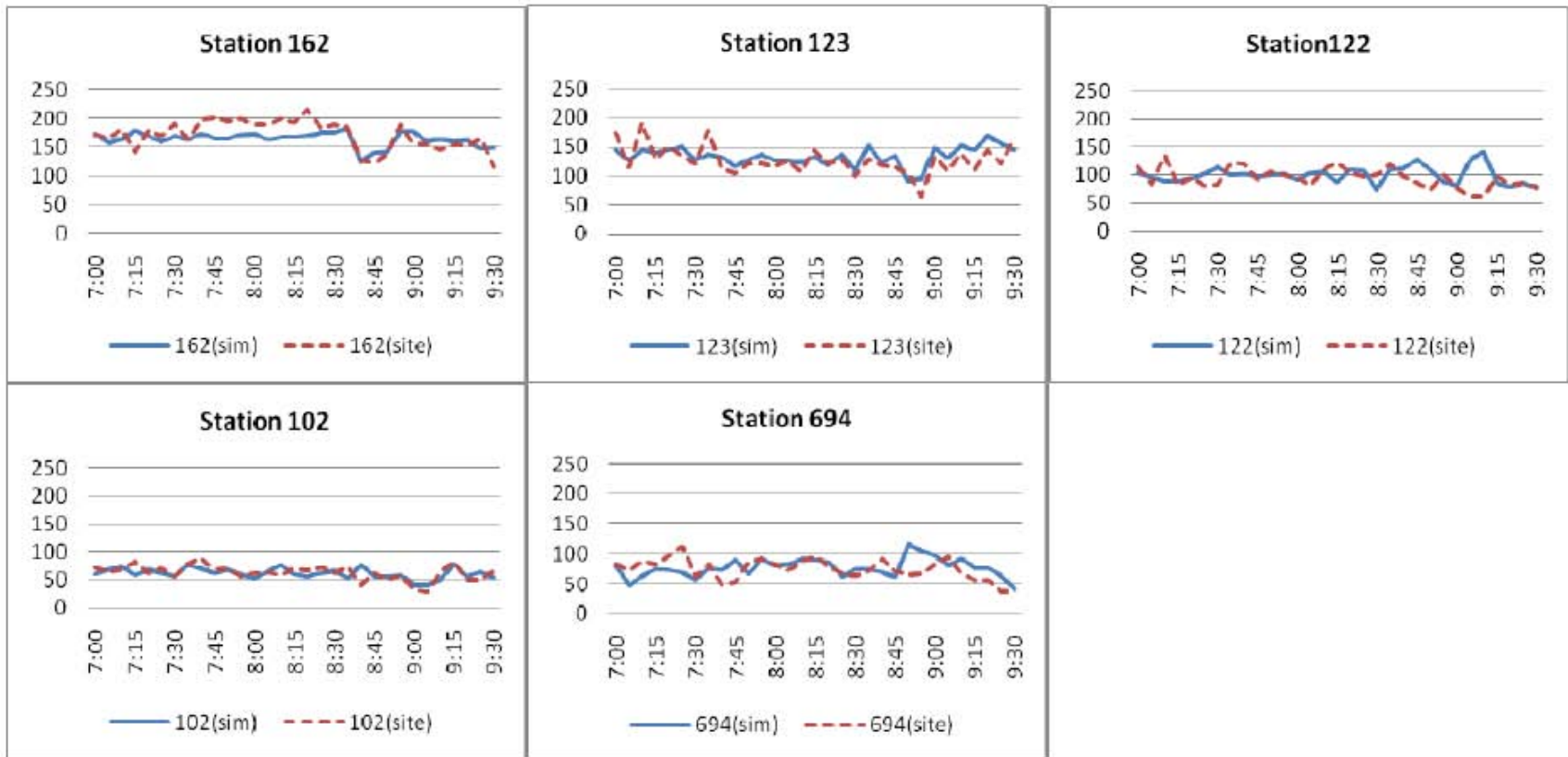


Figure 31. Traffic Counts (veh / 5 min) at Ramps Upstream of Incident 4.

Table 30 presents the travel time excerpt for Incident 4.

**Table 30. Travel Time for Incident 4.**

	0.2	0.4	0.6	0.8	1	1.2	1.4	1.6	1.8	2	2.2	2.4	2.6	2.8	3	3.2	3.4	3.6	3.8	4	4.2	4.4	4.6
8:20	14.31	14.05	15.39	18.37	15.56	16.87	13.12	8.14	5.80	7.98	9.14	10.38	12.13	14.87	15.92	16.24	16.59	19.00	22.27	23.83	24.65	25.11	25.31
8:21	18.82	14.77	14.49	13.90	13.73	12.04	6.81	6.30	7.88	9.20	10.47	11.58	14.47	15.53	15.82	16.58	17.54	20.32	23.29	24.63	24.91	25.37	25.57
8:22	18.84	8.69	6.64	5.31	4.56	5.51	6.62	7.64	9.48	10.87	12.27	13.86	14.78	15.97	17.50	17.88	19.97	21.44	23.48	24.52	24.88	24.96	24.96
8:23	17.19	3.98	4.62	5.51	6.13	7.40	8.36	8.94	10.91	12.61	13.18	14.41	17.30	17.70	19.05	19.89	21.16	22.68	23.45	23.88	24.19	24.44	24.65
8:24	15.93	5.28	6.83	7.08	7.74	9.44	10.08	11.38	11.85	12.45	13.87	16.01	18.24	19.86	20.54	21.52	22.09	22.65	22.83	23.21	23.58	23.76	24.02
8:25	15.12	6.06	8.20	9.37	10.04	11.31	11.08	11.58	12.13	13.19	15.13	17.33	19.76	20.74	21.14	21.46	21.83	22.03	22.35	22.71	22.82	23.09	23.27
8:26	14.57	6.48	9.38	9.91	10.27	11.29	11.86	12.85	14.09	15.10	16.33	18.36	19.92	20.61	20.90	21.14	21.38	21.52	21.83	21.90	22.20	22.30	22.68
8:27	13.87	6.59	9.43	10.54	11.12	12.53	13.09	14.90	15.81	16.50	17.16	18.55	19.62	20.00	20.46	20.52	20.77	21.04	21.06	21.33	21.44	21.70	21.77
8:28	13.38	6.48	10.15	12.27	12.73	14.16	14.83	15.49	16.79	17.54	17.87	18.47	19.00	19.45	19.66	19.96	20.17	20.43	20.59	20.61	20.81	20.81	21.11
8:29	12.40	6.40	10.96	13.66	14.16	15.13	15.65	16.43	17.02	17.67	17.90	18.08	18.40	18.74	19.00	19.20	19.54	19.73	19.90	19.95	20.04	20.11	20.21
8:30	11.53	6.28	11.65	14.65	14.89	15.51	15.96	16.58	16.89	17.08	17.29	17.70	17.86	18.00	18.21	18.58	18.79	18.96	19.07	19.20	19.26	19.42	19.44
8:31	10.87	6.16	11.91	14.55	14.93	15.42	15.83	16.03	16.21	16.45	16.78	16.98	17.21	17.39	17.60	17.73	17.94	18.26	18.29	18.47	18.55	18.66	18.90
8:32	10.34	5.94	11.80	14.40	14.83	15.15	15.11	15.47	15.74	15.91	15.95	16.32	16.52	16.62	16.86	16.91	17.11	17.35	17.69	17.88	17.87	17.84	17.92
8:33	9.90	5.71	11.47	13.87	14.21	14.38	14.58	14.82	14.94	15.13	15.35	15.61	15.80	15.92	16.00	16.12	16.31	16.64	16.80	16.98	17.17	17.23	17.31
8:34	9.06	5.55	11.11	13.18	13.66	13.78	13.93	14.03	14.29	14.44	14.57	14.82	15.02	15.14	15.22	15.33	15.48	15.80	16.05	16.32	16.51	16.81	16.97
8:35	8.14	5.63	10.63	12.45	12.93	13.10	13.14	13.43	13.55	13.69	13.82	13.98	14.22	14.39	14.58	14.69	14.89	14.94	15.27	15.81	16.34	16.62	16.93
8:36	7.49	5.56	10.12	11.72	12.28	12.39	12.54	12.58	12.76	12.92	13.00	13.24	13.45	13.71	13.89	14.00	14.07	14.29	14.63	15.37	16.04	16.84	17.44
8:37	6.70	5.42	9.43	10.94	11.48	11.61	11.68	11.86	11.93	12.05	12.26	12.45	12.81	12.95	13.12	13.29	13.68	13.90	14.30	15.00	16.12	16.97	17.57
8:38	5.93	5.22	8.77	10.08	10.61	10.82	10.88	11.04	11.27	11.31	11.34	11.72	11.99	12.23	12.42	12.76	13.53	14.11	14.42	14.94	16.02	16.90	17.88
8:39	5.20	4.91	8.00	9.24	9.81	9.99	10.12	10.27	10.33	10.57	10.74	10.94	11.26	11.52	12.06	12.56	13.24	14.52	15.12	15.36	15.79	16.96	17.96
8:40	4.54	4.55	7.19	8.39	8.97	9.19	9.24	9.49	9.70	9.74	9.99	10.22	10.70	11.38	11.77	12.38	13.32	14.53	15.65	16.05	16.40	16.86	17.60
8:41	3.72	4.18	6.36	7.55	8.11	8.31	8.45	8.67	8.95	9.09	9.19	9.67	10.47	11.16	11.92	12.60	13.31	14.49	15.76	16.45	16.64	16.77	17.09
8:42	2.93	3.71	5.55	6.70	7.24	7.42	7.62	7.91	8.14	8.36	8.72	9.48	10.38	11.27	12.03	12.70	13.63	14.55	15.57	16.11	16.57	16.76	16.98
8:43	2.19	3.16	4.70	5.85	6.35	6.57	6.80	7.06	7.45	7.82	8.31	9.35	10.97	11.59	12.22	12.87	13.62	14.51	15.21	15.97	16.40	16.76	16.95
8:44	1.39	2.48	3.88	5.02	5.63	5.76	5.93	6.21	6.69	7.49	8.34	9.58	10.99	11.97	12.42	13.00	13.61	14.14	14.89	15.56	16.17	16.55	16.95
8:45	0.63	1.75	3.03	4.16	4.73	4.88	5.11	5.48	6.05	7.00	8.45	9.88	11.13	12.02	12.54	12.89	13.40	14.09	14.71	15.20	15.82	16.51	16.81
8:46	0.21	0.99	2.20	3.32	3.83	4.04	4.29	4.77	5.54	6.63	8.15	9.99	11.03	11.72	12.43	12.88	13.33	13.91	14.46	15.00	15.60	16.03	16.83
8:47	0.11	0.53	1.37	2.48	3.01	3.25	3.57	4.19	5.07	6.31	7.77	9.52	10.82	11.46	12.15	12.85	13.28	13.79	14.41	14.81	15.24	15.97	16.25
8:48	0.11	0.29	0.81	1.67	2.25	2.44	2.88	3.77	4.81	6.05	7.42	9.02	10.54	11.36	11.73	12.52	13.51	13.90	14.30	14.79	15.07	15.41	15.92
8:49	0.11	0.29	0.49	1.04	1.48	1.79	2.34	3.31	4.57	5.77	7.05	8.57	10.15	11.15	11.63	12.15	13.17	14.01	14.30	14.55	14.78	15.14	15.48
8:50	0.11	0.29	0.47	0.73	0.96	1.42	2.02	2.97	4.29	5.51	6.64	8.12	9.68	10.78	11.56	12.03	12.70	13.59	14.21	14.41	14.70	15.23	15.69

When the location and time were determined, the corresponding travel time could be directly read from the table. The table not only provided the travel time during the incident clearance period but also in the queue dissipation period until the flow recovered to the normal condition.

### Queue Length and Dissipation

The end of queue propagation was when the queue reached the farthest location and the corresponding time was the initial time of queue dissipation. The end time of queue dissipation was when the queue was cleared and flow recovered to the normal conditions. This time information could be determined from the speed contour plots and be arranged in a graph, such as that shown in Figure 32, indicating the length of the queue over time.

As can be seen from Figure 32, the maximum queue length was approximately 1.4 miles. The queue built over 70 minutes and then began to dissipate at 14:15.

Queue dissipation could also be determined from the speed contour plots. When the speed returned to free flow conditions, the queue could be considered dissipated.

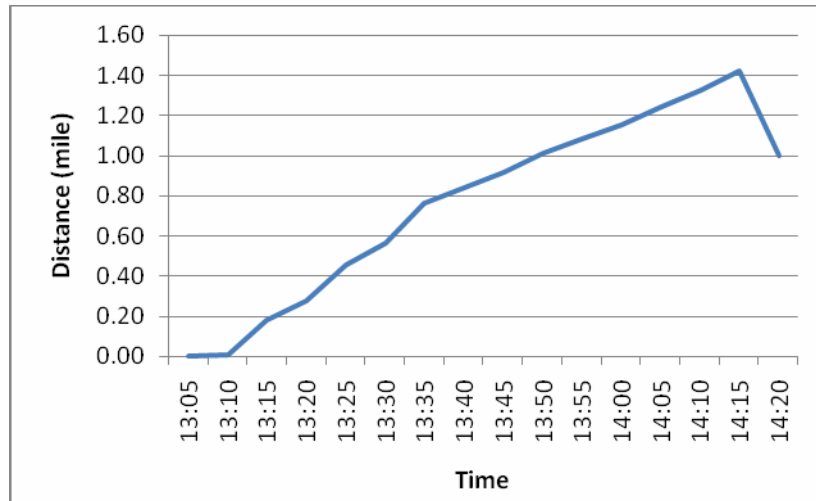


Figure 32. Queue Length and Beginning Recovery for Incident 2.

### Using the Model for Off-Line Simulation

For off-line simulation, all of the inputs were known ahead of time, and the model could be run as previously described. Off-line simulation could be useful for understanding the effects of incidents, whether real or hypothetical.

### Using the Model for Near-Real Time Simulation

To determine the travel time after the incident has been cleared, the incident duration was known and the model could be run as previously described. However, if one desired to run the model during the incident, an estimated incident clearance time could be used. To determine such an estimate, a statistical analysis of several years' incidents could yield an estimate, possibly stratified by incident type, severity, time of day, and number of lanes blocked. Using the estimate, the model could be run and snapshots saved. The snapshots capture all details (e.g., origin, destination, location, speed, etc.) of the vehicles in the network in plain text files that can be saved locally. When the estimate needs to be revised, or the lane blockages changed, the model could be re-run. If the model were still running when the change needed to be made, the "stop" button on the revised interface (not illustrated here) could be used. The new data could then be loaded into the interface or using the file approach. The latest snapshots reflecting the true input conditions could be used with the interface.

## DISCUSSION

The majority of the discussion of the results was presented in the previous section for reading ease. The results indicated that the developed CA model could reproduce speeds and queues found in the analysis of detector information. By tracking each vehicle, the CA model can provide queue lengths and travel times, based on information about the network conditions, such as normal or incident, with the starting time and lane operability.

Additional refinement of incident related parameters would yield more robust parameter values. In particular, the rerouting parameters for incident conditions should be distance or location based and depend on the number of lanes blocked by the incident; however, rerouting was not part of this study. Multiple sets of basic parameters might also be desired in the future to reflect light, “normal,” and heavy traffic days for a particular day of the week.

Another future direction for this work is the incorporation of multiple vehicle types, their OD matrices, and specific rules regarding their behavior. In particular HOV and truck designations could be added.

In addition to the re-routing issue, this study encountered two major difficulties. First, no incident-free day existed for I-66 in 2007; this created a challenge in determining the “typical” flows and corresponding OD tables. Second, detector data were unreliable at times, as indicated by missing data or values that were inconsistent with the network structure. These two challenges required an unanticipated amount of manual work.

## CONCLUSIONS

- The literature review indicated that some macroscopic approaches could capture congestion in portions of the freeway as reflected in detector data; however, these approaches typically had difficulties in the presence of ramps. A study that compared field travel times to those estimated by shockwave analysis and queuing theory revealed underestimated travel time. To avoid these discrepancies, this study examined the cellular automaton microscopic simulation approach. The developed models were capable of reproducing the daily congestion pattern.
- Using the parameters calibrated on the base models and a special set of additional parameters, incidents were successfully simulated in terms of queue propagation speed, distance, and duration. Travel time from any location upstream to the incident zone was estimated by analyzing data for all relevant vehicles. In the case where an incident blocks all lanes, no vehicles were able to pass the incident location and travel times to the off-ramps can be estimated instead.
- Travel time variation collected from the vehicles generally followed expectations from practical experience. Travel time could be directly read from the tables or figures and provided to drivers delayed by the incident.
- In the future, this CA approach, with a few refinements to the parameters, should be subjected to the same testing as the shockwave analysis and queuing theory to determine the accuracy of the results.

## RECOMMENDATIONS

1. *VDOT, particularly the Virginia Transportation Research Council, should further pursue the use of cellular automata approaches for near-real time applications along freeways.* In this initial study, a full 24 hours with roughly 202,000 vehicles was simulated in approximately 90 minutes on a 2006 computer. More efficient coding and data structures as well as faster computers and parallel processing could further improve this speed. Even in its current implementation, especially with the strategy of saving the network state every few minutes, the simulation speed offered great potential for near-real time issues and predictions.
2. *VDOT, particularly the Operations and Security Division, should consider researching or adopting an approach to address detector failures and errors.* A key difficulty encountered in this study that would carry over into any application that used detector information as a major input was that detectors were not perfect sources of information. These devices failed from time to time and could provide erroneous data. Any application that interfaced with the detectors would need an input error checking module that included a method to interpolate the missing or flawed data point(s) from surrounding, functioning detectors.

## COSTS AND BENEFITS ASSESSMENT

Providing accurate information to motorists is a priority for VDOT. Numerous studies have indicated that travel times in particular, are considered valuable to motorists. Incident conditions can significantly complicate the estimation of travel times, particularly as queues build and then dissipate throughout the incident response. Although the tool developed in this study does not attempt to estimate incident duration (with respect to how long lanes will remain closed), it does provide estimates of travel time, as well as an estimate of how long it will take for the queues to dissipate once the lanes are clear, if those parameters are input by the user. Incident characteristics can also be updated as the response continues with revised travel time estimates generated. This tool could become an important component of VDOT's incident management process, providing additional information that could then be distributed on dynamic message signs, 511, and through private media outlets. In the Northern Virginia region it is estimated that incident-induced congestion resulted in over 68 million person-hours of delay in 2007. If this tool and the information it could provide to motorists could eliminate just a fraction of that delay by delaying or diverting trips, significant improvements in mobility would be possible.

As mentioned in earlier sections of this report, there are enhancements to the tool that would improve both the ease of use and the technical robustness of the method. Opportunities to develop and implement these enhancements will be sought through the System Operations Research Advisory Committee process.

## ACKNOWLEDGMENTS

The authors appreciate the opportunity provided by VDOT and the Virginia Transportation Research Council to conduct this study. Specifically, we thank Cathy McGhee for her patience and support.

## REFERENCES

- Ahmed, K.I. *Modeling Drivers' Acceleration and Lane Changing Behavior*. Thesis: Doctor of Science, Department of Civil and Environmental Engineering, Massachusetts Institute of Technology, 1999.
- Barlovic, R., Santen, L., Schadschneider, A. and Schreckenberg, M. Metastable States in Cellular Automata for Traffic Flow. *European Physical Journal B*, Vol. 5, No. 3, 1998, pp. 793-800.
- Benjamin, S.C., Johnson, N.F. and Hui, P.M. Cellular Automata Models of Traffic Flow along a Highway Containing a Junction. *Journal of Physics A: Mathematical and General*, Vol. 29, 1996, pp. 3119-3127.
- Booz Allen Hamilton. *Intelligent Transportation Systems Field Operational Test Cross-Cutting Study: Incident Management: Detection, Verification, and Traffic Management*, 1998. [http://www.itsdocs.fhwa.dot.gov/jpodocs/repts\\_te/6328.pdf](http://www.itsdocs.fhwa.dot.gov/jpodocs/repts_te/6328.pdf). Accessed February 13, 2007.
- Brockfeld, E., Barlovic, R., Schadschneider, A. and Schreckenberg, M. Optimizing Traffic Lights in a Cellular Automaton Model for City Traffic. *Physical Review E (Statistical, Nonlinear, and Soft Matter Physics)*, Vol. 64, No. 5, 2001, pp. 056132-1.
- Campari, E.G. and Levi, G. A Cellular Automata Model for Highway Traffic. *European Physical Journal B*, Vol. 17, No. 1, 2000, pp. 159-66.
- Chowdhury, D., Wolf, D.E. and Schreckenberg, M. Particle Hopping Models for Two-Lane Traffic with Two Kinds of Vehicles: Effects of Lane-Changing Rules. *Physica A: Statistical Mechanics and its Applications*, Vol. 235, No. 3-4, 1997, pp. 417-439.
- Choudhury, C.F. *Modeling Lane-changing Behavior in Presence of Exclusive Lanes*. Thesis: Master of Science in Transportation, Department of Civil and Environmental Engineering, Massachusetts Institute of Technology, 2005.
- Chu, L., Liu, H. X., Oh, J.-S., and Recker, W. A Calibration Procedure for Microscopic Traffic Simulation, *TRB Annual Meeting CD-ROM*, 2004.
- Coifman, B. Estimating Travel Times and Vehicle Trajectories on Freeways Using Dual Loop Detectors. *Transportation Research, Part A (Policy and Practice)*, Vol. 36A, No. 4, 2002, pp. 351-64.

- Corbin, J., Vásconez, K. and Helman, D. Unifying Incident Response. *Public Roads*, Vol. 71, No. 2, 2007. <http://www.tfhr.gov/pubrds/07sep/04.htm>.
- Cremer, M. and Ludwig, J. A Fast Simulation Model for Traffic Flow on the Basis of Boolean Operations. *Mathematics and Computers in Simulation*, Vol. 28, No. 4, 1986, pp. 297-303.
- Diedrich, G., Santen, L., Schadschneider, A. and Zittartz, J. Effect of On- and Off-ramps in Cellular Automata Models for Traffic Flow. *International Journal of Modern Physics C: Computational Physics and Physical Computation*, Vol. 11, No. 2, 2000, pp. 335-345.
- Ez-Zahraouy, H., Benrihane, Z. and Benyoussef, A. The Effect of Off-ramp on the One-Dimensional Cellular Automaton Traffic Flow with Open Boundaries. *International Journal of Modern Physics B*, Vol. 18, No. 16, 2004, pp. 2347-60.
- Fouladvand, M.E. and Lee, H.W. Exactly Solvable Two-Way Traffic Model with Ordered Sequential Update. *Physical Review E (Statistical Physics, Plasmas, Fluids, and Related Interdisciplinary Topics)*, Vol. 60, No. 6, 1999, pp. 6465-79.
- Garib, A., Radwan, A.E. and Al-Deek, H. Estimating Magnitude and Duration of Incident Delays. *Journal of Transportation Engineering*, Vol. 123, No. 6, 1997, pp. 459-466.
- Giuliano, G. Incident Characteristics, Frequency, and Duration on a High Volume Urban Freeway. *Transportation Research – A*, Vol. 23A, No. 5, 1989, pp. 387-396.
- Gomes, G., Might, A. and Horowitz, R. Congested Freeway Microsimulation Model Using VISSIM. *Transportation Research Record 1876*, Transportation Research Board, Washington, DC, 2004, pp. 71-81.
- Hafstein, S.F., Chrobok, R., Pottmeier, A., Schreckenberg, M. and Mazur, F.C. A High-Resolution Cellular Automata Traffic Simulation Model with Application in a Freeway Traffic Information System. *Computer-Aided Civil and Infrastructure Engineering*, Vol. 19, No. 5, 2004, pp. 338-350.
- Highways Agency. *Design Manual for Roads and Bridges - Volume 12*, 1996. <http://www.standardsforhighways.co.uk/dmrb/>.
- Hobeika, A. and Dhulipala, S. Estimation of Travel Times on Urban Freeways under Incident Conditions. *Transportation Research Record 1867*, Transportation Research Board, Washington, DC, 2004, pp. 97-106.
- Transportation Research Board. *Highway Capacity Manual 2000*. Transportation Research Board, 2000.
- IMS Incident Management System, <https://vdotim.cattlab.umd.edu/index.php>. Accessed January 27, 2008.

- Jia, B., Jiang, R. and Wu, Q. The Traffic Bottleneck Effects Caused by the Lane Closing in the Cellular Automata Model. *International Journal of Modern Physics C*, Vol. 14, No. 10, 2003, pp. 1295-303.
- Jia, B., Jiang, R. and Wu, Q. Traffic Behavior Near an Off Ramp in the Cellular Automaton Traffic Model. *Physical Review E (Statistical Physics, Plasmas, Fluids, and Related Interdisciplinary Topics)*, Vol. 69, No. 5, 2004, pp. 056105-1.
- Jia, B., Jiang, R., Wu, Q. and Hu, M. Honk Effect in the Two-Lane Cellular Automaton Model for Traffic Flow. *Physica A: Statistical Mechanics and its Applications*, Vol. 348, March, 2005, pp. 544-552.
- Jia, B., Jiang, R. and Wu, Q. The Effects of Accelerating Lane in the On-Ramp System. *Physica A: Statistical Mechanics and its Applications*, Vol. 345, No. 1-2, 2005, pp. 218-226.
- Jia, B., Gao, Z., Li, K. and Li, X. *Models and Simulations of Traffic System Based on the Theory of Cellular Automaton*. Science Publication, Beijing, 2007.
- Jiang, R., Wu, Q. and Wang, B. Cellular Automata Model Simulating Traffic Interactions between On-Ramp and Main Road. *Physical Review E (Statistical Physics, Plasmas, Fluids, and Related Interdisciplinary Topics)*, Vol. 66, No. 3, 2002, pp. 036104-1.
- Jiang, R. and Wu, Q. Cellular Automata Models for Synchronized Traffic Flow. *Physica A: Statistical Mechanics and its Applications*, Vol. 36, 2003, pp. 381-390.
- Jiang, R., Jia, B. and Wu, Q. The Stochastic Randomization Effect in the On-Ramp System Single-Lane Main Road and Two-Lane Main Road Situations. *Journal of Physics A: Mathematical and General*, Vol. 36, 2003, pp. 11713-11723.
- Khan, A.M. Intelligent Infrastructure-Based Queue-End Warning System for Avoiding Rear Impacts. *IET Intelligent Transport Systems*, Vol. 1, No. 2, 2007, pp.138-143.
- Khattak, A.J., Schofer, J.L. and Wang, M. A Simple Time Sequential Procedure for Predicting Freeway Incident Duration. *IVHS Journal*, Vol. 2, No. 2, 1995, pp. 113-138.
- Knospe, W., Santen, L., Schadschneider, A. and Schreckenberg, M. Disorder Effects in Cellular Automata for Two-Lane Traffic. *Physica A: Statistical Mechanics and its Applications*, Vol. 265, No. 3, 1999, pp. 614-633.
- Knospe, W., Santen, L., Schadschneider, A. and Schreckenberg, M. Towards a Realistic Microscopic Description of Highway Traffic. *Journal of Physics A: Mathematical and General*, Vol. 33, No. 48, 2000, pp. L477-L485.

- Larraga, M.E., del Rio, J.A. and Alvarez-Icaza, L. Cellular Automata for One-Lane Traffic Flow Modeling. *Transportation Research Part C: Emerging Technologies*, Vol. 13, No. 1, 2005, pp. 63-74.
- Lawson, T.W., Lovell, D.J. and Daganzo, C.F. Using Input-Output Diagram to Determine Spatial and Temporal Extents of a Queue Upstream of a Bottleneck. *Transportation Research Record 1572*, Transportation Research Board, Washington, DC, 1996, pp.140-147.
- Li, X., Jia, B., Gao, Z. and Jiang, R. A Realistic Two-Lane Cellular Automata Traffic Model Considering Aggressive Lane-Changing Behavior of Fast Vehicle. *Physica A: Statistical Mechanics and its Applications*, Vol. 367, 2006, pp. 479-486.
- Li, X., Wu, Q. and Jiang, R. Cellular Automaton Model Considering the Velocity Effect of a Car on the Successive Car. *Physical Review E (Statistical Physics, Plasmas, Fluids, and Related Interdisciplinary Topics)*, Vol. 64, No. 6, 2001, pp. 066128.
- Liu, M. *Traffic Flow Modeling and Forecasting Using Cellular Automata and Neural Networks*. Thesis: Master of Science, Computer Science, Palmerston North, Massey University, 2006.
- Munoz, J.C. and Daganzo, C.F. Structure of the Transition Zone Behind Freeway Queues. *Transportation Science*, Vol. 37, No. 3, 2003, pp. 312-29.
- Nagel, K. and Schreckenberg, M. A Cellular Automaton Model for Freeway Traffic. *Journal De Physique I France*, Vol. 2, 1992, pp. 2221-2229.
- Nagel, K., Wolf, D.E., Wagner, P. and Simon, P. Two-Lane Traffic Rules for Cellular Automata: a Systematic Approach. *Physical Review E (Statistical Physics, Plasmas, Fluids, and Related Interdisciplinary Topics)*, Vol. 58, No.2, 1998, pp.1425-1437.
- Nam, D.H. and Drew, D.R. Automatic Measurement of Traffic Variables for Intelligent Transportation Systems Applications. *Transportation Research, Part B (Methodological)*, Vol. 33B, No. 6, 1999, pp. 437-457.
- Nam, D. and Mannering, F. An Exploratory Hazard-Based Analysis of Highway Incident Duration. *Transportation Research – A*, Vol. 34A, No. 2, 2000, pp. 85-102.
- Nassab, K., Schreckenberg, M., Boulmakoul, A. and Ouaskit, S. Effect of the Lane Reduction in the Cellular Automata Models Applied to the Two-Lane Traffic. *Physica A: Statistical Mechanics and its Applications*, Vol. 369, No. 2, 2006, pp. 841-852.
- Oh, J., Jayakrishnan, R., Recker, W. Section Travel Time Estimation from Point Detection Data. *TRB Annual Meeting CD-ROM*, Washington DC, 2003.

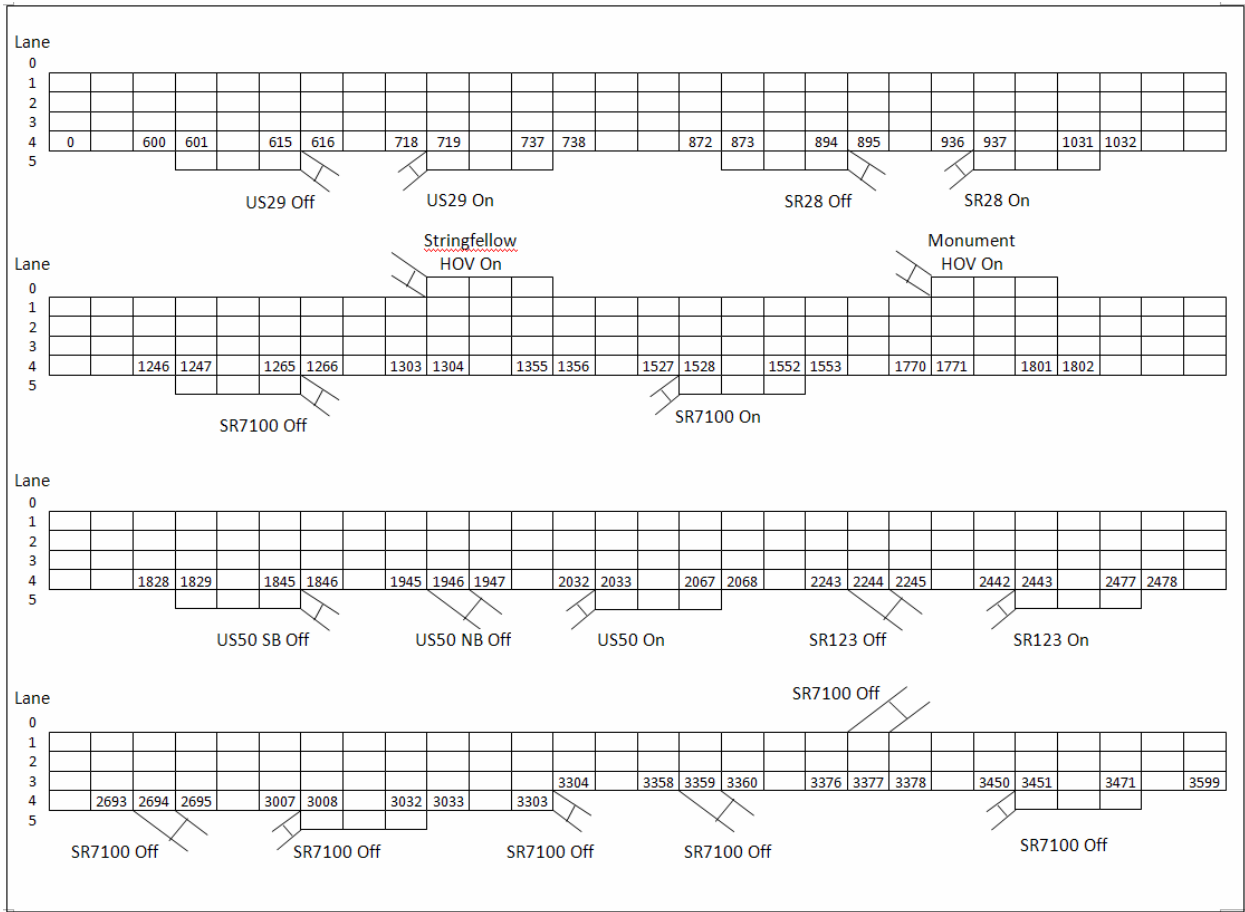
- Ozbay, K. and Kachroo, P. *Incident Management in Intelligent Transportation Systems*. Artech House, Inc., Boston, 1999.
- Park, B. and Qi, H. *Microscopic Simulation Model Calibration and Validation for Freeway Work Zone Network - a Case Study of VISSIM*, IEEE, Piscataway, NJ, 2006.
- Pearce, V. and Subramaniam, S. *Intelligent Transportation Systems. Field Operational Test Cross-Cutting Study: Incident Management - Detection, Verification, and Traffic Management*. FHWA-RD-JPO-034. United States, 1998.
- Petty, K.F., Bickel, P., Ostland, M., Rice, J., Schoenberg, F., Jiming, J. and Ritov, Y. Accurate Estimation of Travel Times from Single-Loop Detectors. *Transportation Research, Part A (Policy and Practice)*, Vol. 32A, No. 1, 1998, pp. 1-17.
- Rakha, H. and Zhang, W. Consistency of Shock-wave and Queuing Theory Procedures for Analysis of Roadway Bottlenecks. *TRB Annual Meeting CD-ROM*, Washington DC, 2005.
- Rickert, M., Nagel, K., Schreckenberg, M. and Latour, A. Two Lane Traffic Simulations Using Cellular Automata. *Physica A: Statistical Mechanics and its Applications*, Vol. 231, No. 4, 1996, pp. 534-550.
- Schadschneider, A. and Schreckenberg, M. Traffic Flow Models with 'Slow-to-Start' Rules. *Annalen der Physik* Vol. 6, 1999, pp. 541-551.
- Schrank, D. and Lomax, T. *2007 Urban Mobility Report*. United States, 2007.
- Simon, P.M. and Gutowitz, H.A. Cellular Automaton Model for Bidirectional Traffic. *Physical Review E (Statistical Physics, Plasmas, Fluids, and Related Interdisciplinary Topics)*, Vol. 57, No. 2, 1998, pp. 2441-4.
- Smith, K. and Smith, B.L. *Forecasting the Clearance Time of Freeway Accidents*. UVACTS-15-0-35. United States, 2001.
- Sullivan, E.C. New Model for Predicting Incidents and Incident Delay. *ASCE Journal of Transportation Engineering*, Vol. 123, 1997, pp. 267-275.
- Takayasu, M. and Takayasu, H.  $1/f$  Noise in a Traffic Model. *Fractals*, Vol. 1, 1993, pp. 860-866.
- TrafficLand. <http://trafficland.com/city/WAS/index.html>. Accessed November 17, 2008.
- Ulam, S. Random Process and Transformations. *Proceedings of the International Congress on Mathematics*, Vol. 2, 1952, pp. 264-275.

- Van Aerde, M. & Assoc. *QUEENSOD Rel. 2.10 - User's Guide: Estimating Origin - Destination Traffic Demands from Link Flow Counts*, M. Van Aerde and Associates, Ltd., Blacksburg, Virginia, 2005.
- Vanajakshi, L.D. *Estimation and Prediction of Travel Time from Loop Detector Data Intelligent Transportation Systems Applications*. Dissertation: Doctor of Philosophy, Civil Engineering, Texas A&M University, 2004.
- VDOT. *High Occupancy Vehicle (HOV) Systems*, <http://www.virginiadot.org/travel/hov-novasched.asp>. Accessed December 29, 2008.
- Wei, C. and Lee, Y. Sequential Forecast of Incident Duration Using Artificial Neural Network Models. *Accident Analysis and Prevention*, Vol. 39, No. 5, 2007, pp. 944-954.
- Wolfram, S. Statistical Mechanics of Cellular Automata. *Reviews of Modern Physics*, Vol. 55, No. 3, 1983, pp. 601 - 644.
- Xia, J. and Chen, M. *Freeway Travel Time Forecasting Under Incident*. University of Kentucky, Lexington, KY, 2007.
- Yeon, J. and Elefteriadou, L. Comparison of Travel Time Estimation Using Three Previously Developed Methods to Field Data Along Freeways. *5th International Symposium on Highway Capacity and Quality of Service*, 2006, pp. 229-238.
- Zhu, L.-H., Chen, S.-D., Kong, L.-J. and Liu, M.-R. The Influence of Tollbooths on Highway Traffic. *Acta Physica Sinica*, Vol. 56, No. 10, 2007, pp. 5674-8.



# APPENDIX A

## CELL LOOK UP FIGURE





## APPENDIX B

### STATION STDEV AND RELATIVE LSE BEFORE AND AFTER DATA PROCESSING FOR THE OTHER DAYS OF THE WEEK

<b>Monday</b>							
<b>Mainline</b>	<b>61</b>	<b>111</b>	<b>121</b>	<b>141</b>	<b>672</b>	<b>161</b>	<b>191</b>
STDEV Before	43.51	45.36	34.43	51.32	36.49	36.00	45.13
STDEV After	25.75	25.90	21.96	27.74	24.08	22.89	27.68
LSE Before	23.95%	24.42%	24.28%	24.13%	25.38%	23.12%	26.72%
LSE After	15.81%	15.75%	17.25%	14.73%	17.95%	16.00%	17.76%
Deletion%	5.00%	5.47%	3.82%	5.76%	4.61%	3.80%	6.50%
<b>Mainline</b>	<b>211</b>	<b>221</b>	<b>231</b>	<b>261</b>	<b>291</b>	<b>351</b>	
STDEV Before	53.54	39.24	56.10	48.49	45.63	49.54	
STDEV After	35.66	23.97	29.37	27.73	26.42	28.94	
LSE Before	31.58%	23.75%	22.00%	22.64%	23.27%	22.08%	
LSE After	21.88%	15.44%	12.70%	13.77%	14.38%	13.67%	
Deletion%	11.41%	4.04%	6.50%	8.03%	5.34%	6.13%	
<b>Ramp</b>	<b>102</b>	<b>122</b>	<b>123</b>	<b>162</b>	<b>173</b>	<b>212</b>	<b>623</b>
STDEV Before	9.92	11.90	18.11	9.14	4.23	6.10	3.05
STDEV After	6.89	9.80	14.74	8.39	4.18	5.64	3.05
LSE Before	43.65%	29.95%	24.47%	31.90%	45.63%	46.68%	51.13%
LSE After	36.72%	26.11%	20.33%	30.34%	45.37%	45.29%	51.13%
Deletion%	0.78%	3.08%	2.24%	0.92%	0.05%	0.96%	0.09%
<b>Ramp</b>	<b>222</b>	<b>273</b>	<b>342</b>	<b>386</b>	<b>388</b>		
STDEV Before	23.05	6.21	9.25	23.25	15.25		
STDEV After	17.14	5.96	8.50	8.72	6.11		
LSE Before	23.73%	40.80%	31.61%	51.47%	53.68%		
LSE After	18.73%	40.11%	30.22%	26.88%	33.56%		
Deletion%	2.80%	0.29%	1.06%	3.41%	4.34%		

<b>Tuesday</b>							
<b>Mainline</b>	<b>61</b>	<b>111</b>	<b>121</b>	<b>141</b>	<b>672</b>	<b>161</b>	<b>191</b>
STDEV Before	46.13	46.47	35.99	50.23	38.73	36.46	48.60
STDEV After	25.48	25.69	21.89	27.54	24.04	22.88	27.94
LSE Before	25.30%	25.35%	26.06%	24.38%	26.54%	23.52%	27.92%
LSE After	15.58%	15.57%	17.62%	14.39%	18.00%	16.04%	17.83%
Deletion%	5.97%	5.87%	4.34%	5.79%	5.22%	4.01%	7.60%
<b>Mainline</b>	<b>211</b>	<b>221</b>	<b>231</b>	<b>261</b>	<b>291</b>	<b>351</b>	
STDEV Before	54.36	37.46	57.14	50.31	46.31	51.78	
STDEV After	36.20	23.31	29.04	27.94	26.56	28.80	
LSE Before	31.56%	23.40%	22.36%	23.00%	23.68%	22.72%	
LSE After	21.92%	15.26%	12.35%	13.44%	14.25%	13.44%	
Deletion%	11.95%	3.59%	6.73%	6.05%	5.15%	5.97%	
<b>Ramp</b>	<b>102</b>	<b>122</b>	<b>123</b>	<b>162</b>	<b>173</b>	<b>212</b>	<b>623</b>
STDEV Before	7.92	11.89	19.84	9.36	4.38	6.88	3.15
STDEV After	7.03	10.08	15.32	8.21	4.27	5.67	3.10
LSE Before	37.48%	30.14%	26.23%	32.43%	48.42%	49.44%	50.12%
LSE After	34.67%	27.06%	20.95%	29.68%	47.99%	45.59%	49.88%
Deletion%	0.83%	1.36%	2.58%	0.99%	0.04%	0.88%	0.03%
<b>Ramp</b>	<b>222</b>	<b>273</b>	<b>342</b>	<b>386</b>	<b>388</b>		
STDEV Before	23.34	6.48	10.13	29.29	21.76		
STDEV After	16.93	6.29	8.94	9.23	6.36		
LSE Before	23.55%	41.54%	32.69%	61.54%	67.83%		
LSE After	18.01%	41.00%	30.39%	28.48%	35.43%		
Deletion%	2.46%	0.17%	1.07%	4.16%	4.38%		

<b>Wednesday</b>							
<b>Mainline</b>	<b>61</b>	<b>111</b>	<b>121</b>	<b>141</b>	<b>672</b>	<b>161</b>	<b>191</b>
STDEV Before	48.23	48.57	38.91	53.78	43.12	40.89	52.74
STDEV After	27.28	27.02	23.24	29.02	25.61	24.19	29.32
LSE Before	25.76%	25.70%	27.15%	25.18%	28.66%	25.77%	29.02%
LSE After	16.68%	16.45%	18.73%	15.24%	19.03%	16.84%	18.33%
Deletion%	6.06%	6.51%	5.25%	6.91%	6.65%	5.30%	8.91%
<b>Mainline</b>	<b>211</b>	<b>221</b>	<b>231</b>	<b>261</b>	<b>291</b>	<b>351</b>	
STDEV Before	56.32	39.36	63.18	55.47	50.94	57.03	
STDEV After	36.86	25.29	30.61	29.62	28.61	30.68	
LSE Before	32.79%	23.92%	23.55%	24.42%	24.79%	24.03%	
LSE After	22.14%	15.93%	12.84%	14.03%	14.92%	13.98%	
Deletion%	12.25%	4.30%	8.59%	8.20%	6.62%	8.09%	
<b>Ramp</b>	<b>102</b>	<b>122</b>	<b>123</b>	<b>162</b>	<b>173</b>	<b>212</b>	<b>623</b>
STDEV Before	8.37	11.98	20.43	10.26	5.08	7.09	3.21
STDEV After	7.28	10.09	16.12	9.01	4.93	5.88	3.21
LSE Before	39.09%	30.33%	26.21%	34.49%	52.49%	50.13%	50.04%
LSE After	35.86%	27.06%	21.02%	31.94%	51.65%	46.29%	50.04%
Deletion%	1.15%	1.97%	2.91%	1.40%	0.16%	1.42%	0.00%
<b>Ramp</b>	<b>222</b>	<b>273</b>	<b>342</b>	<b>386</b>	<b>388</b>		
STDEV Before	24.77	7.41	10.66	17.87	10.80		
STDEV After	18.64	6.48	9.63	10.26	7.10		
LSE Before	24.55%	43.94%	32.48%	48.13%	52.90%		
LSE After	19.08%	41.50%	30.67%	30.47%	40.77%		
Deletion%	2.96%	0.85%	1.15%	2.93%	2.08%		

<b>Thursday</b>							
<b>Mainline</b>	<b>61</b>	<b>111</b>	<b>121</b>	<b>141</b>	<b>672</b>	<b>161</b>	<b>191</b>
STDEV Before	43.35	43.42	32.46	51.19	39.18	36.82	47.28
STDEV After	26.46	26.04	22.24	28.57	25.45	24.42	28.77
LSE Before	24.28%	23.84%	24.99%	23.88%	26.97%	24.44%	27.13%
LSE After	15.81%	15.26%	17.03%	14.28%	18.25%	16.25%	17.46%
Deletion%	4.82%	4.88%	3.29%	5.83%	5.52%	3.75%	7.02%
<b>Mainline</b>	<b>211</b>	<b>221</b>	<b>231</b>	<b>261</b>	<b>291</b>	<b>351</b>	
STDEV Before	55.20	38.53	56.06	51.81	48.70	50.46	
STDEV After	39.03	24.62	31.00	30.37	28.39	29.92	
LSE Before	31.79%	23.28%	21.41%	23.04%	27.03%	21.37%	
LSE After	22.83%	14.97%	12.26%	13.96%	14.28%	13.08%	
Deletion%	11.19%	4.03%	6.72%	6.27%	5.41%	5.91%	
<b>Ramp</b>	<b>102</b>	<b>122</b>	<b>123</b>	<b>162</b>	<b>173</b>	<b>212</b>	<b>623</b>
STDEV Before	7.57	10.82	18.20	9.50	4.39	7.12	3.30
STDEV After	6.86	9.68	14.96	8.66	4.30	5.81	3.28
LSE Before	35.66%	27.65%	23.82%	31.76%	47.25%	48.83%	50.99%
LSE After	33.05%	25.36%	19.78%	29.82%	46.87%	44.77%	50.92%
Deletion%	0.71%	0.94%	1.80%	0.86%	0.06%	1.22%	0.01%
<b>Ramp</b>	<b>222</b>	<b>273</b>	<b>342</b>	<b>386</b>	<b>388</b>		
STDEV Before	23.88	6.59	10.00	11.40	7.28		
STDEV After	17.94	6.33	8.98	9.28	6.74		
LSE Before	23.47%	39.86%	29.90%	30.94%	37.15%		
LSE After	18.31%	38.47%	28.00%	26.56%	35.69%		
Deletion%	2.30%	0.24%	1.06%	1.63%	0.75%		

<b>Saturday</b>							
<b>Mainline</b>	<b>61</b>	<b>111</b>	<b>121</b>	<b>141</b>	<b>672</b>	<b>161</b>	<b>191</b>
STDEV Before	35.07	35.34	29.16	39.73	30.77	31.13	38.03
STDEV After	26.98	27.20	23.11	29.31	24.39	24.89	28.26
LSE Before	23.14%	22.75%	25.08%	21.02%	24.46%	22.44%	22.58%
LSE After	18.54%	18.14%	20.96%	16.13%	19.95%	18.39%	17.85%
Deletion%	3.97%	4.02%	3.39%	4.55%	3.45%	3.08%	5.11%
<b>Mainline</b>	<b>211</b>	<b>221</b>	<b>231</b>	<b>261</b>	<b>291</b>	<b>351</b>	
STDEV Before	48.52	32.05	45.17	40.31	38.83	42.02	
STDEV After	36.84	25.19	30.54	27.84	28.08	28.86	
LSE Before	28.25%	20.58%	18.30%	18.45%	19.49%	17.92%	
LSE After	22.14%	16.75%	13.21%	13.74%	14.86%	13.19%	
Deletion%	10.22%	3.35%	5.84%	4.46%	4.40%	4.96%	
<b>Ramp</b>	<b>102</b>	<b>122</b>	<b>123</b>	<b>162</b>	<b>173</b>	<b>212</b>	<b>623</b>
STDEV Before	7.20	8.07	14.75	7.77	4.54	6.96	4.56
STDEV After	6.83	7.83	12.95	7.51	4.54	4.88	4.42
LSE Before	33.80%	26.93%	19.97%	31.49%	44.62%	50.06%	51.85%
LSE After	32.92%	26.41%	18.21%	30.32%	44.62%	42.97%	51.37%
Deletion%	0.56%	0.33%	1.12%	0.26%	0.00%	1.73%	0.14%
<b>Ramp</b>	<b>222</b>	<b>273</b>	<b>342</b>	<b>386</b>	<b>388</b>		
STDEV Before	19.40	6.07	9.57	10.84	6.96		
STDEV After	16.70	5.77	8.71	9.66	6.56		
LSE Before	20.69%	38.71%	27.24%	25.65%	31.15%		
LSE After	18.59%	37.43%	25.86%	24.13%	30.23%		
Deletion%	1.49%	0.28%	0.90%	1.09%	0.66%		

<b>Sunday</b>							
<b>Mainline</b>	<b>61</b>	<b>111</b>	<b>121</b>	<b>141</b>	<b>672</b>	<b>161</b>	<b>191</b>
STDEV Before	42.56	43.49	37.30	47.13	34.70	34.98	45.90
STDEV After	29.75	30.55	27.53	31.91	25.86	26.63	29.29
LSE Before	30.01%	29.85%	32.88%	27.17%	34.27%	30.70%	30.02%
LSE After	21.72%	21.43%	25.76%	19.48%	24.48%	22.04%	21.40%
Deletion%	7.02%	6.97%	6.39%	7.29%	5.14%	4.81%	9.08%
<b>Mainline</b>	<b>211</b>	<b>221</b>	<b>231</b>	<b>261</b>	<b>291</b>	<b>351</b>	
STDEV Before	50.26	38.30	52.22	46.22	44.58	48.61	
STDEV After	34.22	26.80	31.63	29.66	28.43	30.16	
LSE Before	34.75%	26.77%	23.59%	23.67%	24.95%	22.90%	
LSE After	25.53%	19.95%	16.15%	16.77%	18.08%	16.20%	
Deletion%	13.54%	5.78%	7.76%	6.93%	6.67%	6.91%	
<b>Ramp</b>	<b>102</b>	<b>122</b>	<b>123</b>	<b>162</b>	<b>173</b>	<b>212</b>	<b>623</b>
STDEV Before	7.05	8.28	15.22	7.65	4.37	4.95	3.59
STDEV After	6.65	7.91	12.32	7.28	4.35	4.31	3.57
LSE Before	37.43%	31.67%	24.36%	34.75%	48.58%	49.97%	59.48%
LSE After	36.24%	30.77%	21.22%	33.82%	48.45%	47.59%	59.36%
Deletion%	1.22%	0.51%	2.34%	0.48%	0.01%	0.47%	0.02%
<b>Ramp</b>	<b>222</b>	<b>273</b>	<b>342</b>	<b>386</b>	<b>388</b>		
STDEV Before	18.60	5.41	9.51	11.52	6.08		
STDEV After	14.85	5.17	8.33	9.60	5.76		
LSE Before	23.68%	44.61%	31.80%	31.75%	32.94%		
LSE After	20.36%	42.59%	29.53%	28.94%	32.04%		
Deletion%	2.40%	0.20%	1.24%	1.89%	0.23%		